Aus der

Medizinischen Universitätsklinik und Poliklinik Tübingen

Abteilung VII, Tropenmedizin

Humoral immune response to SARS-CoV-2 infection at the onset of the pandemic in 2020

Inaugural-Dissertation
zur Erlangung des Doktorgrades
der Medizin

der Medizinischen Fakultät
der Eberhard Karls Universität
zu Tübingen

vorgelegt von

Elsner, Käthe

2024

Dekan: Professor Dr. B. Pichler

1. Berichterstatter:in: Professor Dr. B. Mordmüller
2. Berichterstatter:in: Professorin Dr. R. Klein

Tag der Disputation: 30.06.2023

Table of Contents

List of tables

List of figures

List of abbreviations

ANOVA	Analysis of Variance
AUC	Area under the Curve
BMI	Body mass index
bp	base pair
BSA	Bovine serum albumin
CI	confidence interval
CLIA	chemiluminescence immunoassay
COVID-19	coronavirus disease 2019
CRF	Case Report Form
Ct	cycle threshold
CTD	carboxy-terminal domains
CV	coefficient of variation
d	day
D	diversity segment
Da	dalton
ddH_2O	double-distilled water
DNA	deoxyribonucleic acid
E	envelope
EDTA	ethylenediaminetetraacetic acid
ELISA	enzyme-linked immune sorbent assay
Fab	Fragment antigen binding
FACS	Fluorescence activated cell sorting
Fc	Fragment crystalline
g	gram
g	gravity of earth
GFP	green fluorescent protein
h	hour
HEK cells	Human Embryonic Kidney cells
His-tag	hexahistidine-tag
HRP	horseradish peroxidase

IFA	immunofluorescence assay
Ig	Immunoglobulin
J	joining segment
kDA	kilodalton
L	liter
LFIA	lateral flow immunoassay
LLoD	Lower Limit of Quantification
LoB	Limit of Blank
LoD	Limit of Detection
M	molar
m	meter
m-	milli
µ	micro
min	minute
M- Protein	membrane protein
MHC	major histocompatibility complex
N	Nucleocapsid
n-	nano
NCT number	National Clinical Trial number
NTD	amino-terminal domain
OD	optical density
Pa	pascal
RBD	receptor-binding domain
PBS	phosphate buffered saline
PBS-T	PBS + 0.1 % Tween-20
PCR	polymerase chain reaction
RNA	ribonucleic acid
ROC	receiver operating characteristics
rpm	revolutions per minute
RT	room temperature
RT-PCR	reverse-transcription polymerase chain reaction
SARS-CoV-2	Severe acute respiratory syndrome coronavirus type 2

S	spike
sec	second
SDS-page	sodium dodecyl sulfate polyacrylamide gel electrophoresis
SOC	super optimal broth with catabolite repression
TB	terrific broth
TBE	Tris-borate-EDTA
TGS	Tris-Glycine-Sodium dodecyl sulfate
TMB	Tetramethylbenzidine
TNBP	Tri-n-butyl phosphate
V	variable segment

1 Introduction

1.1 COVID-19

The outbreak of Coronavirus disease 19 (COVID-19) was first reported in Wuhan, China in late 2019 [1]. The severe acute respiratory syndrome coronavirus 2 (SARS-CoV-2) spread rapidly worldwide, receiving pandemic status on March 11, 2020 [2]. Already at the beginning of 2021, there had been 82 million confirmed COVID-19 cases and about 1.8 million reported deaths associated with COVID-19 worldwide [3]. Transmission occurs from human to human and the main route of transmission of the virus is via aerosols that are produced, for example, when the infected person breathes, talks, coughs or sneezes and are subsequently inhaled by others [4]. The rapid spread of the virus, as well as the severe courses of the disease, made political actions necessary that affected the everyday life of many people around the world. The economy suffered from repeated periods of lockdowns [5], while quarantine and social distancing strained people's mental health [6]. Hospital staff was permanently stretched to capacity and faced new mental challenges [7]. Scientists were tirelessly researching to gain more knowledge about the virus and the disease and to produce a lifeline from the pandemic - effective vaccines [8].

We began our work in March 2020 with the idea of developing an antibody test to determine whether an infection has been passed, to estimate the proportion of those who have recovered and may be immune, and to determine the antibody formation after vaccination. But by March 2020 little was known about the disease and there was little in the way of diagnostic capabilities. The reverse transcription polymerase chain reaction (RT-PCR), which is detecting the ribonucleic acid of the virus, was the only test option available for the detection of acute infections. First rapid antigen tests were available later in October 2020 [9]. Antibody tests for the detection and analysis of the humoral immune response to SARS-CoV-2 did not yet exist on the market. Reliable antibody tests, like Enzyme-linked Immunosorbent Assays (ELISA) were urgently needed.

People suffering from COVID-19 present diverse symptoms. The extent of symptoms varies widely from asymptomatic cases or cases with mild flu-like symptoms

to severe courses requiring intensive medical care [10]. SARS-CoV-2 primarily attacks the respiratory system [11]. Frequently reported symptoms are sore throat, cough, rhinitis, fever and other pneumonia associated symptoms as well as olfactory and/or gustatory disturbances [12].

1.2 Severe acute respiratory syndrome coronavirus 2

To develop an antibody test, one must first become aware of the structure of SARS-CoV-2 in order to make a choice for a suitable antigen.

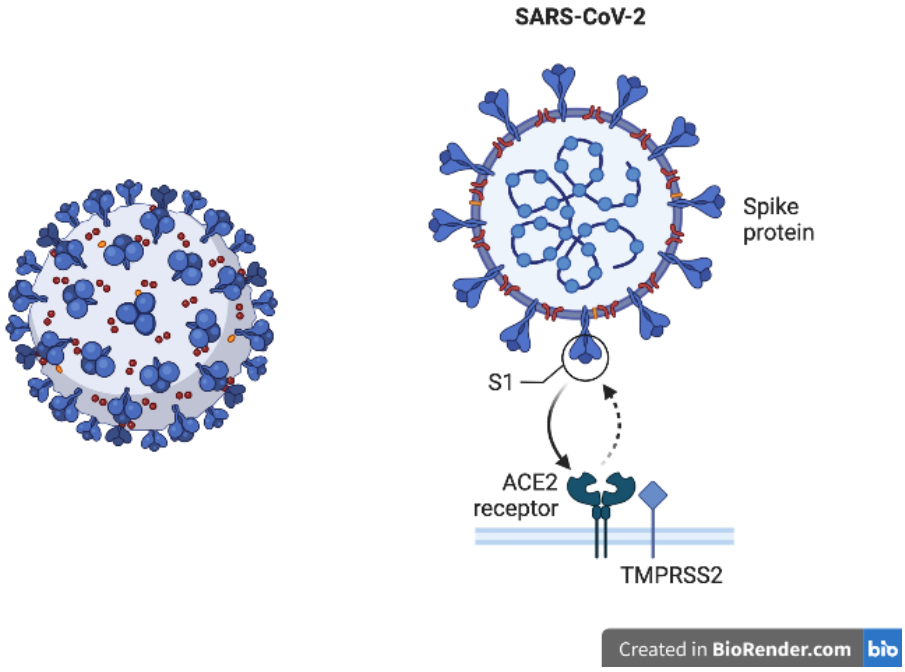

Figure 1: Structure of SARS-CoV-2 (own creation).

SARS-CoV-2 belongs to the group of beta-coronaviruses. They have a single-stranded positive sense RNA genome that is enveloped. The genome codes for four structural proteins: spike protein (S), envelope protein (E), membrane protein (M) and nucleoprotein (N) [13]. The coronavirus owes its name to the spike proteins, which give it a crown-like structure. The S protein is a large glycoprotein (approximately 180 kDa)[14] that is assembled into a homotrimer and protrudes from the surface anchored in the viral membrane [15]. Upon interaction with the cell membrane, structural changes of the S protein occur, so that the virus fuses with the cell membrane [14]. It contains a S1 receptor-binding subunit for cell entry and

a membrane-fusion S2 subunit. The S1 subunit in turn comprises an amino-terminal domain, a receptor binding domain (RBD) and two carboxy-terminal domains (CTD1, CTD2) and is highly conserved [15]. The RBD binds to angiotensin-converting enzyme 2 (ACE2) to enter the target cells [16]. ACE2 is a metallopeptidase which is, among other cells, abundantly expressed on the epithelial cells in the lung and on enterocytes of the small intestine [17]. Cellular serine proteases TMPRSS2 divide S into S1 and S2, leading to activation of the protein for cell entry [14] (see figure 1).

The N protein together with the genome forms the nucleocapsid which is surrounded by E and M proteins [13]. The described proteins are potential antigens for antibody testing. Immune cells develop antibodies against structural proteins. Selection criteria for the antigen are immunogenicity, avidity, conservation and use in vaccines. Most vaccines target the S protein [18]. RBD is the main target of neutralizing antibodies triggered by natural infections or vaccinations [15], what makes it highly immunogenic and interesting for our test. Another important criterion of antigens is the binding strength (avidity). This enables high sensitivity and specificity as well as a long persistence of detection [19]. High avidity has been demonstrated for RBD and S protein [19].

1.3 Immunology

The human immune system protects the body from infections by attacking foreign structures called antigens [20]. In addition to the non-specific immune system with cellular and humoral components, there is the specific immune system, which can also be divided into humoral and cellular components [20]. In this work, the focus is on the humoral specific immune response, which includes the antibody response.

The humoral immune response belongs to the acquired immune system and serves to eliminate free pathogens in plasma with the help of specific antibodies that bind to the pathogens declared as foreign by the body according to the lock-and-key principle. Thus, it is highly specific against pathogens, but is activated with a delay [20].

The antibodies enable the fight against pathogens and are secreted by activated

and differentiated B cells. B cells, which are antigen presenting cells, carry B cell receptors on their surface, which can recognize antigens. Each naive B lymphocyte carries a specific B cell receptor. Antigens bind to this receptor and these, together with T cells, activate the B cell via MHC II receptors and cytokines. The activated B cell divides to produce clones with the same antigen receptor (clonal selection), which may secrete specific antibodies. Antibody secreting B cells are called plasmablasts or plasma cells. In addition, memory B cells are generated that can be rapidly reactivated into antibody-producing effector B cells upon renewed contact with the antigen, thus it is preventing or attenuating renewed infection. These cells are called memory B cells [20].

Antibodies are part of the humoral specific immune response. They occur in bound form as well as freely in plasma or secretions. The bound antibodies are located as B cell receptors on the B lymphocytes. Antibodies are polypeptides consisting of two fragments with a Y-shaped structure. The Fab fragment (Fragment antigen binding) contains the antigen binding site and has a variable region. The Fc fragment (Fragment crystalline) is responsible for most of the effector functions of antibodies. Antibodies can also be divided into light and heavy chains. There are two types of immunoglobulin light chains: λ- and κ- chains. The heavy chains can be divided into μ, δ, γ, α, and ε chains. According to their Greek names, they determine the five different classes of immunoglobulins: IgM, IgD, IgA, IgG, and IgE [20].

Now, how is the specificity of antigen receptors, or antibodies to antigens, achieved? The high specificity is made possible by several mechanisms. First, the B cell receptor as an antibody has variable and constant parts. The variable parts are responsible for antigen recognition and obtain enormous diversity by various mechanisms. One important mechanism is that of somatic recombination. During lymphocyte maturation, the variable domains of the immunoglobulin light and heavy chains are encoded by specific gene segments: variable segment (V), joining segment (J) and diversity segment (D), which encodes only the heavy chain. Somatic recombination randomly rearranges and links the V(D)J segments. Thus, each cell expresses a unique receptor and a human has

approximately 10^8 to 10^{11} different lymphocyte specificities [20].

The secreted antibodies are acting by neutralization, opsonization, cellular inhibition, or complement activation [21]. The different functions depend on the antibody class. IgM is produced first after activation of a B cell. It is a pentamer found only in the bloodstream, not in tissues due to its comparatively large mass. IgM has high avidity, with low affinity. It is responsible for complement activation by interaction with complement factor C1. It also occurs bound on B cells as a B cell receptor. IgM thus plays a special role in the early phase of the immune response. In the absence of T helper cells, activated B cells secrete only IgM isotype antibodies [20]. IgM accounts for 10% of immunoglobulins and has a half-life of 10 days [20,22].

If the B cell then comes into contact with a T helper cell, cytokines induce isotype switching. For example, IgG is then formed. IgG has four isotopes, IgG1 - IgG4. It counts as the main immunoglobulin and accounts for 70-75% of immunoglobulins. It is found intravascularly and extravascularly and has a half-life of 7-20 days, giving it the longest survival time. Functions include neutralization of toxins and viruses, opsonization, complement activation, and antibody dependent cellular cytotoxicity. Repeated contact with the protein antigen results in the production of antibodies with increased affinity (affinity maturation). The increase in affinity occurs through point mutations in the variable regions of the antibodies. This is called somatic hypermutation. Therefore, IgG is one of the antibodies with very high affinity [20].

The isotope of immunoglobulins is also influenced by the location of the immune response. For example, IgA is produced in mucous membranes where it can be secreted and neutralizes microbes and microbial toxins. Because pathogens are frequently inhaled or swallowed, the immune response via IgA at the mucous membranes is particularly important [20]. IgA, also like IgG, has a high affinity and both play an important role in neutralizing viruses by blocking binding sites and interfering with viral functional mechanisms [21]. It is divided into isotopes IgA1 and IgA2. It accounts for 15-20% of immunoglobulins and occurs as monomer and dimer [20]. IgA has a serum half-life of only 6 days[22].

IgE plays a role in the activation of mast cells and eosinophilic granulocytes. This mechanism plays a role in parasite defense and in the hypersensitivity reaction and will therefore not be discussed further here. IgD, as already mentioned, occurs as a naive B cell receptor on the surfaces of B lymphocytes and accounts for only less than 1% of total globulins [20].

1.3.1 Specific humoral immune response against SARS-CoV-2

When we started developing an antibody detection assay in March 2020, little information was known about time courses and levels of the different antibody classes during a SARS-CoV-2 infection. The number of publications about the immune response to SARS-CoV-2 has risen sharply since then. In the following paragraphs, the current knowledge (by January 2021) about the immune response to COVID-19 infection is summarized. It contains important points for the development of an antibody screening test.

The antibodies bind to different antigens of SARS-CoV-2 to combat the virus. At that time, the best studied antibodies were against S, N and RBD proteins. Brochot et al. observed a higher sensitivity (the ability to correctly identify patients with SARS-CoV-2 antibodies [23]) of antibody screening tests when using RBD as antigen, compared to S1 and S2 proteins [24]. Furthermore, a very high specificity to correctly identify patients without SARS-CoV-2 antibodies was reported by using RBD as antigen in ELISAs as well [25].

In the following, the kinetics of antibodies after infection with SARS-CoV-2 will be described. Many studies do not explicitly describe against which antigen the specific antibodies are directed. Therefore, IgM, IgG and IgA antibody classes are generally reported. In the review by Post et al. that examined antibody kinetics in the first three months after infection, most studies describe an increase in IgM before IgG and IgA. The mean or median of time from symptom onset to seroconversion is four to 14 days for IgM and 12 to 15 days for IgG. Seroconversion for IgA is most commonly described within four to 11 days [26]. Thus, the antibody classes IgM, IgG and IgA are detectable in most infected individuals within the first two weeks after symptom onset [26-28].

The dynamics of antibody levels over time varies among classes. IgM refers to a

rapid increase followed by a decrease in the third to fifth week. After six weeks, IgM could no longer be detected in most cases [26]. IgG levels, on the other hand, showed a high peak with a plateau followed by a decline. However, persistence of IgG antibody levels at low levels for the observation period of three months has been described [26]. Thus, IgG response has the longest half-life compared to the IgA and IgM antibody classes with a peak around three to seven weeks after symptom onset [26,29]. Sun et al. observed that S- specific IgG then decreased more slowly compared to N- specific IgG [30]. In addition, neutralization titers correlated with S- and RBD-IgG antibodies, which are immunogenic [29-33], whereas the correlation of neutralizing antibodies to anti-RBD IgA and IgM is limited [26]. Meanwhile it is known that the level of antibodies correlates with the severity of the disease. Subjects with mild symptoms or no symptoms at all frequently develop fewer antibodies than subjects with severe symptoms. Neutralization titers can be very low or even undetectable in individuals with no symptoms or mild course of disease [26,28].

For the development of an antibody test, the following conclusions can be drawn from this chapter.

For a high quality of the test it seems reasonable to choose an anti-RBD IgG and anti-RBD IgA antibody test, because RBD as antigen shows a high specificity, sensitivity, affinity and immunogenicity and IgG and IgA in general have a high affinity. Moreover, IgG in general but also specifically after COVID-19 infection shows a long half-life and persistence of antibody levels for at least 3 months [26]. Thus, a passed infection would still be detectable by the test for a long time. IgM, on the other hand, would be less suitable for the test, since the rapid drop in antibody levels [26] means that the time frame for detecting a passed-through infection is relatively small.

IgG and IgA are also interesting in terms of their function, since, as described in this chapter, they have a neutralizing effect by blocking the binding sites and interfering with the functional mechanisms of viruses.

1.4 Serological methods

There are two categories of diagnostics for COVID-19: molecular detection of viral RNA and serological diagnostics with the search for antibodies, a reaction of the body to the infection [34]. I would like to focus on serological diagnostics and present different methods below, one of which we selected for our test.

What is the purpose of antibody detection? The first thing is to get a better understanding of the disease. How does the immune system react to contact with the virus? Who develops specific antibodies and who does not? Which responses predict disease outcome? For this purpose, it is necessary to investigate exactly what the concentration and kinetic of the antibody concentration in plasma is like. Antibody tests are also a tool to conduct epidemiological studies that assess disease prevalence in different regions or settings, such as among particularly exposed hospital personnel or in children. Serological tests are also useful for the assessment of an outbreak of the disease, at a time period when the virus is no longer detectable with RT-PCR. Antibody levels may also provide an indication of whether immunity has been achieved following infection or vaccination. Thus, the proportion of individuals with potentially protective antibodies in the population could contribute to policy decisions regarding public health measures to reduce the incidence of infection. Serological assays can also be a surrogate for vaccine efficacy. Moreover, it could theoretically be used to guide the timing of vaccination campaigns including the need for booster vaccinations. In the following, immunological assays are presented.

Gong et. al. described four different serological methods for COVID-19 diagnosis. These are the ELISA, chemiluminescence immunoassay (CLIA), lateral flow immunoassay (LFIA) and immunofluorescence assay (IFA). Each of these methods has its advantages and disadvantages [35].

ELISA is an established method that has been widely used since 1970 until today [36]. Also, at the Institute of Tropical Medicine this method for the detection of antibodies is well implemented. There are different variants of the ELISA. Among others, the indirect detection method, the sandwich method and the double antibody method [37]. The indirect method is most commonly used in COVID-19

diagnostics [35], so I will to present it in more detail.

The indirect ELISA can be used for the quantitative detection of specific antibodies in serum or plasma. For the detection of serological responses to infections, an antigen of the pathogen is bound to a plate. Antibodies (if present) from the subject's plasma or serum bind to the antigen. These antibodies are subsequently marked by a second antibody. This allows to measure specific antibody levels [38]. The average time required for the test is 2-8 h [35].
The CLIA has a similar mode of operation as the ELISA. The difference is that it requires a chemical reaction to reveal positive samples by glowing. The time required is 0.5-2 h. A large detection instrument, a chemical immuno-luminescence analyzer, is required [35]. The LFIA is a paper-based detection and analysis platform. By aspirating the sample, fixed antibodies on the test strip can interact with target molecules [35]. Thus, specific antibodies against SARS-CoV-2 can be detected. It is cost-effective, portable, rapid (3-30 min) and versatile. However, no quantification of antibodies is possible [35].
IFA works with SARS-CoV-2 infected animal cells fixed on glass slides. Serum is then added to the sample to be tested. Binding antibodies can be labeled with fluorescent protein by adding goat anti-human secondary antibodies. These can be assessed via the fluorescence microscope. Again, however, exact quantification of the specific antibodies is difficult [35].
Which serological test is best suited for our projects? We have said that we want to measure the concentration and kinetics of specific antibodies. Accordingly, the LFIA and IFA are unsuitable for our project because the results cannot be quantified precisely [35]. If we consider the CLIA and the ELISA, we find that the procedures are very similar. We decided to use the ELISA despite the longer test duration because the method is well established at the institute and the appropriate equipment is available.

1.5 Disorders of taste as a symptom of COVID-19

Loss or disturbance of the sense of taste and smell has been shown to be a distinctive symptom of COVID-19 with high incidence [39]. Unlike the ordinary

disturbances of these senses as in the case of a blocked nose, it occurs even without a cold and usually persists for several days to weeks and can be severe with almost complete loss of the sense [12]. It was reported as a highly specific symptom for COVID-19 [40]. A meta-analysis showed that nearly 40% of approximately 138,000 infected individuals suffered from taste disorders [41]. Taste and olfactory disturbances were investigated as pre-test criteria for diagnostic testing because they were found to be good predictors of RT-PCR positivity for the alpha and delta variants of SARS-COV-2 and were the only symptom in some cases [42-44]. A link between loss of taste and a high viral load has been observed [45]. However, little is known about whether seroconversion occurs in people with loss of taste and whether this symptom is associated with the height of antibody levels.

1.6 Objectives of this thesis

The primary objective of the study was to establish a SARS-CoV-2 ELISA and to conduct epidemiological and immunological studies in the early phase of the SARS-CoV-2 pandemic. The goal was to develop a quantitative assay that could be used to test the effect of vaccinations and assess immunity. We also wanted to develop a low-cost ELISA with similar or better performance than commercial tests for implementation at the Centre de Recherches Médicales de Lambaréné, Gabon. Such a test could be of great use to investigate the epidemiology of COVID-19 in Gabon.

The goal was to optimize the developed test and compare it with commercial tests that came on the market during the thesis. Another objective was to collect a cohort of infected persons from the first and the beginning of the second wave (the ´TüCoV-Study`) in order to quantify the specific antibodies against SARS-COV-2 using the developed test. We then wanted to investigate correlations between symptoms and antibody levels. In particular, the influence of taste disturbances, which are considered very specific, and the influence of fever on antibody levels.

In this work, we aimed to address the question of what factors besides PCR positivity are reliable indicators of antibody positivity as a proxy for immunity.

Accordingly, in summary, we pursued the following aims and objectives:

- Develop a quantitative SARS-CoV-2 IgG and IgA ELISA
- Corroborate whether these ELISAs detect SARS-CoV-2 specific antibodies
- Evaluate if there is a relation between symptoms and antibody levels
- Analyze which factors additional to a RT-PCR positive test predict antibody positivity under the hypothesis that a model that includes both disease symptoms and diagnostics can predict seroconversion better than PCR alone.

2 Methods

To develop ELISAs that have high sensitivity and specificity, can detect passed-through infection, and can quantify levels of specific SARS-CoV-2 antibodies, we followed the steps outlined in figure 2. We started with the selection of an antigen. We then multiplied the corresponding plasmid to express the antigen. As a next step, we surveyed the `TüCoV´ study and collected blood samples. This was then used to develop the ELISAs, which were subsequently validated with precision tests. With the validated assays, we measured all samples to then use the results to set a cut-off for seroconversion and perform statistical analysis. In this chapter, the individual steps are described in more detail. A complete list of materials and devices used for developing the ELISAs is given in the appendix.

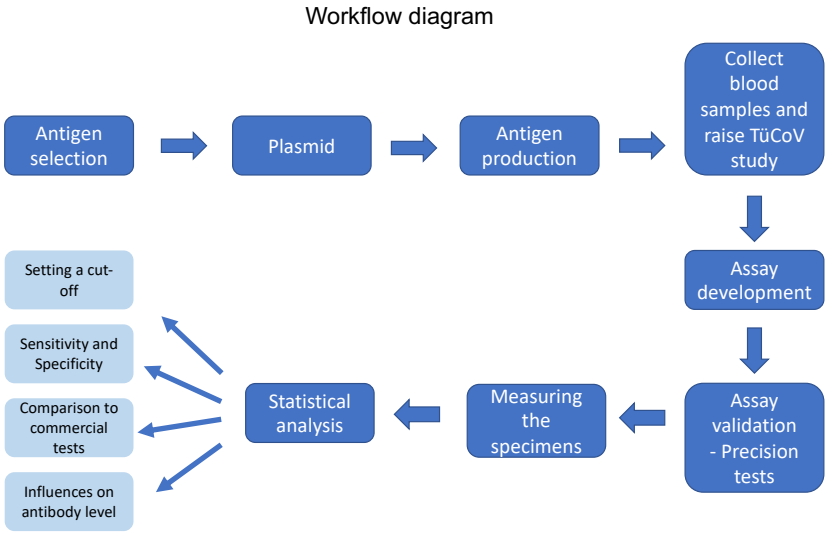

Figure 2: Workflow diagram of this thesis.

2.1 Antigen selection

To be considered a diagnostic-quality antibody screening test, it should have high sensitivity and specificity. Selecting the proper antigen for the test is thus a key step for achieving this goal.

We chose S1 RBD as the antigen for the ELISAs because it meets our criteria for a good antigen (stated in the introduction) as it is sensitive, specific, immunogenic, and is often a component of the vaccines being developed.

2.2 Plasmid

2.2.1 Amplification of the plasmids

The following reagent was obtained through BEI Resources, NIAID, NIH: Vector pCAGGS Containing the SARS-Related Coronavirus 2, Wuhan-Hu-1 Spike Glycoprotein Receptor Binding Domain (RBD), NR-52309. The plasmid pCAGGs-CoV2-RBD, encoding for the RBD protein of SARS-CoV-2 was kindly provided by Florian Krammer (Icahn School of Medicine at Mount Sinai, New York. The plasmids were amplified previously for the transfection into human embryonal kidney (HEK) 293 F cells for expression of the RBD protein. The RBD contains a C-terminal hexahistidine-tag (His-tag) for purification of the protein. Furthermore, we had a CMV-Sports-CoV2-RBD plasmid available, kindly provided by Andrea

Weierich from our institute, to compare the level of protein expression of pCAGGs and pCMV-Sport vectors in 3.2. The pCMV construct is a C-terminal twin strep-tag followed by a His-tag. Both sequences of the plasmids are provided in the appendix.

2.2.1.1 Transformation into competent cells

The plasmids were transformed into chemically competent Top 10 *Escherichia coli* cells (Thermo Fischer, cat. #C404010) and Stellar competent cells, *Escherichia coli* HST08 strain (Takara, cat. #636766). Approximately 30 ng of each plasmid was added to 50 µl of competent cells. Afterwards, the solutions were placed on ice for 30 min. Stellar cells were heat-shocked for 60 sec and Top 10 cells for 30 sec at 42°C, then placed on ice for 1-2 min. Prewarmed SOC medium was added to a final volume of 500 µl and incubated on a shaker at 300 rpm for 45 min at 37°C. 50 µl of each solution was subsequently streaked on carbenicillin-plates. Plates were incubated overnight at 37°C and colonies counted the next day.

2.2.1.2 Purification of the plasmids

Purification of the plasmids was performed according to the manual of Plasmid Purification Handbook from July 2009 (QIAGEN, Hilden) with minor modifications. A single colony of the cells, containing the plasmid was inoculated in 200 ml of TB media and incubated at 37°C on a shaker for 16 h. For harvest, the cells were centrifuged at 4000 x g for 15 min at 4°C. The resulted pellet was resuspended in 10 ml Buffer P1. 10 ml of Buffer P2 was added and components were mixed by inverting the tube 6 times. The mixture was incubated for 5 min at room temperature. After addition of 10 ml of chilled Buffer P3, the solution was mixed immediately by inverting 6 times. Subsequently, the reaction tube was incubated on ice for 15 min and centrifuged at 4000 x g for 30 min at 4°C. The supernatant containing the plasmid was separated. The QIAGEN-tip 500, column that contains 25 ml, optimized to bind plasmid DNA, was equilibrated by applying 10 ml Buffer QBT. The supernatant containing the plasmid was applied to the column and likewise entered the resin by gravity flow. Afterwards, the QIAGEN-tip was

washed with 2x 10 ml of Buffer QC. Plasmid DNA was eluted with 15 ml Elution Buffer and collected in a falcon tube. 10.5 ml Isopropanol was added and the solution was centrifuged at 4000 x g for 30 min after mixing of components. The supernatant was discarded careful, the remaining DNA pellet was washed with 5 ml of 70% ethanol and centrifuged again at 4000 x g for 10 min. The supernatant was decanted once again. Under sterile conditions, the plasmid-pellet was dried and redissolved with 100 µl sterile filtered Milli-Q water. The concentrations of plasmids were measured by Nanodrop and diluted to a final concentration of 1 µg/µl in sterile filtered Milli-Q water.

2.2.1.3 Agarose gel electrophoresis

Agarose gel electrophoresis was performed to check purity of the plasmids. The gel was prepared with 1% agarose in TBE buffer and left in a gel slide with for 30 min to harden. 50 - 500 ng of DNA was added to 6 µl loading buffer and 1 µl SYBR Green and filled up with nuclease-free H_2O to a total volume of 20 µl. As a size-marker, 7 µl of 1 kb Plus DNA ladder (1,000 µg/ml) from New England BioLabs Inc. was applied and mixed with 2 µl loading buffer and 1 µl SYBR Green. Samples and marker were filled into the pouches of the gel and electrophoresis run with 110 V for 1 h. The gel was placed on the Gel Stick Imager (Intas Science Imaging Instruments GmbH) to see the results.

2.3 Antigen Expression

2.3.1 Cell culture of HEK 293 F cells

HEK 293 F cells are modified clones from human embryonal kidney (HEK) cells. They were cultured for the expression of SARS-CoV-2 antigens, which are required for the ELISA. HEK 293 F cells were used for all performed transformations. All procedures were performed under sterile conditions. No antibiotics were added. The user instruction manual (Thermo Fisher Scientific, Carlsbad) provided by the Expi293™ Expression System Kit (Thermo Fischer, #A14635) was used during the experiments.

2.3.1.1 Thawing of HEK 293 F cells

Cells were frozen with 10% Dimethyl sulfoxide, a cryoprotective substance. One vial, containing 1 ml at $1*10^7$ cells/ml, was thawed by gentle agitation in 37°C water bath. When the cells were almost thawed, they were transferred in a centrifuge tube with 5 ml of preheated medium and centrifuged for 5 min at 125 x g. The supernatant was discarded and the pellet was resuspended with fresh preheated medium to a final volume of 30 ml and transferred into a 125 ml Erlenmeyer flask with vent cap. Cells were incubated on an orbital shaker at 125 rpm, 37°C, 8% CO_2 and humidified atmosphere. The following day, the medium was changed. The viability and density of the cells were evaluated, using a Neubauer counting chamber and Trypan Blue solution.

2.3.1.2 Maintenance of the cells

HEK 293 F cells were cultured in 30 ml Expi293 Expression medium from the Expi293™ Expression System Kit (Thermo Fischer). The culture was incubated on an orbital shaker at 125 rpm, 37°C, 8% CO_2 and humidified atmosphere. Cell density and viability were monitored every 2-3 days. Cells were seeded at $3 - 5*10^5$ cells/ml and diluted when they reached a number of $2 - 3*10^6$ cells/ml. If the dilution was less than 1:2, the medium was replaced by centrifuging the cells at 125 x g for 5 min and resuspending the pellet with fresh, prewarmed medium.

2.3.2 Transfection of pCAGGs-CoV2-RBD and pCMV-Sport-CoV2-RBD

The plasmids were transfected into HEK 293 F cells for production of the RBD protein. The method described below, is representative for both performed transfections. Two 30 ml cultures were prepared for transfection. One week in advance, the cultures were kept in a logarithmic growth phase and viability was above 95%. One day before the transfection, the cultures were seeded at approximately $2.5*10^6$ cells/ml. At the day of transfection $7.5*10^7$ cells in 25.5 ml Expi293 Expression medium for each culture were prepared. Next, lipid-DNA complexes were prepared by diluting 30 µg total plasmid DNA in 1.5 ml Opti-MEM I medium for one transfection culture. Green fluorescent protein (GFP)

control vector was co-transfected to assess the transfection rate. Total plasmid-DNA was composed of 5% GFP vector and 95% antigen-plasmid. 80 µl Expifectamine reagent was also applied to 1.5 mL Opti-MEM I medium respectively and mixed gently. After incubation of 5 min at room temperature, suspensions of plasmids and Expifectamine were mixed to obtain a volume of 3 ml and incubated for exactly 20 min at room temperature to allow complexes to form. Lipid-DNA complexes were added to the cells into the shaker flasks to a total volume of 28.5 ml and incubated on orbital shaker at 37°C, 8% CO_2, 125 rpm and humidified atmosphere. 16-18 h after transfection, 150 µl of Transfection Enhancer 1 and 1.5 ml of Transfection Enhancer 2 were added to the transfected cultures to reach the final volume of 30 ml.

2.3.3 Monitoring of Transfection

Transfection rate and viability were monitored on day 1, day 3 and day 6 using flow cytometry (FACS) and the Neubauer counting chamber. Cell density and viability was determined with the Neubauer counting chamber. Transfection rate was measured by detecting the green fluorescent protein with FACS. For FACS, 50 µl sample were taken from transfected and non-transfected cultures as negative control and mixed with 500 µl 1x PBS by vortexing at low speed. Thereupon, 5 µl Propidium Iodide Staining Solution (PI) 1.0 mg/ml was added and samples were vortexed once again and incubated for 10 min to measure the viability of the cells. PI cannot diffuse into cells with an intact membrane. It emits light (between 600-700 nm) that can be detected by flow cytometry. In this way, dead cells can be distinguished from intact cells.

2.3.4 Harvesting the Proteins

The proteins were harvested on day three and day six of transfection. On day three the cultures were transferred into 50 ml tubes and centrifuged on low speed 133 x g for 3 min to ensure cell viability. The supernatant containing the protein was transferred into another 50 ml tube and centrifuged at 4000 x g for 10 min at 4°C. The transparent supernatant was stored at -80°C and combined with the protein sample of the second harvest. The cell-pellet was resuspended with

preheated medium to a volume of 30 ml and incubated again. On day six the cells were centrifuged at 4000 x g for 10 min at 4°C, combined with the day three supernatant and purified immediately.

2.3.5 Purification of RBD and S1 protein

2.3.5.1 His- Tag purification

The RBD, containing a C-terminal His-tag, was purified with the help of ÄKTAprime plus (GE Healthcare) and HisTrap HP column (GE healthcare, Munich). During the purification, the His-tag of the RBD protein binds to the column and is thus separated. Because of the volume of the sample (approximately 100 ml), a pump was used to let load the column. The buffers were filtered in advance with help of vacuum-riven filtration system (Vakuubrand GmbH & Co, serial no. 17088802) using 0.22 µm Millipore Express PLUS filter (Merck). To prepare the samples, they were filtered with a 0.45 µm Millipore filter (Merck) attached to a 50 ml Luer lock syringe. 5x wash buffer was added, so that the sample finally contains 1x wash buffer. To prepare the HisTrap column, it was flushed gently with 10 ml MilliQ water and equilibrated with 10 ml wash buffer. After the initializing of the Äkta system, done with the setting “System wash”, the purification step was done by using the method template “Ion exchange gradient elution”. A flow rate of 1 ml/min and a maximum pressure of 0.5 mPa was applied. After the injection of the sample, the column was washed with 20 ml wash buffer and the protein was eluted with 15 ml of elution buffer. Fractions of 500 µl were collected during elution and the following wash with 10 ml wash buffer. Fractions were analyzed with SDS-Page as described in the following.

2.3.5.2 Strep-Tag purification

The RBD protein from the pCMV-Sport vector was further purified using its Strep-tag. The second purification step was done with help of StrepTrap™ HP column. The pCMV-Sport vector encodes for a strep tag at one side of the RBD protein, which binds to the column. The Äkta system, the column and the sample were prepared and initialized as described for the His tag purification. A 5 ml loop was used to inject the sample. A flow rate of 1 ml/min and a maximum pressure of

0.5 mPa was applied. After the injection of the sample, the column was washed with 10 ml wash buffer and the protein was eluted with 5 ml of elution buffer, containing 2.5 mM Desthiobiotin. Fractions of 500 µl were collected during elution and the following wash with 5 ml wash buffer. Fractions were analyzed once again with help of SDS-Page as described in the following.

2.3.5.3 SDS Page (Sodium Dodecyl Sulfate Polyacrylamide Gel Electrophoresis)

SDS page was performed to separate the proteins accordingly to their size and to assess purity and size of proteins. 10% or 15% separating gel and 6% stacking gel were prepared. The samples were diluted in 5x loading-buffer (recipe is in the list of materials in the appendix) to a final concentration of 1x. The samples were boiled at 95°C for 5 min. 20 µl of each sample was added to the stacking gel. Different purified fractions were applied on the gel to figure out which fractions contain the target protein. The RBD protein donated by Florian Krammer (Icahn School of Medicine at Mount Sinai, New York) was used as a positive control. Additionally, 10 µl of a molecular-weight size marker (Precision Plus Protein Unstained Standards, Bio-Rad) was added. The electrophoretic separation was performed in TGS buffer with 130 - 160 V for 1 h. The separating gel was put into Coomassie Brilliant Blue staining solution (Bio-Rad), followed by destaining solution for 1 h to analyze the samples.

2.3.5.4 Exchange of the buffer

The fractions with the highest protein concentrations were pooled. The protein was transferred into PBS buffer by using Amicon Ultra-4 centrifugal filters Ultracel 30 K, 10 ml (Merck, Darmstadt).

The sample was centrifuged at 4000 x g for 5 min at 4°C. PBS was added to the left over in the filter by pipetting up and down to release the protein from the filter. Sample was centrifuged again as described before. The procedure was repeated 4 times to wash out the buffers from purification. The sample was transferred into Eppendorf tubes 1,5 ml. The RBD concentration was determined with NanoDrop and diluted to 1 mg/ml in PBS supplemented with protease inhibitors (Roche; ref.

11697498001).

2.4 Collect blood samples and conduct TüCoV Study

2.4.1 Plasma samples

The screened plasma samples came from three different studies described below. Two studies were clinical trials, which investigated the efficacy of Hydroxychloroquine against COVID-19. The third was the TüCoV study, which was designed to investigate the immune response against SARS-CoV-2 in COVID-19 convalescent participants. A pool of negative controls, CoVNeg was prepared using samples from donors. Furthermore, pre- pandemic plasma samples from earlier than 2019 were measured. All plasma samples were stored at -60°C.

2.4.2 Studies

2.4.2.1 COMIHY and COV-HCQ study

The first study conducted at the Institute for Tropical Medicine, Tübingen, named “Hydroxychloroquine for the treatment of mild coronavirus disease 2019 – COVID-19 (COMIHY)”, registered at Clinicaltrial.gov (NCT04340544), included 19 participants, who had a positive SARS-CoV-2 RT-PCR and did not need to be treated in a hospital, due to mild symptoms. Blood and saliva were drawn at three timepoints, on day one, day 14 and day 28. The second one is named "Randomized controlled trial of hydroxychloroquine versus placebo for the treatment of adult patients with acute coronavirus disease 2019 – COVID-19 (COV-HCQ)" with the register number 2020-001224-33. It included 18 participants, who were tested SARS-CoV-2 positive and required hospitalization due to severe COVID-19-related symptoms. Participants were recruited from Tübingen, Bahlingen and Reutlingen in Southwest Germany. Blood was taken at four timepoints, on day one, day seven, day 14 and day 30. Individual blood samples are missing for some timepoints.

2.4.2.2 TüCoV study

TüCoV was a cross-sectional investigation of immune response in a COVID-19 convalescent study population. The study was reviewed by the Ethics Committee

(project number: 247/2020BO1; 256/2020BO2). In advance ELISA- or RT-PCR-confirmed (by general practitioner or testing station) COVID-19 cases from Tübingen and surroundings were recruited. We also invited relatives of confirmed positive participants to take part in the study as contact persons. Recruitment of participants started on the 27.05.2020. Data from 138 blood samples of the subjects collected up to the 04.12.2020 were included in the present study. Saliva, plasma and serum were sampled at one single timepoint. All participants completed a questionnaire to record gender, age and BMI, as well as the date of symptom onset and the range of symptoms.

2.4.2.3 Negative controls

CoVNeg samples were collected in May and June 2020 from individuals who work at the Institute. Hence, they are not pre-pandemic and one cannot rule out that some individuals had COVID-19 before sampling. Participants who had a proven COVID-19 infection were excluded. For evaluation of in-house ELISAs, 32 pre-pandemic samples were used.

2.5 In-house ELISA (Enzyme linked immunosorbent assay)

2.5.1 Development of the Assays

To reduce background signal and to get a specific binding of antibodies in the plasma, we tested several blocking solutions, sample diluents, diluents of the secondary antibody and secondary antibody concentrations. The development and optimization of the ELISAs is described in 3.3.

2.5.2 Procedure of the ELISAs

The illustration shows briefly the main steps in carrying out the IgA and IgG in-house ELISA. The procedures are described in detail below.

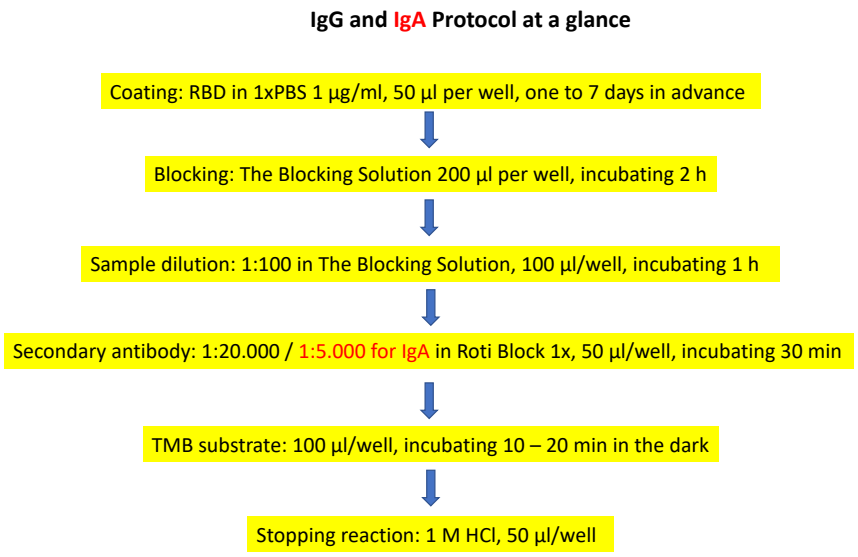

Figure 3: RBD SARS-CoV-2 IgG and IgA ELISA protocol at a glance.

Changes for IgA are marked in red.

2.5.2.1 SARS-CoV-2-RBD IgG in-house ELISA

The ELISA was performed to determine the quantity of SARS-CoV-2 IgG antibodies in plasma samples and to detect seroconversion. The plate was coated 1-7 days in advance with the RBD protein in a concentration of 1 µg/ml in PBS. Each well of the 96-well Costar microtiter high binding plates (Corning) was filled with 50 µl protein solution, then sealed with parafilm and incubated at 4°C. The plate was washed once with PBS before applying The Blocking Solution (Candor). The blocking buffer was incubated for 2 h at room temperature (RT) on a microplate shaker at 600 - 900 rpm. The samples were pre-diluted on non-binding plates with a starter dilution of 1:100 in The Blocking Solution. Each sample was measured in three serial 2-fold dilutions which were prepared on non-binding plates, to avoid false results and to quantify the concentration of bound IgG.

The plate was washed three times with PBS-T before 100 µl of the samples were transferred from the non-binding plate to the high-binding plate and incubated on a shaker at 600 - 900 rpm at RT. After one hour of incubation plates were washed again. Goat-anti-human IgG was diluted in a ratio of 1:20.000 in Roti Block 1x (Roth) and 50 µl of the solution was added to each well. The secondary antibody

was incubated for 30 min on a shaker at 600 - 900 rpm at RT. After washing the plate four times, 100 µl TMB substrate was applied for visualization of the antibody capture. When the absorption of positive control measured at 350 nm with CLARIOstar plus microplate reader (BMG LABTECH GmbH, Ortenberg, Germany) was around 1.3 to 1.6 OD the reaction was stopped by adding 50 µl 1 M HCl. To analyze the results, absorption was measured at 450 nm. Plasma from a PCR positive tested person was used as positive control. Values are given as concentrations in ng/ml, which were determined by a dilution series of highly pure human IgG (ThermoFisher) with known concentrations which was coated on the same plates.

2.5.2.2 SARS-CoV-2-RBD-IgA in-house ELISA

The IgA ELISA was performed as described in the method of the IgG in-house ELISA to detect the presence or absence of IgA antibodies against SARS-CoV-2. As secondary antibody, Goat-anti-human Serum IgA, HRP conjugated, was used in a concentration of 1:5000. Two determinations of the positive control were made on each plate.

2.5.3 Assay validation - precision tests

2.5.3.1 Intra- and inter-assay precision

To determine reproducibility of the designed ELISAs, intra- and inter-assay precision was assessed following the method described in the book `Immunoassays´ [38]. To measure the intra-assay precision seven serial 12-fold dilutions were made, to get a signal of saturation down to background-signal. The means, standard deviations and coefficients of variation were calculated. The inter- assay precision was made on three different days by the same operator. Exactly the same pipetting scheme was performed. The means, standard deviations and coefficients of variation were calculated and presented in a table and figure. The cut-off of coefficients of variation was set at 10% for the intra-assay and at 15% for the inter-assay for a good reproducibility [46]. Basic calculations and the figures were made with Microsoft Excel, version 16.42.

2.6 Measurement of the specimens

2.6.1 In-house ELISAs

The screening of the study samples was performed with the developed and optimized in-house IgA and IgG SARS-CoV-2 ELISA as described in 2.5.2, to examine the presence or absence of specific IgA and IgG antibodies. Samples were measured in duplicates and in dilutions of 1:100, 1:500 and 1:2,500. OD values were normalized to the positive control. The positive control was compared to a highly pure human IgG which was precoated as dilution series and whose exact IgG concentration was known. Thus, by relating all results of the samples to the positive control, we determined the exact concentration of specifically bound IgG in µg/ml. A sigmoidal standard curve of the dilution series (eight dilutions repeated three times) of the positive control was generated with four parameter logistic regression using the R package epiR Version 0.9-43. Samples with unknown concentration were interpolated to this standard. Subsequently, for each sample measured in duplicate, an average of the duplicates was calculated, provided that these OD values did not differ by more than 20%. The mean value of the duplicates was chosen as the final OD value. Now the mean value of the sample was normalized to the positive control, of which we know how many µg/ml IgG it contains. The IgG concentrations in the samples could be calculated through the ratio and the known concentration of the positive control.

The same procedure was done for the IgA ELISA. A sigmoidal standard curve was generated from the positive control of the IgA ELISA. Also, the mean values were determined from the OD values of the IgA ELISA and then normalized to the positive control.

2.6.2 Commercial ELISAs

To evaluate and compare the results of the in-house ELISAs, commercial tests were performed. The EUROIMMUN SARS-CoV-2 IgA, IgG and NCP-IgG ELISA (EUROIMMUN Medizinische Labordiagnostika AG, Lübeck) were done following the manufacturer´s instructions. The IgA and IgG assays are coated with recombinant S1 antigen of SARS-CoV-2. In the NCP-IgG ELISA, the plates are coated with the N protein as antigen. The OD was measured at 450 nm and a ratio was

calculated with a calibrator which was provided with the kit. The instructions specify a dilution of 1:101 of the samples.

In addition, we performed Mediagnost IgG and IgA immunoassays (Mediagnost®, Gesellschaft für Forschung und Herstellung von Diagnostika GmbH, Reutlingen) which uses RBD as antigen, the same antigen as the in-house ELISAs. The instructions of the manual indicate a sample dilution of 1:201. The cut-off values were calculated by multiplying the mean of the OD values of the negative controls three times and five times. The measured samples below the mean of the triple negative controls were negative. The sample values between the mean of the triple negative controls and the mean of the fivefold negative controls were borderline samples and the sample values above the mean of the fivefold negative controls were considered positive. The IgA ELISA from Mediagnost was not yet on the market at the time of the study and kindly provided as a test sample. An IgA ELISA from Beijing Wantai Biological Pharmacy Enterprise Co., Ltd. was used as well to compare the ELISAs and analyze the samples. In this assay, the OD values of the samples are divided by the mean value of the negative controls plus 0.3. The cut-off to positivity is 1.0. All tests described are semi-quantitative tests, which intended to detect positivity but reach saturation at high values.

2.7 Statistical analysis

2.7.1 Defining a cut-off value

The set threshold value depends on the purpose of a test. This value separates positive from negative samples. In general practice, tests can be optimized for specificity or sensitivity. Typically, an increase in one of the two parameters leads to a decrease in the other. Depending on the question, the focus is on sensitivity or specificity. For example, in a population where the infection rate is low, it is more important to have high sensitivity to detect the few who have developed antibodies. On the other hand, if the infection rate of SARS-COV-2 is very high, the test should have high specificity. In both cases, one must weigh whether false-positive or false-negative results are more acceptable. To determine a cut-off value, we used the receiver operating characteristic (ROC) curve generated with GraphPad Prism 8. For this purpose, the PCR-confirmed TüCoV samples (n

= 83) were used as positive samples and the CoVNeg study (n = 34) and the pre-pandemic samples (n = 32) were used as negative samples to generate the ROC curves.

2.7.2 Sensitivity and Specificity of the ELISAs

To determine the sensitivity and specificity of the ELISAs, pie charts of proportions of positive and negative measured samples were made with PCR positive individuals. We chose PCR results as reference to estimate the sensitivity of the ELISAs, as it has become the gold standard in the diagnostics of COVID-19. Samples from time D01 and D07 of the COMHIY and CoV HCQ studies were not selected because antibodies are not expected to be detected until day 10. Hence, these samples might decrease the sensitivity of the tests untruly. Results from CoVNeg and pre-pandemic samples were used to measure the specificity.

2.7.3 Comparison of the in-house ELISAs with commercial tests

In order to be able to evaluate the quality characteristics like sensitivity, specificity and separability and to figure out whether the in-house ELISAs could compete on these criterions with commercialized tests, a comparison between them was done. In addition, the study can provide information which antigen is best suited for the detection of past SARS-CoV-2 infection. Therefore, ROC curve analysis was created for all performed ELISAs and the AUC was used to compare the diagnostic quality, measured as the correct attribution to positive and negative samples. Furthermore, the sensitivity and specificity of all ELISAs were compared and illustrated with pie charts as described for the in-house ELISAs above. For the Mediagnost ELISAs a smaller sample size of negative controls was used, because less plates were available. Finally, Graph Pad Prism 8 was used to generate graphs showing each sample value, each compared from the in-house ELISA (in µg/ml) to a commercial test (OD values). For this comparison, all determined values of the study samples available were base-10 log-transformed. Before logarithmizing in order not to lose the values of “0” one was added to each sample before the logarithm was applied.

2.7.4 Analysis of the Case Report Form

The statistical analysis of the Case Report Form (CRF) was performed to find factors statistically associated with the antibody level. Moreover, the aim was to estimate which symptoms, besides a positive PCR test, indicate a COVID-19 infection. Hence, we investigated the data of the TüCoV population, as we systematically collected data on symptoms using a CRF for these participants. Participants without confirmed test in advance (contact persons of infected family members) who have been measured negative in all ELISAs, were not included in the calculations (n = 7). Therefore, in total 131 samples were included in the analysis. Descriptive statistics were used to describe the baseline characteristics of the cohort. Continuous variables were described with help of the mean of the variable and the range. IgG levels of classified groups (divided on the basis of categorical variables) are compared in terms of median and interquartile range, because data were not normally distributed, not even after transformation.

A linear regression was carried out for the continuous variables and the independent-sample t-test for the categorial variables. The dependent variable was the IgG antibody level, determined with the quantitative in-house ELISA. The antibody levels were not normally distributed. Therefore, they were base-10 log-transformed after 1 was added to not lose values of 0. Normal distribution was assessed by investigating kurtosis, skewness as well as the histogram. The unpaired t-test was used for the numeric variables with the logarithmized dependent variable. We evaluated the association of the IgG antibody level after infection of COVID-19 on demographic parameters. Analysis of variance (ANOVA) was used with fever and disorders of taste as independent variables and IgG antibody level values as the dependent variable. Before running the model data were inspected to support the following assumptions:

1. Normal distribution of the quantitative variable
2. Normal distribution of the residuals of the regression
3. Homoscedasticity by a scatterplot of the residuals
4. Multicollinearity
5. Homogeneity of variance by Levene´s test

Bivariate logistic regression analysis was performed to find a predictor for antibody positivity or negativity (dependent variable), besides the gold standard RT-PCR. Only the PCR positive samples (n = 85) were considered for the bivariate logistic regression, as I wanted to find an additional clinical predictor to the PCR test for seroconversion.

All statistical tests were two-tailed. The significance level was set at $p \leq 0.05$. The results are reported with 95% confidence intervals (95% CI). The analysis was carried out using SPSS (IBM 26 Corp, Armonk, NY). Basic calculations were made with Microsoft Excel, version 16.42.

3 Results

3.1 Plasmid

Expression of recombinant proteins for the development of diagnostics can be achieved by transfection of specific plasmids encoding a suitable expression cassette into specific cell lines (protein expressing cells). The result of the purification of the plasmid is shown here.

After transformation of the plasmid into competent *E. coli* (Top 10 or Stellar) (described in 2.2.1.1), single colonies were grown on the plates overnight. After purification, 100 µl of pCAGGS-CoV2-RBD plasmid diluted in sterile MilliQ water with a concentration of 147 µg/µl was received by transformation into the *E. coli* Stellar cells and a concentration of 81 µg/µl by transformation into *E. coli* Top 10 cells. Plasmids were diluted to a final concentration of 1 µg/µl.

3.1.1 Agarose gel electrophoresis

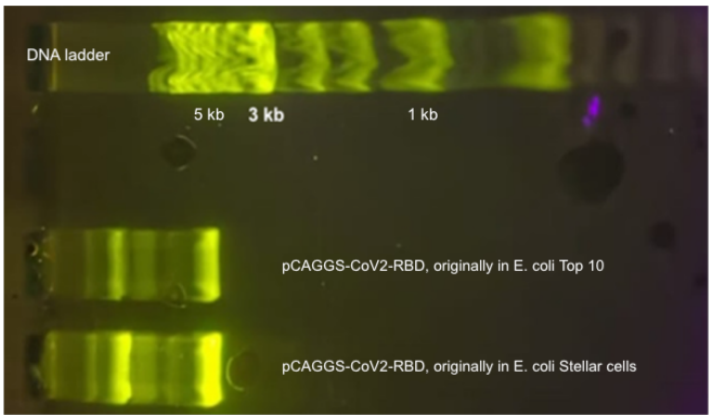

Figure 4: 1% Agarose gel, plasmids pCAGGS-CoV2-RBD (own production).

First band 1 kb DNA ladder, second band: pCAGGS-CoV2-RBD originally in E- coli Top 10 cells, third band: pCAGGS-CoV-2-RBD originally in E. coli Stellar cells

Figure 4 presents the Agarose gel run for the purified plasmids. The gel showed two distinct bands for each plasmid. The bands of the plasmids were at the same height. The plasmid was little contaminated, with hardly any remnants of genomic DNA detectable. We measure a size of approximately 5500 bp. The first band corresponded to the plasmid in form of a circular ring and the second band

corresponded to the supercoiled plasmid. The pCMV-Sport-CoV2-RBD plasmid was kindly provided by Andrea Weierich from our Institute.

3.2 Antigen production

3.2.1 Transfection of pCAGGs-CoV2-RBD and pCMV-Sport-CoV2-RBD plasmids

The transfection of the plasmids into HEK 293 F cells for the production of the RBD and the monitoring of the transfection-rate and viability of the cells was performed as described in 2.3.2. Two cultures per plasmid were transfected.

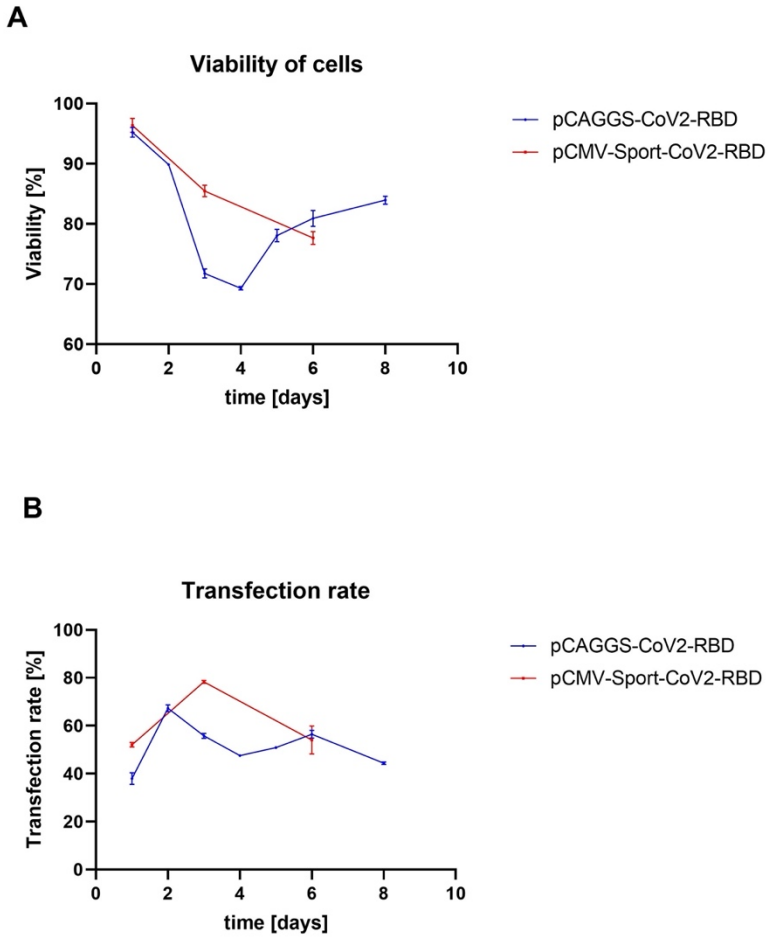

Figure 5: Transfection rate and viability of HEK 293 F cells

Means of two cultures are dotted with error bars showing the range. Blue: values of cells transfected with pCAGGS-CoV2-RBD plasmid. Red: values of cells transfected with pCMV-Sport-CoV2-RBD plasmid.

The transfection of the pCAGGS-CoV2-RBD and the pCMV-Sport-CoV2-RBD

plasmids into HEK 293 F cells was successful. The transfection of the pCMV-Sport-CoV2-RBD plasmid was slightly more efficient compared to the transfection of the plasmid with the pCAGGS vector. The transfection rate of the pCMV-Sport-CoV2-RBD plasmid started at a higher level (51 and 53%). Also, on the days of harvest, day three and six, the transfection-rate of the pCMV-Sport-CoV2-RBD plasmid was higher. In terms of viability, the pCMV-Sport-CoV2-RBD plasmid achieved higher values as well, except on day six of transfection (see figure 5.B).

3.2.2 Purification of the protein

3.2.2.1 His-Tag and Strep-Tag purification

The protein was purified using His-Tag purification for both proteins. Strep-Tag purification was additionally performed for the RBD produced with the pCMV-Sport-CoV2-RBD plasmid. The proteins were purified as described in 2.3.5.

A B

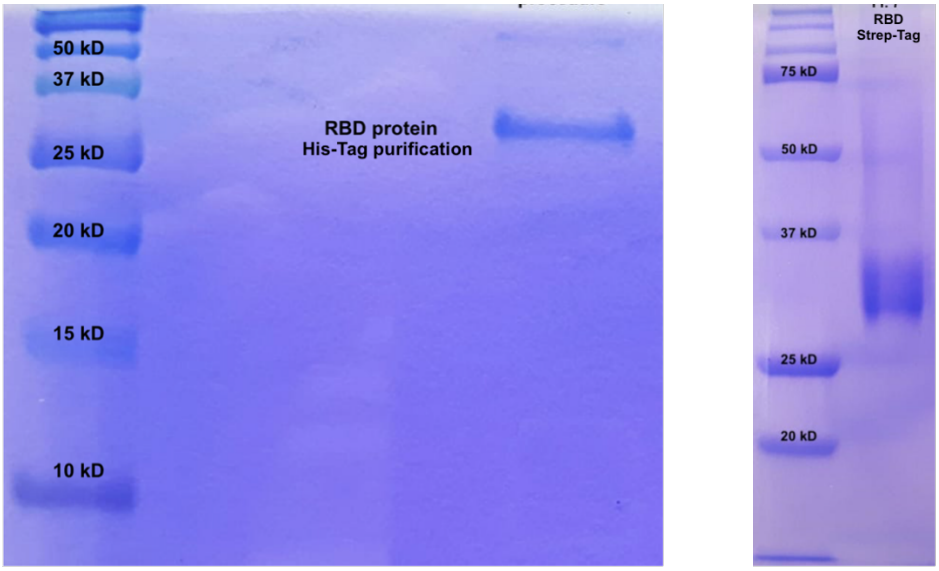

Figure 6: SDS-page of purified RBD protein.

A. Gel of 15% acrylamide.; results of His-Tag purification. B. Gel of 10% acrylamide; results of second purification with Strep-Tag. Marker: Precision Plus Unstained Standards (Bio-Rad).

After the first purification, one band between 25 and 37 kDa appeared. Minor contaminations could be observed (light band above the RBD protein) (figure 6.A). After the second purification there was a wide band between 25 and 37 kDa to be seen, as well as some smaller contaminations (see figure 6.B). The size of the analyzed RBD proteins was larger than 25 kDa. A theoretical molecular

weight of 25.9 kDa was described by BEI resources for the RBD, where we expect this recognizable increase in size due to numerous glycosylations of the protein. Apart from that, the band in the gel was difficult to evaluate because it ran smeared due to too high concentration of protein.

3.3 SARS-CoV-2 ELISA development

In the following sections, results are shown that led to the standardization of the IgG in-house ELISA protocol. Different experiments were conducted in order to find the optimal blocking buffer, coating buffer, sample diluent and antibody diluent. Positive controls chosen were primarily a sample from an employee previously PCR-confirmed to have COVID-19. Other samples from PCR confirmed COVID-19 cases were also chosen. Samples that previously measured positive in the IgG ELISA were used to generate the IgA ELISA.

Pre-pandemic samples were used as negative controls. CoVNeg samples that previously measured negative in the IgG ELISA were also used to develop the IgA ELISA.

3.3.1 IgG assay optimization

3.3.1.1 Optimization of blocking

To figure out a blocking solution, which makes it possible to distinguish positive from negative samples and which results in low background-reactivity, two experiments were performed. The ELISA was performed as described in 2.5.2, modifications are noted.

In the first experiment seven different blocking solutions were tested. Casein 1% (Thermo Scientific), powdered milk (ROTH) 5% (w/v) in PBS-T, Pierce™ Protein-Free (PBS) Blocking Buffer (Thermo Scientific), Roti®-Block 10x (ROTH) and 1x, Gelatin from cold water fish skin (SIGMA) in PBS supplemented with 0.1% Tween-20 and BSA: Albumin bovine fraction 5% (SERVA), supplemented with 0.1% Tween-20 as well. The 96 well high-binding plate was coated with antigen 0.5 µg/ml in PBS. The samples were diluted in respective blocking buffer in a dilution of 1:200. The secondary antibody was also diluted in the respective blocking buffers.

In the second experiment another four blocking solutions were tested. The Blocking Solution, Plate Block™ and Smart Block™ by Candor and milk powder, Blotting-Grade-Blocker (BIO-Rad) 5% (w/v) in PBS-T. LowCross Buffer (Candor) was used as sample diluent (1:100) and secondary antibody diluent.

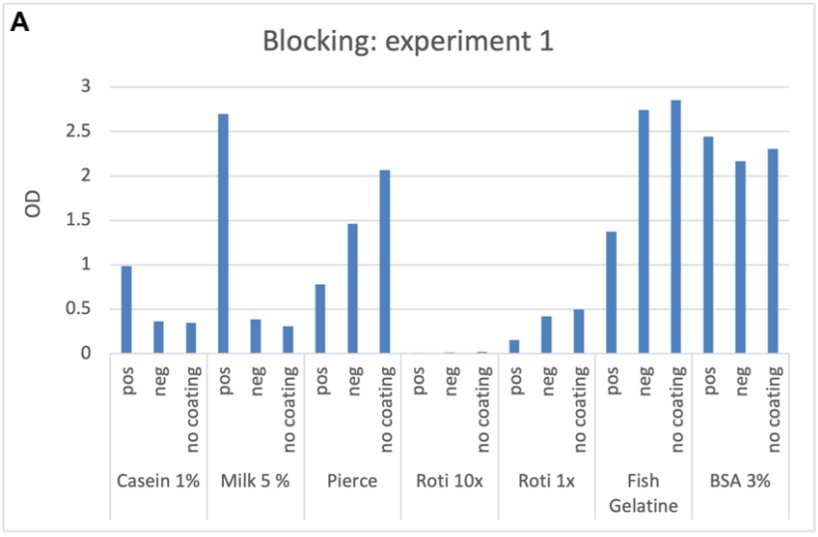

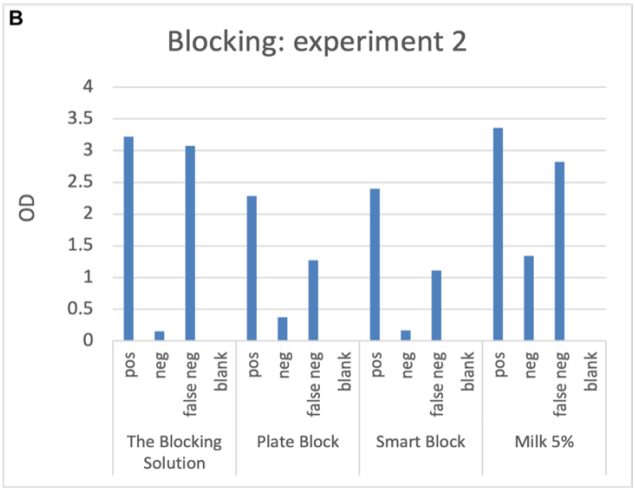

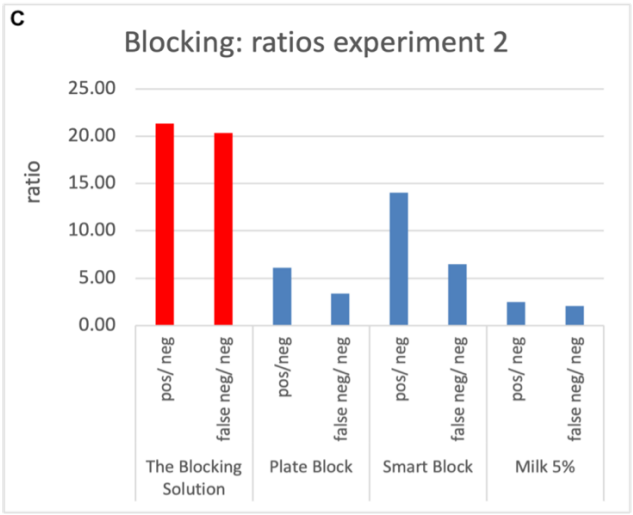

Figure 7: Testing of blocking buffers for SARS-CoV-2 IgG ELISA.

A. ODs of the first experiment. One positive sample (pos) and a negative sample (neg) were tested with each blocking buffer. One negative sample was applied as control on a row which was not coated in advance (blank). B. ODs of the second experiment. Three samples were applied on each blocking. A positive (pos), a negative (neg) and a positive sample which falsely appeared with low OD values in previous experiments (false neg). C. Ratio of positive sample to negative control and false negative sample to negative control is shown. Best ratios are marked red.

The highest absorption values were seen for The Blocking Solution, Milk 5% and fish gelatin for positive control but also for negative controls (figure 7.A, B). The best ratio of positive to negative sample showed The Blocking Solution (figure 7.C). Even the positive sample, which wrongly appeared with low OD values in former experiments (false negative sample), came out with a high OD of approximately three under these conditions. In addition, the negative control was very low in absorption (OD_{450} of < 0.25). The background signal at the uncoated plate was low for The Blocking Solution, Smart Block, Plate Block, Milk 5% and Roti Block but very high for fish gelatin and BSA 3% (figure 7.A, B). All in all, blocking with The Blocking Solution allowed specific antibody binding and blocked negative controls as desired. Therefore, The Blocking Solution was applied for further ELISAs.

3.3.1.2 Optimization of coating buffer

The next experiment aimed to determine a coating buffer. Candor coating buffer and PBS were compared. The ELISA was performed as described in 2.5.2. There was no distinct difference in the OD_{450} to be seen (data not shown). Hence, we chose PBS as coating buffer to reduce costs.

3.3.1.3 Optimization of sample diluent

The objective of this experiment was to figure out an optimal sample diluent, which minimized background-reactivity and unspecific antibody binding. Three buffers were compared, PBS, LowCross Buffer and The Blocking Solution (Candor). The secondary antibody was diluted in LowCross Buffer. Other steps were performed as described in 2.5.2.

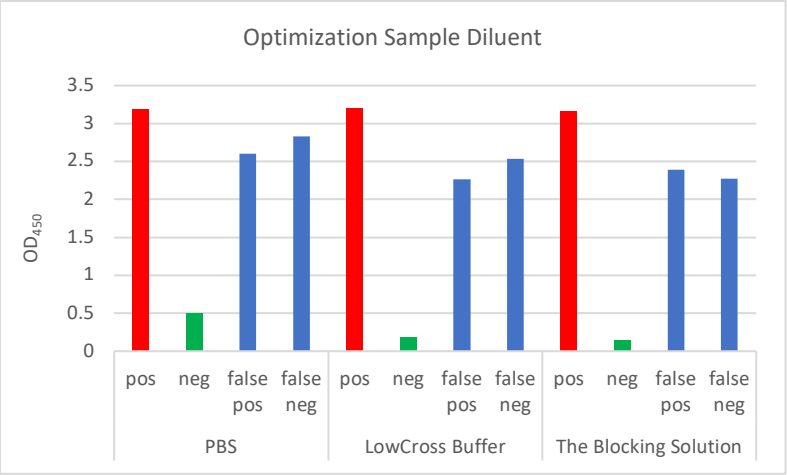

Figure 8: Testing of sample diluents for SARS-CoV-2 IgG ELISA.

Absorption at OD_{450} was measured for three different diluents. Positive control (red) and negative control (green) were applied as well as a sample which wrongly appeared negative and positive in previous assays (blue). Measurements were performed in serial dilutions. Dilution of 1:100 is pictured.

In all diluents, the positive control had a distinct signal. For PBS as diluent, the negative control reacted stronger than in LowCross Buffer and The Blocking Solution. The false positive sample had a strong signal for all buffers, due to unspecific binding (see figure 8). Though, none of the diluents could block the falsely positive sample and no distinct differences between the diluents were seen. The Blocking Solution was selected as sample diluent, because it was less expensive than LowCross Buffer.

3.3.1.4 Elimination of unspecific antibody binding.

The objective of this experiment was to eliminate the false positive signal, which still remained strong in the last experiment by testing six secondary antibody diluents. Smart Block (Candor) was used as blocking buffer as well as sample diluent. Further steps were performed as described in 2.5.2. As secondary antibody diluent LowCross Buffer, PBS 1x, Smart Block, Roti Block 1x and 10x and conjugate from the EUROIMMUN IgG Anti-SARS-CoV-2 ELISA kit were used.

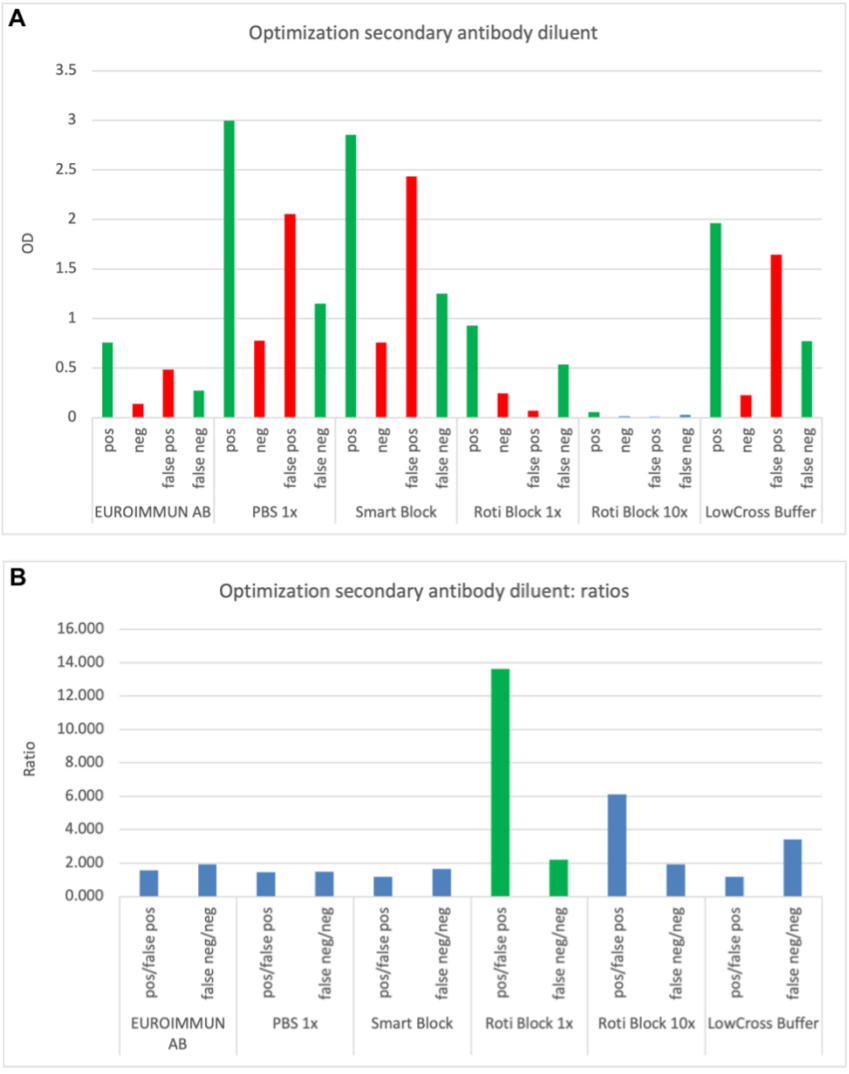

Figure 9: Optimization of secondary antibody diluent for IgG ELISA.

A. OD_{450} of positive (green) and negative (red) plasma samples in six different secondary antibody diluents. B. Ratio of positive to false positive samples and of false negative to negative samples. Diluent with highest ratio is marked green.

Solely Roti Block 1x blocked the unspecific antibody capture of the false positive sample and thereby showed the best ratio of positive control to the false positive sample. The ratio of the false negative sample to the negative control was the highest by using LowCross buffer, followed by Roti Block 1x (figure 9.B). Roti Block 10x as blocking solution for secondary antibodies came out with very low signal in all samples (figure 9.A). For the other diluents the positive samples appeared with a distinct signal, but the falsely positive samples came out with high signal as well (figure 9.A). Therefore, Roti Block 1x was used as secondary antibody diluent, since it showed the best results for eliminating unspecific binding, while remaining a strong signal of positive controls. Finding Roti Block 1x as the right antibody diluent was the key factor in improving specificity in the in-house ELISA.

3.3.2 IgA assay optimization

We started the development of the in-house SARS-CoV-2 IgA ELISA with the recipe of the in-house SARS-CoV-2 IgG ELISA and checked, whether other buffers or concentrations were more suitable. In the following section, results are shown that led to the standardization of the IgA in-house ELISA.

3.3.2.1 Optimizing secondary antibody dilution

To find the appropriate dilution of the secondary antibody for the IgA assay, four dilutions were compared. The IgA assay was performed as described in 2.5.2 on one single plate with secondary antibody dilutions of 1:5,000, 1:10,000, 1:15,000 and 1:20,000 diluted in Roti Block 1x.

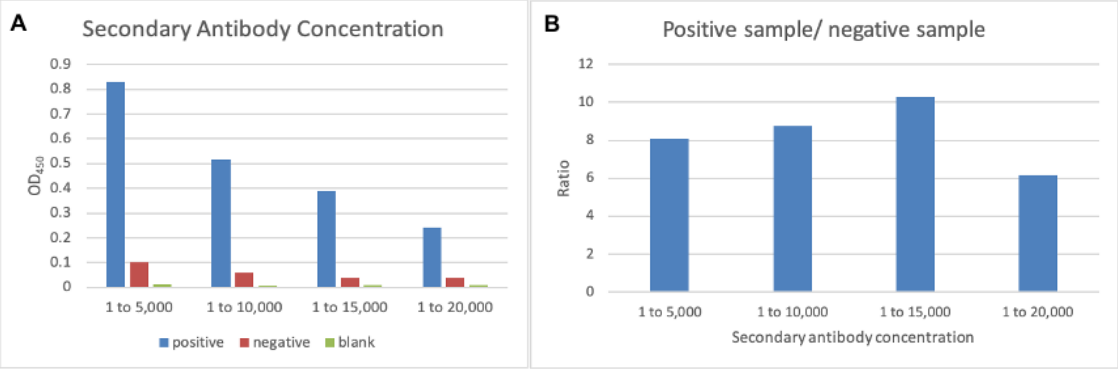

Figure 10: Optimization of secondary antibody concentration for IgA ELISA.

A. OD_{450} of positive and negative control and of a blank. Four secondary antibody dilutions are compared. B. Ratio of positive to negative sample under condition of these dilutions.

The results illustrate an increased signal in the positive samples, when the concentration of the secondary antibody is high. Likewise, the signal of the negative control became stronger, the higher the concentration of antibodies (figure 10.A). The most distinct signal of positive control was measured in dilutions of 1:5,000 and 1:10,000. (figure 10.A). The ratio of positive to negative sample is the highest at an antibody dilution of 1:15,000 (figure 10.B). On the other hand, the signal of the positive control became quite low in concentrations lower than 1:10,000 (figure 10.A). Therefore, secondary antibody dilution of 1:5,000 was selected for the ELISA protocol to achieve a good signal strength, even if the ratio was minimally worse compared to the dilution of 1:10,000.

3.3.2.2 Comparison of blocking buffers

To figure out, whether another blocking buffer works better for the IgA than The Blocking Solution, which was optimal for the IgG ELISA, 12 different blocking buffers were compared. Besides The Blocking Solution (Candor), Smart Block, Plate Block (Candor), Blocker™ Casein in PBS (Thermo Scientific), Pierce™ Protein-Free (PBS) (Thermo Scientific), BSA: Albumin bovine fraction 5% (SERVA), BSA 5% with EDTA 2 mM, Nonfat dry milk 3% and 5% (w/v) (Bio-Rad) and Roti Block 0.5x, 1x and 2x (ROTH) were applied and incubated for 2 h.

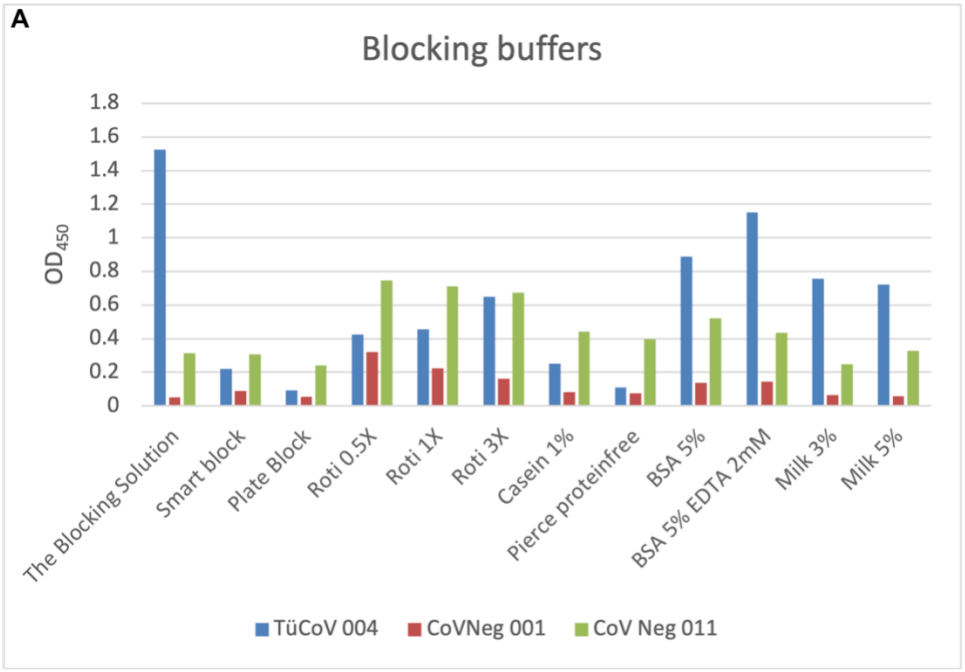

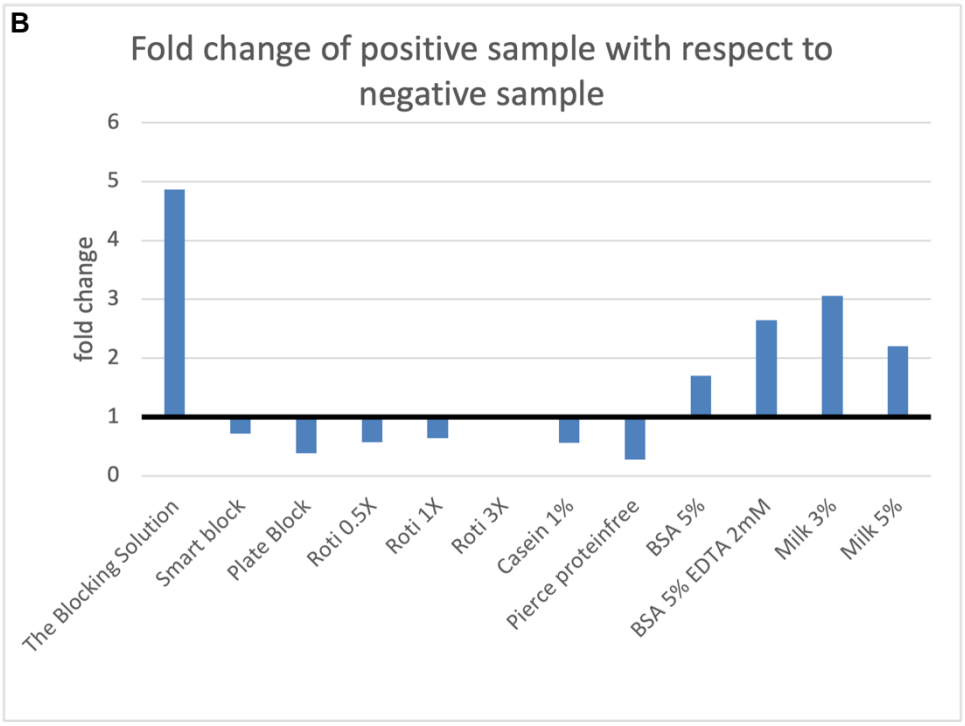

Figure 11: Comparison of blocking buffers for SARS-CoV-2 IgA ELISA.

A. The positive sample (TüCoV 004), a negative sample (CoVNeg 001) and a negative sample with remarkably high OD values (CoVNeg 011) plotted for all blocking scenarios. B. Blocking buffers are compared with the fold change of positive control (TüCoV 004) with respect to negative sample (CoVNeg 011).

The strongest signal for the positive control was seen with The Blocking Solution, whereas the reactions of the false positive sample under conditions of Plate Block and Milk 3% were comparably low, followed by The Blocking Solution and Smart

Block (see figure 11.A). Certainly, the signal of positive control was decreased in blocking scenarios with Smart Block, Plate Block, Milk 3%, Roti Block, Casein and Pierce protein-free (figure 11.A). Regarding the fold change, these blocking solutions did not differ between positive and negative samples. The comparison of the different blocking solutions showed with The Blocking solution the highest fold change of positive and negative controls (figure 11.B). Therefore, it was included in the standard protocol for the IgA ELISA as it was already used for the IgG assay.

3.3.2.3 Comparison of secondary antibody diluents

As individual negative samples continued to appear with high signal, seven different secondary antibody diluents were tried out to block unspecific antibody binding. The assay was performed as described in 2.5.2, modifications are mentioned. As diluents Roti Block 1x and 3x (ROTH), LowCross Buffer, LowCross Buffer mild, LowCross Buffer strong, LowCross Buffer HRP stab and The Blocking Solution (all by Candor) were applied.

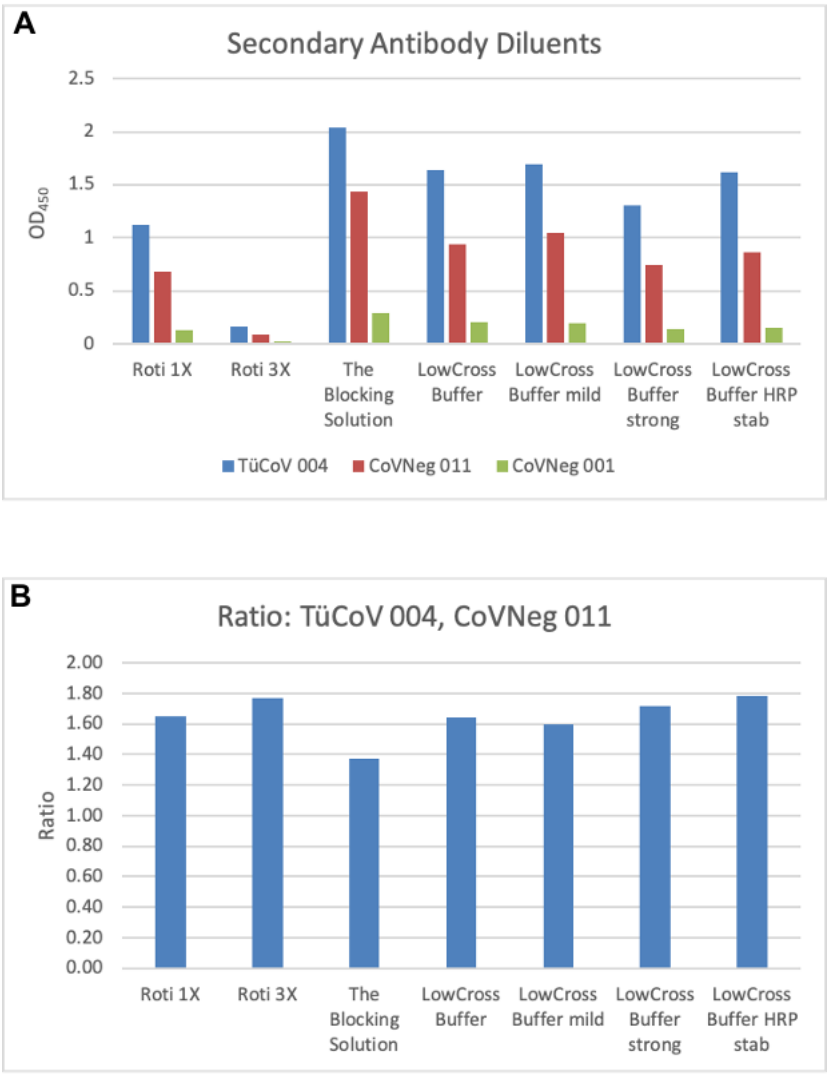

Figure 12: Comparison of secondary antibody diluents for SARS-CoV-2 IgA ELISA.

A. OD values of a positive, a negative and a negative sample which reacted strongly in previous assays, under condition of seven different antibody diluents. B. Ratio of a positive sample (TüCoV 004) to the negative one with high OD values (CoVNeg 011) for the different diluents.

The Blocking Solution showed the highest signal strength for all samples (figure 12.A). Roti Block 3x resulted in very low signal intensity. Certainly, for the ratio, lowest values were seen, when The Blocking Solution was used as diluent. A high ratio stands for a good distinction between positive and negative samples. There is no big difference in ratios between the other buffers used (figure 12.B). Still, the background signal of CoVNeg 011 appeared to be high in all scenarios compared to CoVNeg 001. Roti Block 1x was confirmed as good antibody diluent and chosen for further performances, due to lower costs compared to diluents

from Candor.

3.3.2.4 Determining the impact of temperature to the signal strength

We observed variations in signal due to the hot summer months, hence, incubation temperatures were compared. Two plates were prepared and treated strictly the same way by a single operator, as described in 2.5.2. But one plate was incubated at room temperature (22°C) the second plate was incubated at 37°C for all incubation steps.

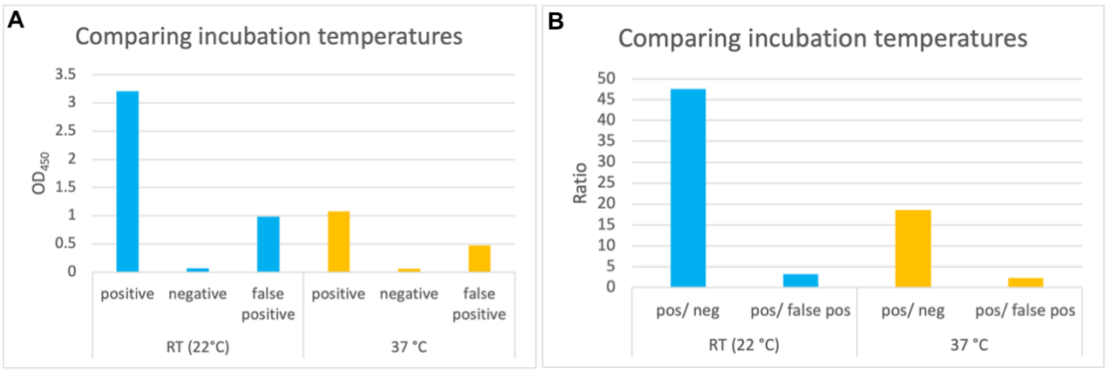

Figure 13: Impact of hot temperature to the signal strength of SARS-CoV-2 IgA ELISA.

A. The OD_{450} values of positive and negative control and of a negative sample with high OD values (CoVNeg 011), under condition of 22°C incubation temperature (blue) and 37° C incubation temperature (orange) respectively. B. Ratio of positive to negative control; ratio of the positive sample to sample with falsely high signal.

Figure 13.A. shows that the OD values were significantly higher at RT. More than three times for the positive sample and twice as high for the CoVNeg 011 value. The negative control on the other hand remained low under both conditions, which had a positive effect on the ratio of positive to negative sample at RT (figure 13.B). Compared to 37°C, incubation at 22°C delivers a better signal strength for positive samples. A distinct impact on the ratio of CoVNeg 011 to the positive control couldn't be measured. Hence, we carried out further assays in an air-conditioned room with controlled temperature conditions of approximately 22°C.

3.4 Evaluation and Validation

3.4.1 Intra-assay precision in-house SARS-CoV-2 IgG ELISA

To figure out the precision and stability of the in-house IgG ELISA, 12-fold determinations were made on one plate, beginning in saturated signal and ending in

background signal. The ELISA was performed as described in 2.5.2.

Figure 14: Intra-assay precision profile in-house SARS-CoV-2 IgG ELISA.

A. single measurements of 12 repeat determinations of TP 04. The dilution series started at a dilution of 1:50 and was continued in 1:3 dilution steps. B. coefficients of variation for each dilution. The red line marks the precision cut-off value of 10%.

We observed the signal was in saturation at a dilution of 1:50 and fell to background noise at the last dilution of 1:36,450 (see figure 14.A). The figures present a high intra-assay precision with an average coefficient of variation (CV) of 4% and below 10% (threshold for high precision assays) for all applied dilutions. Thus, study samples can be diluted up to 1 to_36,450 without problems for sample replicates.

3.4.2 Inter-assay precision in-house SARS-CoV-2 IgG ELISA

To determine the inter-assay precision of the in-house SARS-CoV-2 IgG ELISA, the same operator repeated the same ELISA on different days.

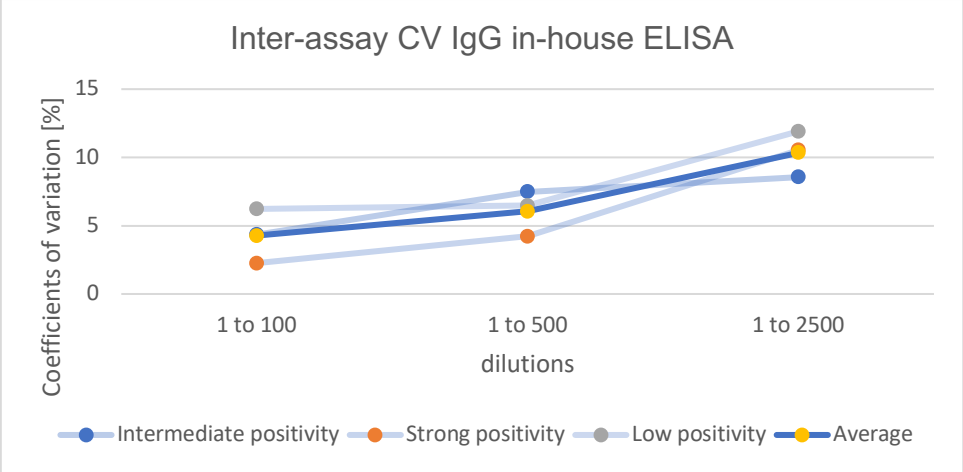

Figure 15: Inter-assay coefficients of variation of the SARS-CoV-2 IgG ELISA.

Average of variation coefficient of each sample is plotted as well as an average of variation coefficients for all concentrations respectively (dark blue line with yellow dots). A strongly reacting sample, a medium reacting sample and a low reacting sample were applied onto the plate. Each sample was measured in a dilution of 1:100, 1:500 and 1:2,500.

Regarding the sample concentration of 1:100 and 1:500, the sample with the strongest signal had the lowest CV (figure 15). Thus, it was the most precise, regarding the OD values with those concentrations. Overall, the results showed that more precise values were obtained with higher concentrations. The CV only differed slightly with repeated measurements on different days. The average of the CV of different days showed, the lower the concentration of the sample, the more the measurements vary. The slightly reacting sample almost reached a CV of 12% at a dilution of 1:2,500. The mean value of the CV in the strongest dilution (1:2,500) was 10.3% (see figure 15). The average CV of the inter-assay precision in the IgG in-house ELISA is 6.9%.

3.4.3 Intra-assay precision in-house SARS-CoV-2 IgA ELISA

To determine the stability in the assay, the sample COM 03 D01 as positive control was applied to a plate 12 times in serial dilutions, starting at signal saturation, 1:100, and going on in dilution-steps of 1:3, ending in background-signal. Further

procedure is described in 3.4.1.

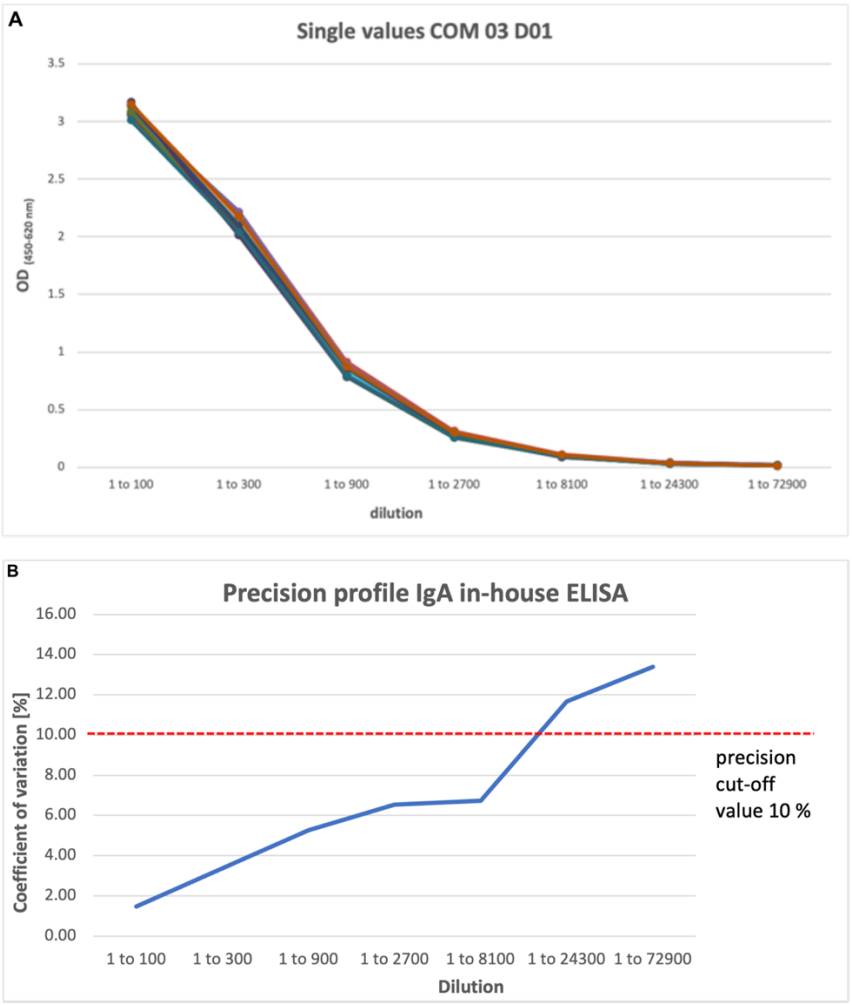

Figure 16: Intra-assay precision profile SARS-CoV-2 IgA ELISA.

A. Single measurements of 12 repeat determinations of COM 03 D01 on one plate. B. Coefficient of variation for each dilution. A line marks the precision cut-off value of 10%.

Individual measurements of the positive control varied only minimally (see figure 16.A). The results provided a CV lower than 10% up to a dilution of approximately 1:20,000 where we set the threshold for high precision (precision cut-off) (figure 16.B). The average CV of the intra-assay precision is 6.9%

3.4.4 Inter-assay precision in-house SARS-CoV-2 IgA ELISA

We aimed to figure out the inter-assay precision of the in-house SARS-CoV-2 IgA ELISA to check the internal consistency of the assay, by repeating exactly the

same ELISA on different days by the same operator. The signal strength of the samples was assessed within these samples and cannot be generalized. This means that the "very strong positive sample" only counts as very strong in comparison to the other samples used for the test, but does not generally represent the highest level of IgA antibody. Each sample was measured in triplicate and in a dilution of 1:100, 1:500 and 1:2,500.

The CV of the OD values varied within the samples between 5.6% of the sample with strong positivity, to 25.2% of the sample with intermediate positivity in dilutions of 1:100 (figure 17).

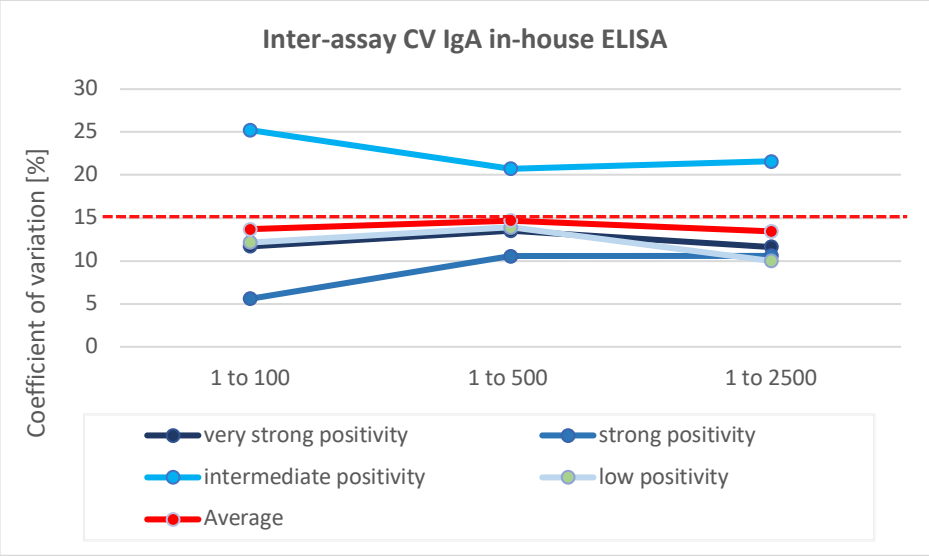

Figure 17: Inter-assay coefficients of variation of OD values in SARS-CoV-2 IgA ELISA.

The CV of four samples with different signal strength is plotted in the graph for three different dilutions, as well as the mean value (red) of these coefficients of variation. The dotted red line marks the precision cut-off value of 15%.

The CV is between 5 and 15%, except for the sample with intermediate positivity, which shows a coefficient up to 25% (figure 17). The average of CV is 13.9%.

3.5 Measurement of the specimens with the in-house ELISAs

To examine the presence or absence of specific IgA and IgG antibodies in the study samples, the screening was performed with the developed and optimized in-house IgA and IgG SARS-CoV-2 ELISA, as described in 2.5.2, to examine the

presence or absence of specific IgA and IgG antibodies. The following figures present the results of screening to get an overview of the antibody levels in the studies.

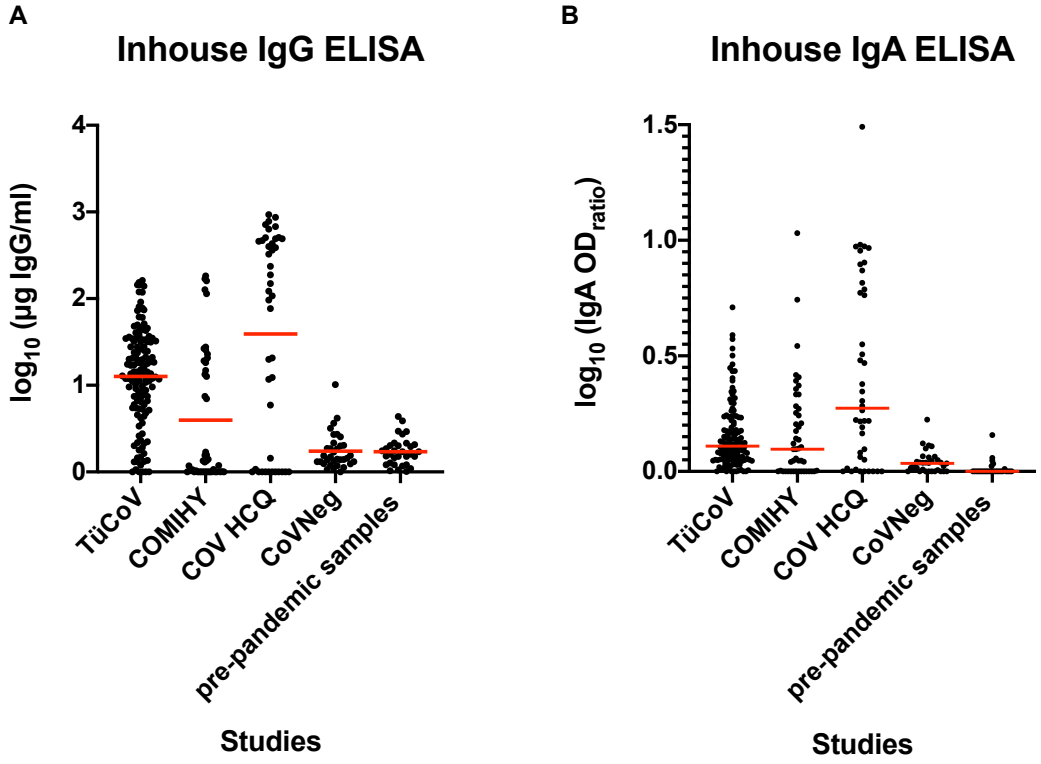

Figure 18: Results of study screening with the IgG and IgA SARS-CoV-2 ELISAs.

The OD values were set in ratio to the positive controls. The unit for the IgG values is in µg IgG/ml. For IgA and IgG the results were logarithmized in order to be able to display the results more accurately. The red line marks the mean of the results for every study.

The graphs above show that the highest single values and the highest means in both classes of antibodies were reached in the CoV HCQ study with hospitalized COVID-19 patients. The COMIHY samples containing outpatients were widely distributed on the y-axis and the mean value was the lowest compared to the other SARS-CoV-2 positive samples, especially in the IgG antibody class. In contrast, the antibody levels from the TüCoV study cohort are less variant. The CoVNeg and pre-pandemic samples were on a low level. The mean of pre-pandemic samples was slightly lower than the mean of the CoVNeg study.

3.6 Statistical analysis of data

3.6.1 Evaluation of the screening

3.6.1.1 Determining the threshold values and the diagnostic quality

We used the ROC- curve as a tool to choose the optimal threshold, to describe assay performance and to determine sensitivity and specificity of the assays. The PCR-confirmed TüCoV samples (n = 83) were used as positive samples and the CoVNeg study (n = 34) and the pre-pandemic samples (n = 32) were used as negative samples to generate the ROC curves. Figure 19 provides the ROC curves and the area under the ROC curve (AUC ROC) for the in-house IgG and IgA ELISA, respectively.

A

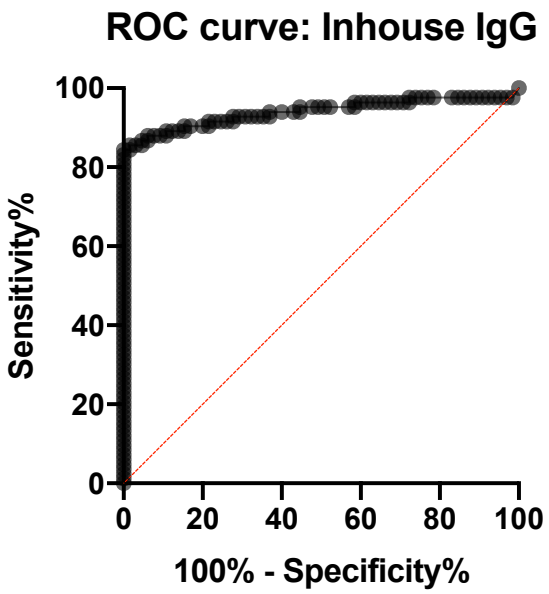

AUC: 0.941

95% CI: 0.899 to 0.983

P value: <0.0001

B

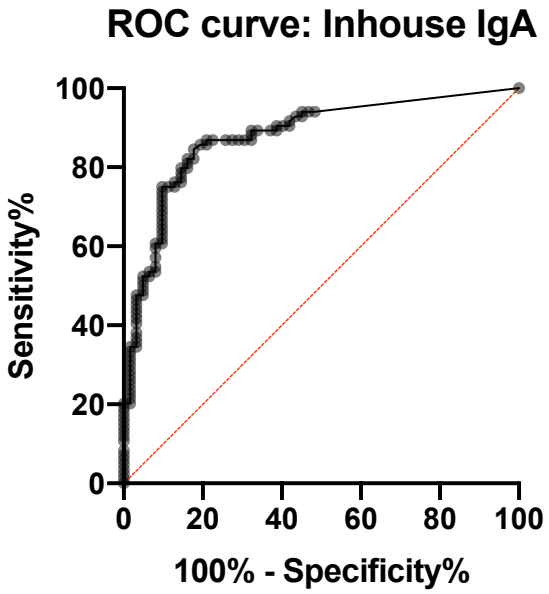

AUC: 0.879

95% CI: 0.8225 to 0.9364

P value: <0.0001

Figure 19: ROC curves of in-house SARS-CoV-2 IgG (A) and IgA (B) ELISA.

Curves were generated with 66 negative and 83 PCR-confirmed positive samples from the TüCoV cohort. The AUC was determined, including a confidence interval (CI) of 95%. The red diagonal line marks the level, where the true positive rate is equal to the false positive rate.

With the help of the ROC curve the cut-off of the IgG ELISA was set to 3.5 µg/ml. This resulted in a sensitivity of 84.3% with a 95% CI of 75.0 – 90.6% and a specificity of 100% with a 95% CI of 94.5 – 100%.

For the IgA ELISA a cut-off at 0.326 OD was chosen. Thus, we reached a sensitivity of 47.6% with a 95% CI of 37.3 – 58.2% and a specificity of 96.8% with a 95% CI of 89.0 – 99.4%.

For further assessment of the developed ELISAs, we took a look at the AUC ROC. With the AUC ROC, the degree of separability of positive and negative samples, and thereby the diagnostic quality, can be measured.
The IgG ELISA reached an AUC of 0.941 with a CI 95% of 0.899 to 0.983 and a P value of <0.0001. The developed IgA ELISA showed a slightly lower AUC of 0.879 with a CI 95% of 0.823 to 0.936 and a P value of <0.0001 (figures 19.A, B).

3.6.1.2 ELISA negative samples in the study cohorts

With the determined threshold it is apparent that many samples which were RT-PCR confirmed positive, came out as negative in the ELISA. According to the in-house IgG ELISA, 56.3% of the COMIHY participants (n = 9), 33.3% of the CoV HCQ participants (n = 6) and 16.7% of the RT-PCR positive TüCoV samples (n = 14) had no seroconversion at any timepoint. In total 24.6% of the RT-PCR positive tested individuals (n = 29) were measured negative in the in-house ELISA.

3.6.2 Sensitivity and specificity

The following paragraph presents the pie charts, to get a more distinct survey of the sensitivities and specificities of the ELISAs. Charts were created like described in 2.7.2.

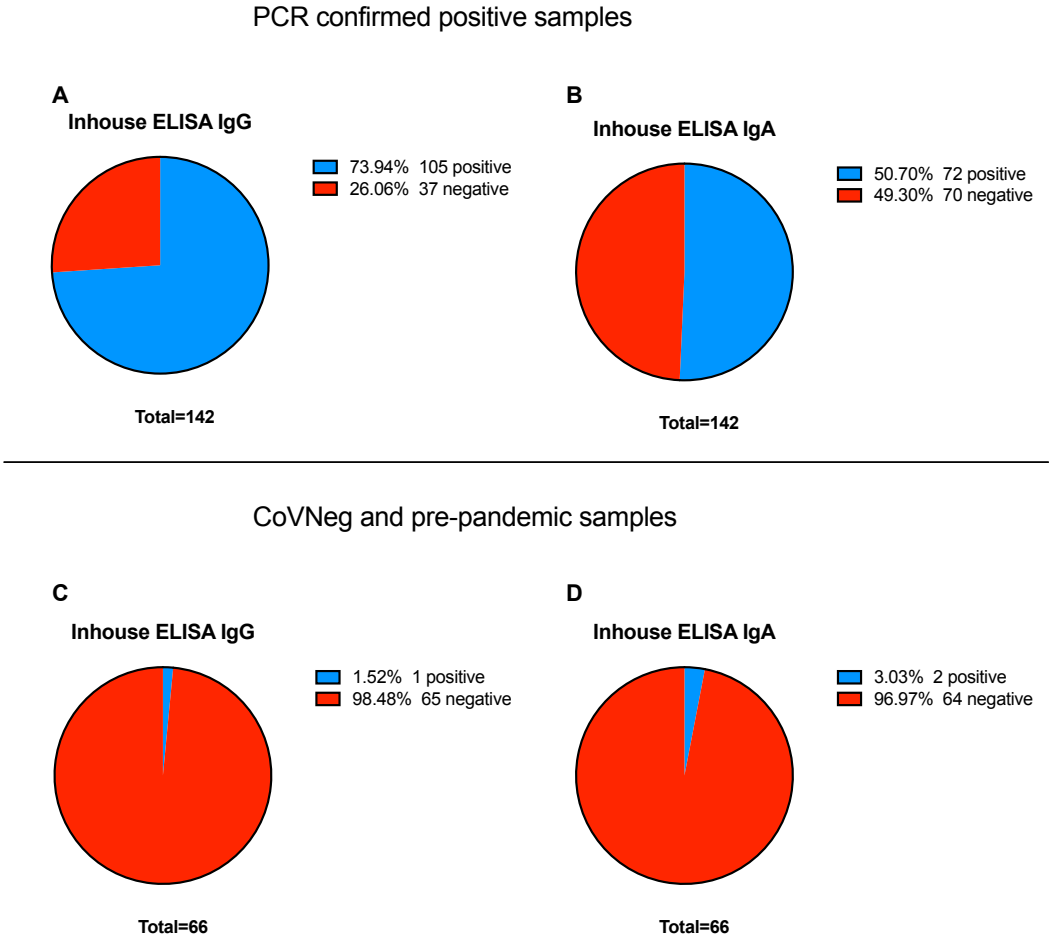

Figure 20: Sensitivity and Specificity of in-house IgG and IgA ELISA.

Figures A and B provide the sensitivity (blue) of the developed IgG and IgA ELISA with PCR-confirmed positive samples as a reference. Figure C and D refer to the specificity (red) of the IgG and IgA ELIASs with CoVNeg study samples and pre-pandemic samples as reference.

142 samples from SARS-CoV-2 PCR positive confirmed subjects out of all cohorts were measured with the IgG and IgA in-house ELISA. The top half of the figure shows the sensitivities of the developed tests. The IgG ELISA possessed a sensitivity of 73.94% when measuring all cohorts. According to this, it detected 105 samples as positives with the selected cut-off, while 37 samples did not show detectable antibody levels (figure 20.A). The IgA ELISA had a lower sensitivity of 50.7% and 72 positive measured samples out of 142 PCR-positive samples (figure 20.B). Figure 20 C and D present the specificities of the tests. The specificity of the IgG ELISA was 98.48% with one sample measuring positive out of 66 negative samples in total. In the IgA ELISA one sample was measured positive.

3.6.3 Comparison with commercial tests

To get a better picture of the functionality and to find out how the selected RBD antigen performed compared to other antigens used in commercialized ELISAs, we set the results of the developed tests in relation to other ELISAs as described in 2.7.3. In the following paragraphs, individual samples, as well as AUC, sensitivities and specificities are compared.

3.6.3.1 Comparing separability

For further assessment of the developed ELISAs, the ROC curve analysis were applied to the commercial ELISAs in a similar way. The results are presented in the following figures.

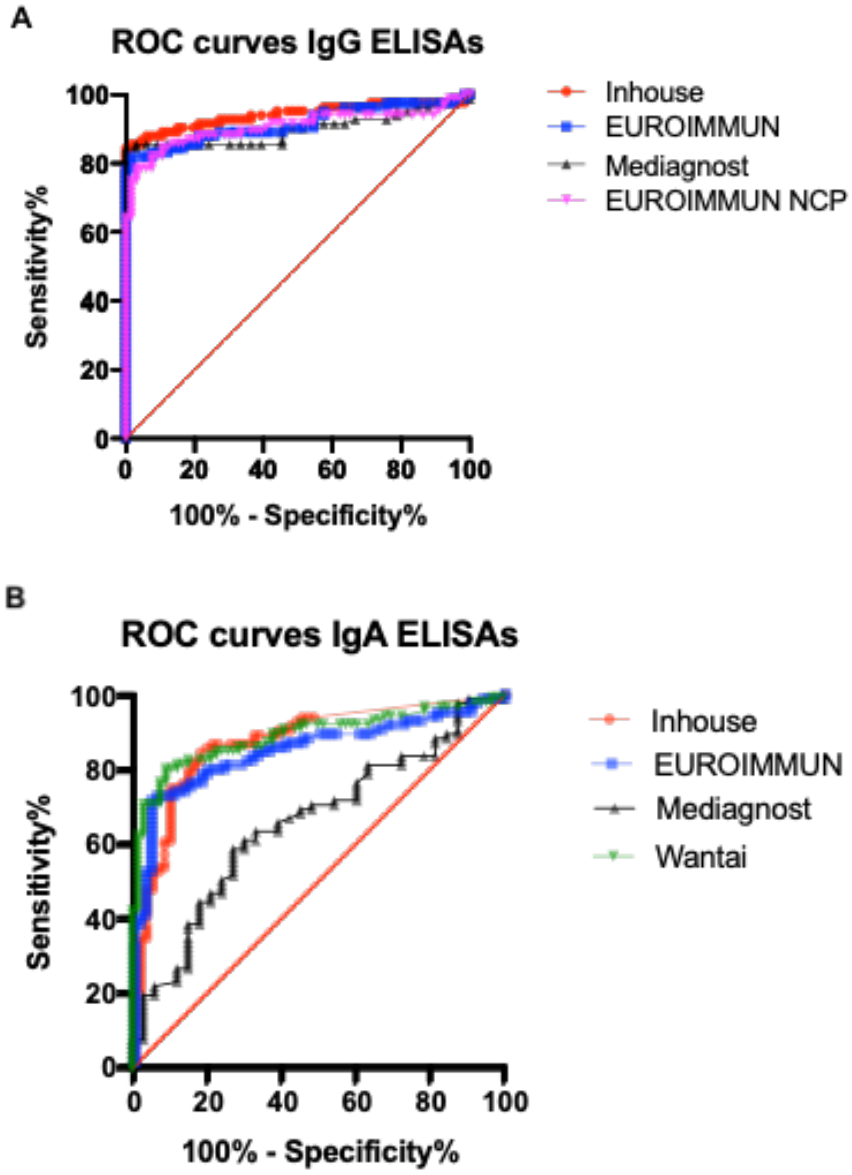

Figure 21: ROC curves of the in-house and commercial IgG and IgA ELISAs.

Curves were generated with 66 negative samples for the in-house and EUROIMMUN ELISAs and 34 negative samples measured with Mediagnost ELISA, as well as 83 PCR-confirmed positive samples from the TüCoV study. The AUC was measured for each test, including a 95% CI. The diagonal line marks the level, where the true positive rate is equal to the false positive rate.

Regarding the IgG ELISAs, the figure 21 A shows that the largest AUC with a value of 0.941 and the highest ROC curve was reached by the in-house IgG ELISA. It was followed by the EUROIMMUN IgG ELISA with an AUC of 0.915 and the NCP ELISA from EUROIMMUN with an AUC of 0.904, followed by an AUC of 0.901 from the Mediagnost test. Finally, all IgG ELISAs showed a high

degree of separability of negative to positive samples with decent differences. The largest AUC of the IgA ELISAs instead, refers to the Wantai IgA ELISA with a value of 0.895, directly followed by the in-house IgA ELISA with a size of 0.879 and the EUROIMMUN IgA ELISA with 0.853. Certainly, the ELISA from Mediagnost came out with a smaller AUC of 0.651. Indeed, all ELISAs showed a p value <0.05. In generally, the IgA assays came out with a smaller AUC as the IgG ELISAs (figure 21.B).

3.6.3.2 Sensitivity and specificity in comparison

To assess the determined sensitivity and specificity of the developed ELISAs, pie charts were made with the same samples as described in 2.7.2, which we used for comparison in the following.

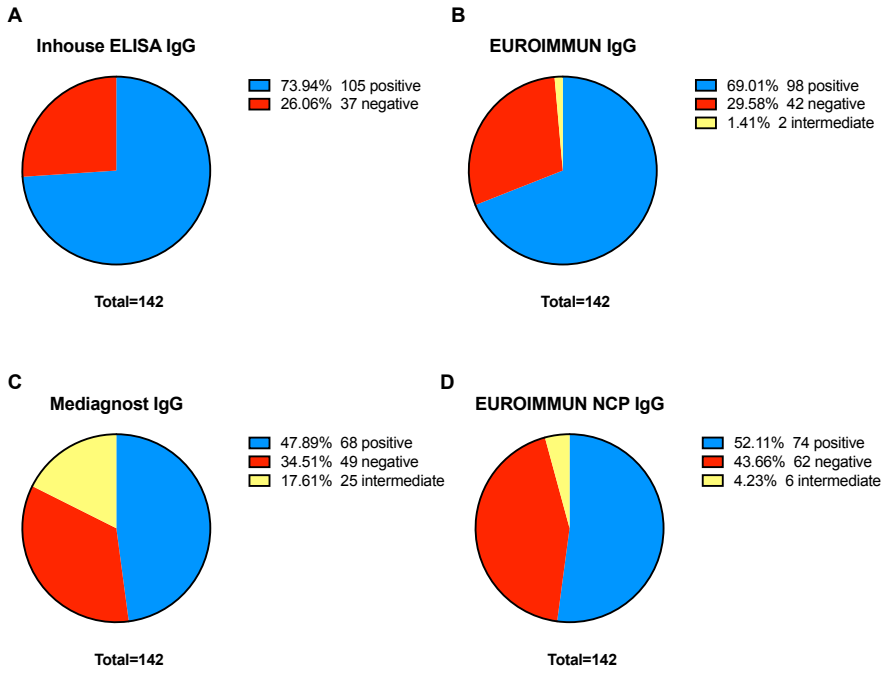

Figure 22: Pie charts of sensitivity of IgG ELISAs

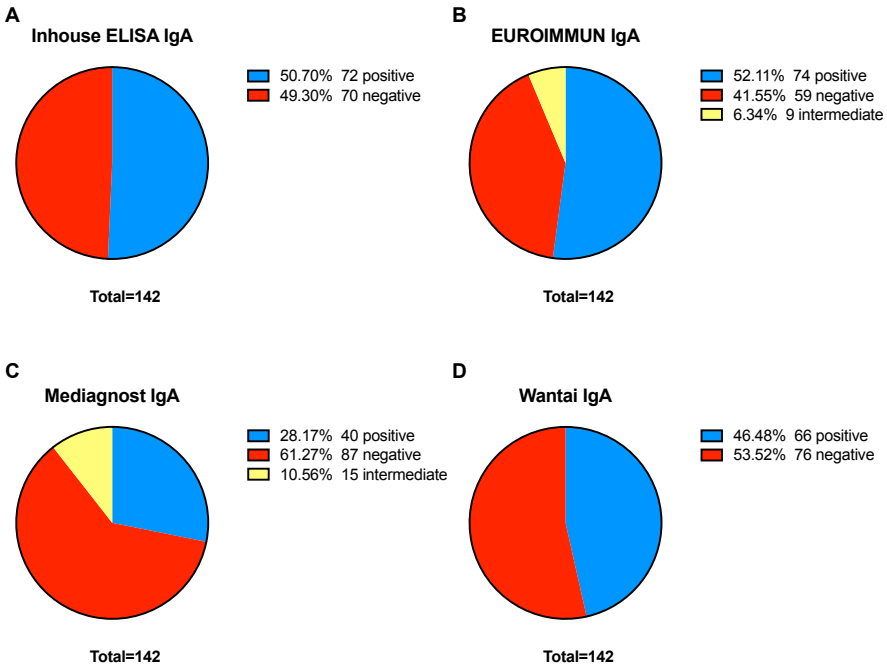

Figure 23: Pie charts of sensitivities of IgA ELISAs.

In total 142 PCR positive samples were measured. The sensitivity is represented by the blue field and provided in percentage beside the pie charts.

What stands out in the figure 22 is that the highest number of true positive rate refers to the in-house IgG ELISA with already mentioned 73.9%. Followed by the EUROIMMUN IgG ELISA with 69.0%. Especially the EUROIMMUN test with NCP as antigen showed a much lower sensitivity of 52.1%. Also, the Mediagnost IgG ELISA with 47.9% had a low sensitivity, which was already indicated by the smaller AUC in the previous figure. Figure 23 compares the true positive rate of the IgA ELISAs. It is apparent that the EUROIMMUN IgA ELISA had a slightly higher sensitivity than the in-house IgA ELISA by determining two more samples as true positive. Wantai showed the third best rate with 46.5%, followed by Mediagnost with only 28.2%.

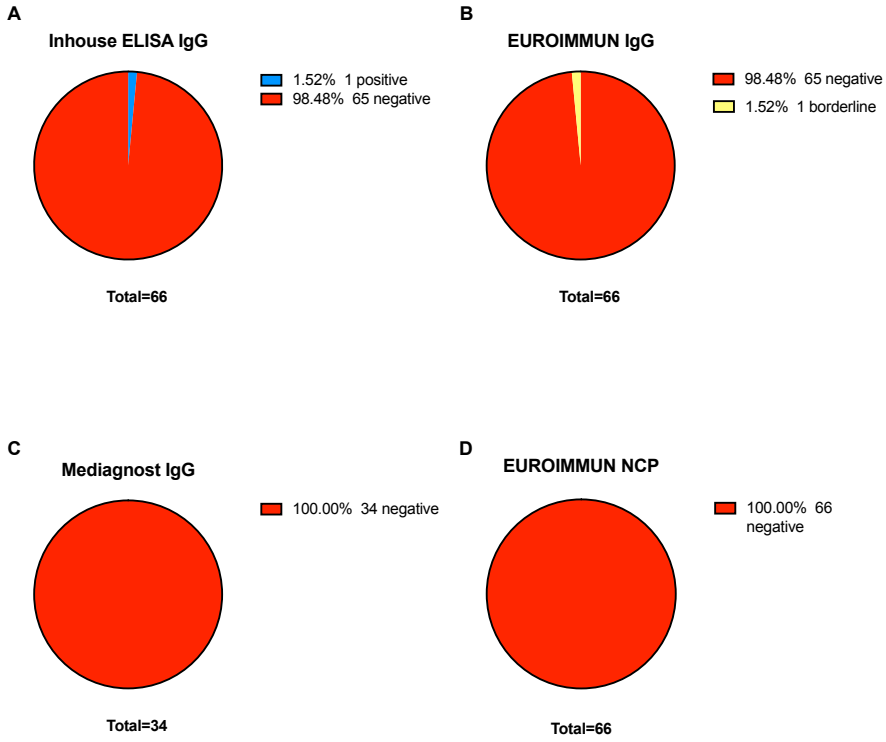

Figure 24: Pie charts of specificity of the IgG ELISAs

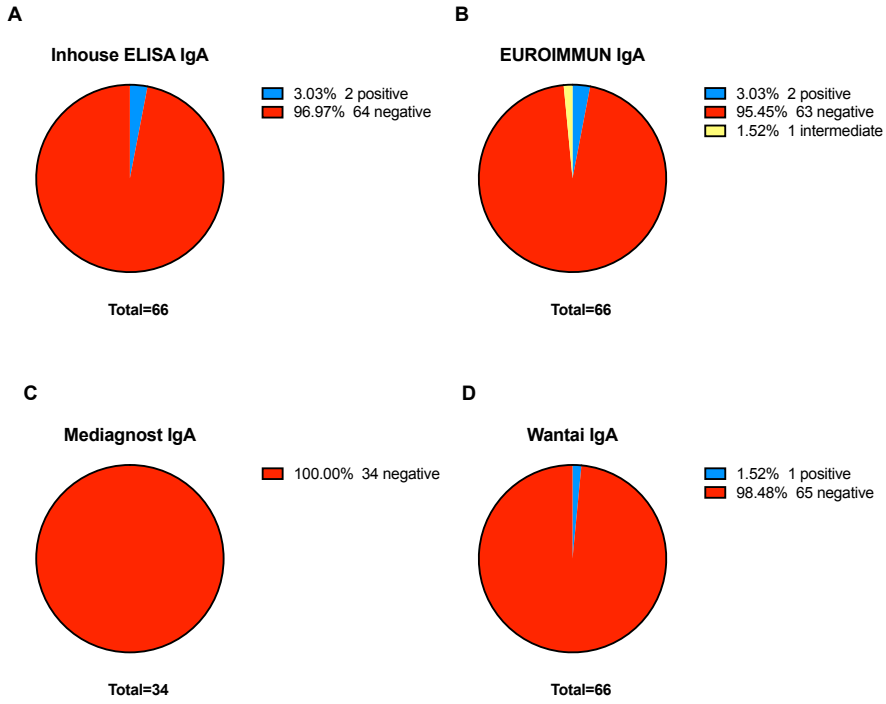

Figure 25: Pie charts of specificity of IgA ELISAs.

In total 66 negative samples were measured, except the Mediagnost ELISA with just 34 samples measured. The specificity is represented by the red field and provided in percentage beside the pie charts.

Figure 24 compares the true negative rate of the IgG ELISAs. The in-house ELISA and the EUROIMMUN ELISA shared the same specificity of 98.5%. Mediagnost and EUROIMMUN NCP showed a hundred percent true positive rate, but at the expense of sensitivity as we have seen before in figure 22. Figure 25 compares the true negative rate of the IgA ELISAs. The Mediagnost IgA ELISA also presented a hundred percent specificity but as mentioned before, with a lower sensitivity. The Wantai IgA ELISA determined just one sample as false positive, while the in-house ELISA and EUROIMMUN IgA assay identified two samples as false positive, as well as one borderline result in the EUROIMMUN IgA assay.

3.6.3.3 Comparison of individual samples

In the following figures, individual measurements of samples are presented in order to focus on individual results of different ELISAs.

A

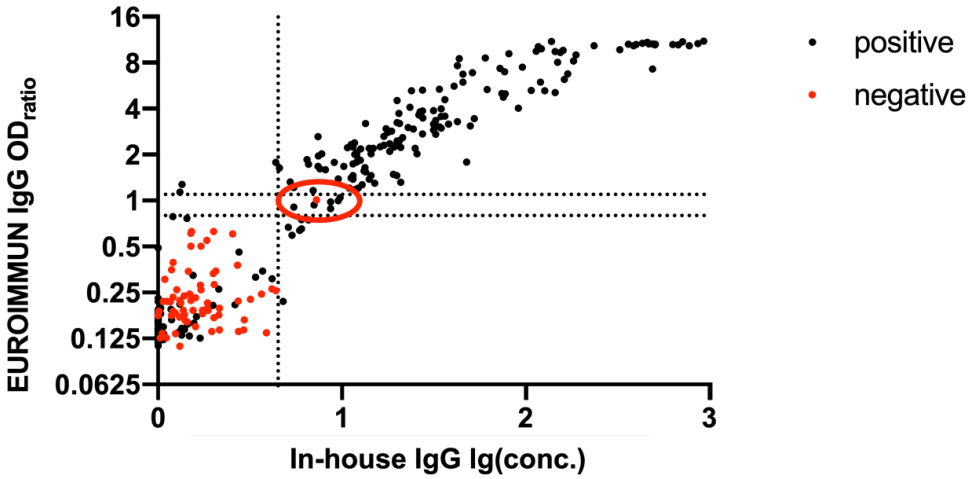
Inhouse IgG vs. EUROIMMUN IgG
EUROIMMUN IgG OD ratio
16
8
4
2
1
0.5
0.25
0.125
0.0625
0
1
2
3
In-house IgG lg(conc.)
positive
negative

B

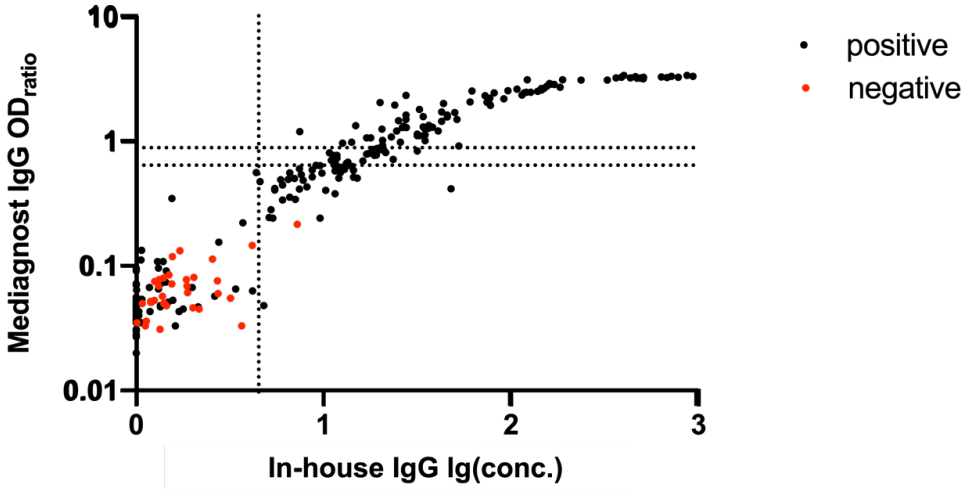
Inhouse IgG vs. Mediagnost IgG
Mediagnost IgG OD ratio
10
1
0.1
0.01
0
1
2
3
In-house IgG lg(conc.)
positive
negative

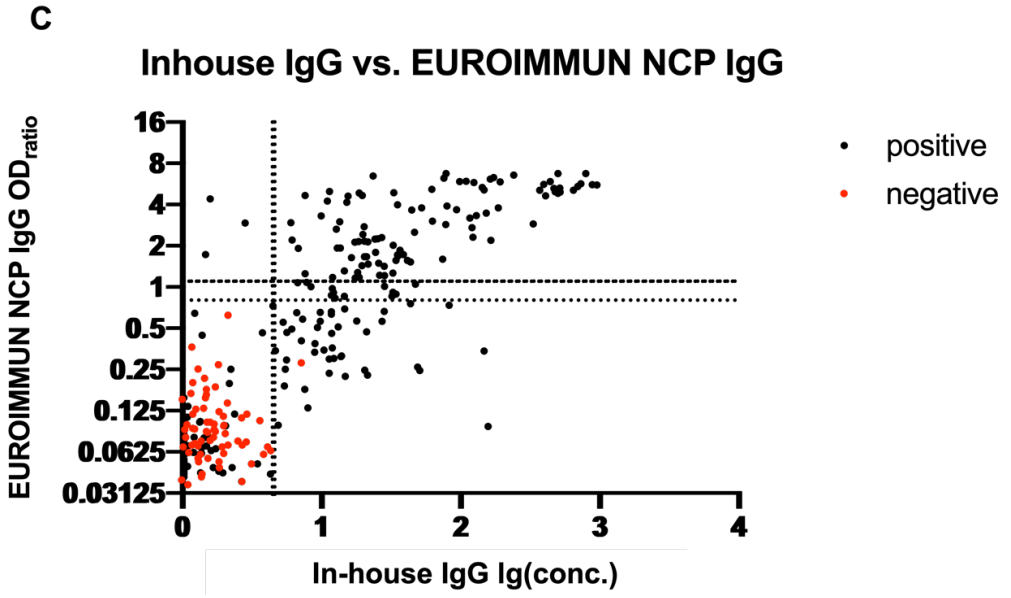

Figure 26: Comparison of SARS-CoV-2 IgG ELISAs.

On the x axis, the results of the in-house IgG ELISA are plotted. The y axis refers to the commercial ELISAs. The dotted lines are cut-off values of the tests. EUROIMMUN specifies an intermediate range in the tests, which lies between 0.8 and 1.1. Mediagnost uses cut-offs, which vary in each plate. Therefore, the highest and the lowest threshold of the plates were plotted. The positive samples are RT-PCR- and ELISA confirmed study samples (n = 219). The negative samples (n = 66), plotted in red, refer to the CoVNeg and pre-pandemic sample collection. The pre-pandemic samples were not measured by the Mediagnost test. The sample circled in red in figure A is a health-care worker, who had symptoms of fever but was not tested PCR positive.

The cut-off lines divide the samples into four fields. The lower left quadrant contains the samples read as negative by both tests; the upper right field contains the samples determined as positive by both tests. The upper left quadrant comprises the samples read as positive by the commercial ELISA, but read negative by the in-house ELISA. The lower right field on the other hand, comprises samples determined as positive by the in-house ELISA but negative by the commercial ELISA.

The figures 26 A, B, C show once again that even if the ELISA-confirmed positive samples (not just PCR-confirmed positive ones) were included, the in-house ELISA detect more positive samples and thus was more sensitive than the commercial ELISAs. This is shown by the higher number of samples from recovered individuals in the lower right quadrants, compared to the upper left quadrants.

Considering the negative samples, it becomes clear that all commercial ELISAs show 100% specificity, as there were no negative samples (red dots) in the upper

quadrants. The in-house IgG ELISA determined one negative sample as positive (red circled dot) in the lower right quadrant (figure 26.A). In this illustration it can be seen that even the EUROIMMUN IgG ELISA determined it as a borderline sample. This CoVNeg sample was collected from a health care worker, who declared to have had symptoms like fever in April 2020 but was not tested positive by PCR. When comparing the positive samples (black dots) from EUROIMMUN and the in-house ELISA (figure 26.A), it is noticeable that the two tests agree in scoring most samples. This means that both do not measure specific antibodies against SARS-CoV-2 in many of the same PCR- or ELISA-positive samples, whereas, there are many distinctions in the comparison with Mediagnost and EUROIMMUN NCP (figure 26 B, C).
It can also be seen that the samples of the commercial ELISAs did not go beyond a certain value and were therefore saturated. They are sold only as semi-quantitative assays. In contrast the in-house ELISA did not reach saturation, as appropriate sample dilutions were always applied (figure 26 A, B, C).

The following figures (figure 27) serve for further comparison of the IgA ELISAs, with the possibility to evaluate individual samples.

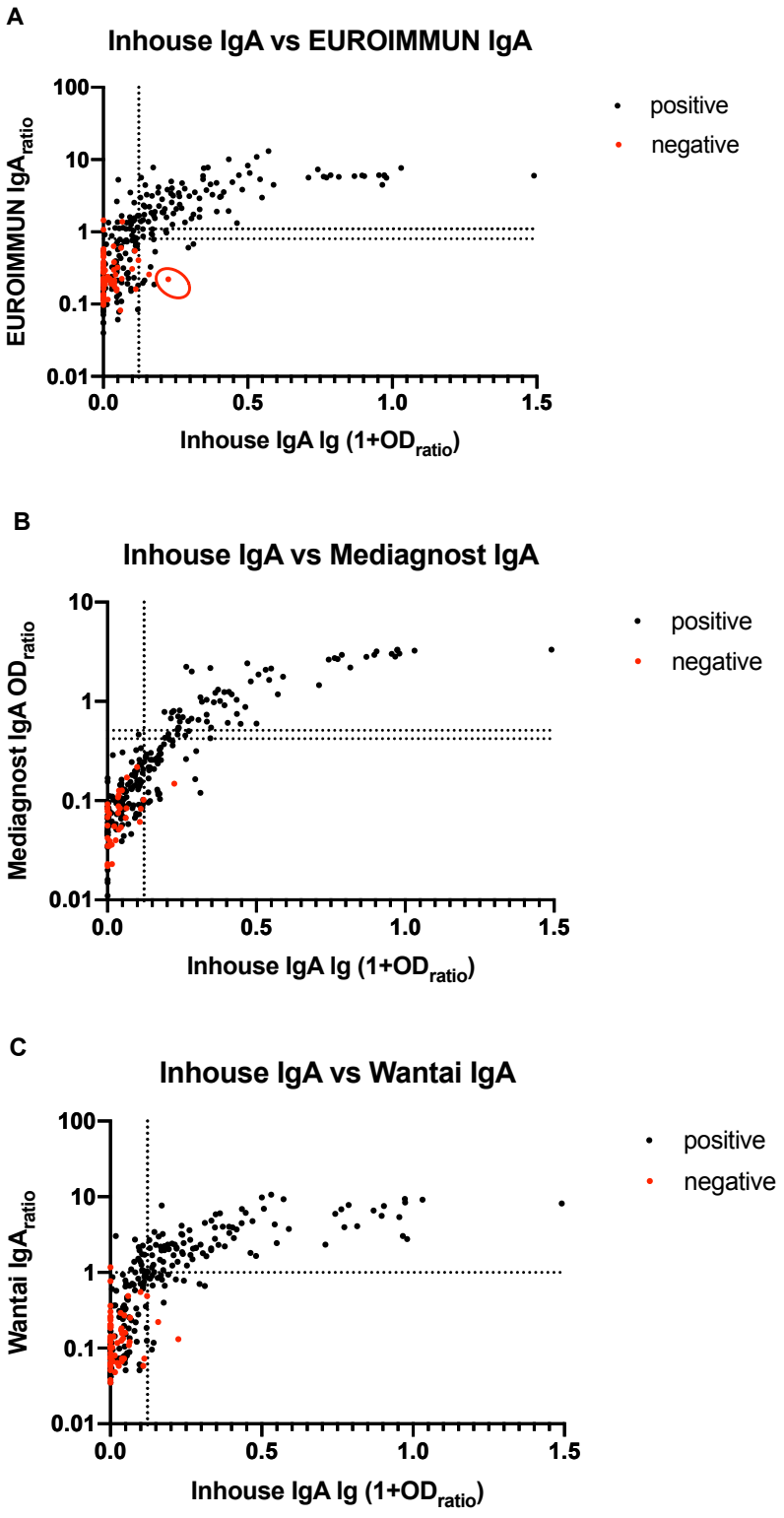

Figure 27: Comparison of SARS-CoV-2 IgA ELISAs.

On the x axis, the results of the in-house IgA ELISA are plotted. The y axis refers to the commercial ELISAs. The values of the in-house ELISA were logarithmized. The dotted lines are cut-off values. EUROIMMUN specifies an intermediate range in the tests, which lies between 0.8 and 1.1. Mediagnost uses cut-offs, which vary in each plate. Therefore, the highest and the lowest threshold of the plates were plotted. The positive samples are RT-

PCR- and ELISA confirmed positive study samples (n = 219). The negative samples (n = 66), plotted in red, refer to the CoVNeg and pre-pandemic sample collection. Mediagnost did not measure the pre-pandemic samples. The sample circled in red had hemolytic discoloration.

What stands out is that many PCR-confirmed cases appeared negative in all IgA ELISAs (figure 27.A, B, C). The EUROIMMUN IgA assay determined two samples from uninfected individuals as positive, they were from the CoVNeg study. One was determined as borderline sample by the EUROIMMUN IgA assay (figure 27.A). The borderline sample was from the pre-pandemic collection. The in-house ELISA determined two samples as positives, which should not contain specific antibodies. One of them, the red marked sample has attracted attention by hemolytic discoloration (figure 27.A). The second one was a pre-pandemic sample, which should definitively not be determined as positive. The ELISA from Mediagnost had no false positive samples, but it did not show a good true positive rate neither, as there were many infected individuals determined as negative, even more than in the other tests (figure 27.B). In contrast, test from Wantai detected only one false positive sample (figure 27.C). However, this was not the same sample that the in-house ELISA found to be positive.

3.7 Analysis of the Case Report Form

The ELISA study showed that the antibody levels of infected individuals varied greatly. In the COMIHY study, for example, which included subjects with less severe symptoms, many samples were measured negatively, by all conducted ELISAs.

It is also noticeable that the quantitative in-house test measured extremely high antibody levels in some samples. Therefore, in the following chapter the TüCoV study will be introduced in more detail. It was recruited with a Case Report Form (CRF). Moreover, the variables that might have influenced the antibody levels were further examined.

3.7.1 Descriptive statistic of the TüCoV study

131 participants from the TüCoV study were included for statistical analysis. Out of these 131 individuals, 85 test persons were tested RT-PCR positive and 45 were tested ELISA positive by routine clinical laboratories before participating.

One was not tested in advance, but was a family member of an infected person, thus, contact person and ELISA positive in our tests. The composition of the study population is described below and summarized in table 1 and 2.

Within the study population more females (n = 79, 60%) than males (n = 52, 40%) were recruited (binominal test, two-tailed, p = 0.02). The mean of age was 38.7 years (range, 15 – 75 years). The average time between the onset of symptoms and blood sampling was 120.8 days (range, 23 – 173 days). 24.5 was the mean of body mass index (BMI) with a range of 16.65 – 41.67. None of them were hospitalized. 126 claimed to have had symptoms, whereas five did not suffer from any symptoms. Symptoms reported were fever (n = 71), disorders of taste (n = 80), cough (n = 84), dry cough (n = 62), fatigue (n = 107), exhaustion (n = 108), diarrhea (n = 37), rhinitis (n = 45), headache (n = 70), joint pain (n = 69), skeletal pain (n = 18) and nausea (n = 21). Nine reported to smoke of which one was an electro cigarettes smoker. 43.5% had pre-existing conditions like cardiovascular disease (n = 5), hypertension (n = 18), pulmonary disease (n = 9), allergies (n = 26), diabetes mellitus (n = 2) and other pre-existing conditions like hypothyroidism (n = 12), Hashimoto-thyroiditis (n = 1), glaucoma (n = 1), osteopenia (n = 1), psoriasis (n = 1), neurodermatitis (n = 1), hyperuricemia (n = 1), migraine (n = 1) and a congenital lack of IgA in one person were indicated. The table below summarizes the main characteristics of the cohort.

Table 1: Descriptive statistics of TüCoV, continuous variables

Continuous variables	Observations	Mean	Range
Age [years]	131	38.65	15 - 75
BMI	131	24.54	16.65 - 41.67
Time period: Symptoms - blood drawing [days]	124	120.81	23 - 173

Table 2: Descriptive statistics TüCoV, categorical variables.

Categorical variables	Observations [n]	Observations [%]	Antibody levels median	Antibody levels Inter-quartil-range
Female	79	60.3	13.47	6.43 - 33.41
Male	52	39.7	12.55	4.53 - 29.5
ELISA-confirmed positive	45	34.4	17.02	6.94 - 33.5
PCR- confirmed Positive	85	64.9	12.2	5.54 - 30.92
Symptoms	126	96.2	13.81	6.6 - 32.8
No symptoms	5	3.8	0.48	0.21 - 1.37
Fever	71	54.2	17.02	8.72 - 41.56
No fever	60	45.8	10.29	3.78 - 29.74
Taste disorders	80	61.1	16.36	8.61 - 36.42
Diarrhea	37	28.2	15.06	7.69 - 32.39
Cough	84	64.1	16.36	6.8 - 35.51
Dry cough	62	47.3	15.5	6.41 - 33.99
Fatigue	107	81.7	13.35	6.43 - 31.01
Exhaustion	108	82.4	14.6	6.69 - 32.44
Rhinitis	45	34.4	12.2	5.57 - 26.53
Headache	70	53.4	14.6	6.71 - 31.61
Joint pain	69	52.7	16.48	9.41 - 35.17
Skelettal pain	18	13.7	12.99	4.85 - 34.84
Nausea	21	16.0	10.51	3.58 - 41.03
Nonsmoker	122	93.1	14.6	6.24 - 33.43
Smoker	9	6.9	7.8	2.81 - 11.47
Pre-existing conditions	57	43.5	16.48	6.73 - 32.60
Cardiovascular disease	5	3.8	13.35	8.21 - 43.62
Hypertension	18	13.7	21.53	9.55 - 48.59
Pulmonary disease	9	6.9	19.95	14.79 - 39.77
Allergies	26	19.8	17.1	8.23 - 27.52
Diabetes mellitus	2	1.5	38.46	
Rheumatism	0	0.0		
Positive tested contact person	78	59.5	16.44	8.46 - 33.43
Stay in risk area	26	19.8	11.29	4.84 - 47.51

As already mentioned, 61% had gustatory dysfunction, of which 62% (n = 52)

were female. The median of the age of participants with gustatory disorders was 31 years (range 19 – 70 years) and the median of the BMIs amounted to 24.3 (range 16.65 – 41.67).

3.7.2 Influence of individual independent variables

To figure out whether there are independent variables with an impact on the antibody level statistical analysis was performed as described in 2.7.4. All pre-existing conditions are summarized in one variable. The variables for mild cold such as headache, rhinitis and similar were not included because they are only mild symptoms that are measured and evaluated very subjectively.

Table 3: Linear regression of continuous variables.

Continuous variables	Beta	CI 95 %	P value
Age	0.002	-0.004 - 0.007	0.5
BMI	0.007	-0.016 - 0.030	0.54
Time period: Symptoms to blood drawing [days]	-0.002	-0.005 - 0.001	0.28

Table 4: independent-sample t-tests of categorical variables.

Categorical variables	Mean difference	CI 95%	P value
Male - Female	-0.133	-0.32 - 0.06	0.17
ELISA - PCR	0.014	-0.18 - 0.21	0.885
No symptoms - Symptoms	-0.968	-1.43 – (-0.51)	0.000***
No fever - Fever	-0.266	-0.45 – (-0.08)	0.005**
Taste disorders	0.296	0.11 - 0.48	0.002**
Diarrhea	0.067	-0.14 - 0.28	0.524
Dry cough	0.05	-0.14 - 0.24	0.596
Pre-existing conditions	0.778	-0.11 - 0.27	0.416
Positive tested contact person	0.214	0.03 - 0.40	0.025*
Stay in the risk area	0.102	-0.13 - 0.34	0.391
*** p<0.001, ** p<0.01, * p<0.05			

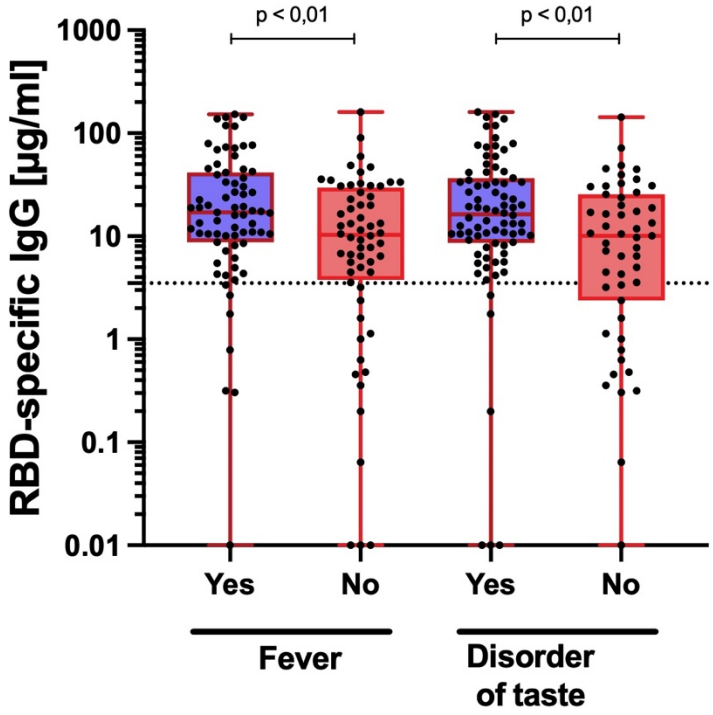

Figure 28: Scatter dot plot of IgG antibody levels in individuals with and without symptoms.

Box-whiskers-plot; dotted line: cut-off (3.5) for antibody-positivity.

It is striking that there was a significant difference of antibody levels between individuals with and without fever (figure 28, $p<0.01$) as well as between participants reporting disorders of taste and no disorders of taste (figure 28, $p<0.01$). In both cases, antibody levels were higher in the presence of the symptoms (independent sample t-test, table 4 and figure 28). None of the continuous variables had a significant impact on the IgG antibody level (table 3, $p>0.05$). Participants of high or low antibody level were comparable in terms of age, BMI, sex, as well as in symptoms like diarrhea and dry cough (table 3, 4). Individuals without symptoms had significantly lower antibody levels than participants who reported symptoms (table 4, $p<0.05$). The confidence interval in this variable was relatively wide compared to the other variables. Nevertheless, no antibodies were detectable for participants indicating no symptoms. No significant effect on antibody level could be attributed to the inclusion criteria of the study, positive ELISA or positive PCR nor on the time interval between the onset of symptoms and the drawing of blood, which varied in the individuals (table 4, $p>0.05$). In addition, pre-existing conditions showed no significant effect to the number of antibodies produced (table 4,

p>0.05). Likewise, residence in a corona risk area had no influence. However, contacts of COVID-19 infected people had significantly higher antibody levels than people who did not report a direct contact (table 4, p<0.05).

3.7.3 Factorial ANOVA

A factorial ANOVA was conducted to examine the impact of disorders of taste and fever on IgG antibody level as well as the interaction between the effect of taste disorders and fever. Homogeneity of variances was asserted using Levene´s Test which showed that equal variances could be assumed (p = 0.895).

Table 5: Factorial ANOVA, dependent variable: IgG antibody level.

	df	F	P value
Fever	1	6.72	0.011*
Disorders of taste	1	7.58	0.007**
Fever * Disorders of taste	1	1.10	0.297

R Squared = 0.121, Adjusted R Squared = 0.100

*** p<0.001, ** p<0.01, * p<0.05

Test persons with fever and disorders of taste showed higher antibody levels (factorial ANVOVA, table 5). There was a statistically significant difference of antibody levels in participants reporting fever and those without fever (F (1, 131) = 6.72, p<0.05) and even a bigger difference of antibody levels in participants reporting disorders of taste compared to those without disorders of taste (F (1,131) = 7.58, p<0.01). There were just six cases out of 80 (7.5%) who claimed to have had gustatory disorders, but had no seroconversion. Conversely, we observed a seroconversion of 92.5% for participants with taste disorders. There was no statistically significant interaction between the effect of taste disorders and fever on antibody levels (F (1,131) = 1.097, p = 0.297). With this model, the level of antibodies could be predicted by 10% (Adjusted R Squared = 0.100, table 5).

3.7.4 Prediction of positive or negative ELISA result

As we figured out, a positive PCR test alone cannot predict reliably whether

antibodies to SARS-CoV-2 will be generated. Therefore, the question had arisen what else can be considered as additional predictor for antibody positivity besides the PCR test. For this purpose, a binary logistic regression was created, with the binary dependent variable antibody positive or negative. Fever and disorders of taste had already shown an effect on antibody levels in the ANOVA, so these variables were now tested as predictors.

Table 6: Seroconversion of RT-PCR positive individuals. Categorized by occurrence of symptoms.

		Seroconversion	
		yes	no
		72	13
fever	yes	43	5
	no	29	8
disorders of taste	yes	55	4
	no	17	9
contact person	yes	46	7
	no	26	6

Table 7: Binary logistic regression, dependent variable: IgG antibody positive, negative.

	df	Exp(B)	95% CI	P value
Fever	1	2.4	0.85 - 6.76	0.098
Disorders of taste	1	4.3	1.49 - 12.20	0.007**
Contact person	1	2.0	0.75 - 5.58	0.165

Interestingly, taste disorders increased the probability that the IgG ELISA of the affected person was positive by a factor of 4.3 ($p<0.05$) (binary logistic regression, table 7). Among those confirmed RT-PCR positives, seroconversion was 93.2%, as there were only 4 cases out of 59 (6.8%) with disorders of taste that showed no seroconversion (see table 6). In comparison, people without taste disorders in this cohort (n = 26, 30.6%, table 6) had a 4.3-fold lower probability that the test result was positive (table 7). The variable `disorders of taste´ had a wide 95% CI. The results show that the symptom fever and being a contact person were not adequate predictors of antibody positivity (binary logistic regression, $p>0.05$, table 7). The model accounted for 19% of the variability of the outcome

(Nagelkerke R^2 = 0.190). The Hosmer and Lemeshow test denoted good model fit ($p>0.05$).

4 Discussion

In the following section, I will discuss the results and place them into context with the literature available up to January 2022. The order is based on the results section.

4.1 SARS-CoV-2 ELISA development

The steps in the development of the ELISA, from amplification of the plasmid, to transfection into HEK 293 F cells, to harvesting of the protein were successful. Purifications were successful as well and both purified RBD worked out as antigen in the in-house ELISAs. Amanat et. al. also used mammalian cells (HEK293 F cells) to express RBD. They compared the expression of mammalian cells with expression in insect cells, and mammalian cells achieved much higher yields [47]. It is also noteworthy that it was also apparent in their SDS page that RBD was greater than 25 kDa, similar to our SDS page result [47].

By trying different buffers and solutions, as well as conditions such as temperature, we arrived at the aforementioned standard protocol for our in-house ELISAs, which we used for all subsequent determinations of antibody levels. The special thing at the beginning of our work in March 2020 was that we had no guidance for the development of a SARS-CoV-2 ELISA, because at that time there was no reviewed protocol for implementation of a SARS-CoV-2 ELISA and no commercial assays available for comparison. In the protocol of the ELISAs, it is noticeable that different buffers proved to be optimal for blocking and for secondary antibody dilution. Presumably, preventing nonspecific binding during blocking requires different conditions than preventing nonspecific binding of the secondary antibody. It is also noteworthy that the otherwise considered common and very effective blocking reagents such as BSA [48] were not convincing in our tests.

4.2 Evaluation and validation

4.2.1 Precision of the in-house IgA and IgG ELISA

The results of the in-house IgA ELISA showed a good intra-assay precision for dilutions of 1:100 up to approximately 1:24,300. We set a precision cut-off at a CV of 10%, what is considered to be good [46]. This means that we measured with a precision of 90 to 98.5% up to a dilution of approximately 1:24,300. For further tests, it was sufficient to use dilutions of 1:100, 1:500 and 1:2,500 to get a quantitative test score. Hence, our measurements were highly precise with between 93.5 and 98.5% precision.

The intra-assay precision of the IgG ELISA was very high with a CV of 4%. We set the cut-off at 10%, which is still considered acceptable [46]. We only used dilutions of 1:100, 1:500 and 1:2,500 (no stronger dilutions) in further ELISAs with an estimated precision of 95 to 99%.

The inter-assay CV for the IgG ELISAs was very good with an average value of 6.9% [46]. In the inter-assay precision tests of the IgA ELISA, one sample exceeded the 15% mark, but the average of CV was with 13.9% below 15%. It showed that the OD values of different plates on varying timepoints were comparable. We had a good reproducibility.

In summary, we have stable assay performances for the IgG and the IgA in-house ELISA. Krähling et. al have also implemented an IgG SARS-CoV-2 S1 ELISA. For evaluation, they determined the precision of the test as we did. They achieved an intra-assay CV of 5.3%, where our IgG in-house ELISA is still below with 4.0%. Their inter-assay CV was 7.9%, with our IgG test performing better at 6.9% [49]. However, they also had different operators in the inter-assay precision testing, whereas we performed the tests with the same operator, which may have an impact on the inter-assay precision. All in all, the IgG in-house ELISA presented a better performance in precision than the IgA in-house ELISA. Moreover, the IgA ELISA passed the precision tests as well. The slightly poorer precision of the IgA ELISA could be due to human error in the performance or to a lower robustness compared to the IgG ELISA, which was also shown in the effects of temperature. Therefore, robustness could be investigated in further experiments for example in terms of variability in incubation times. It would be interesting to know if the test

results would remain stable in case of variations in the performance.

In general, it would be good to perform further experiments to validate the tests. For further assessment of the inter-assay precision (reproducibility), one could use different operators, different equipment or increase the repetitions of the measurements to more than three times. For further evaluation and validation of the in-house ELISAs the following methods according to international quality guidelines would be useful besides precision (what we already tested) and robustness: Limit of Detection (LoD), Lower Limit of Quantification (LLoQ), dilution linearity and accuracy [50].

LoD is the calculated lowest concentration of the analyte for possible detection. The difference between low positive sample and signal in the absence of sample. It is calculated with help of the Limit of Blank (LoB). LoB is the highest concentration measured when replicates of blanks are measured [51].

LLoQ is the lowest concentration of analyte that can be accurately measured. Hence, it determines the precision of the test at low concentrations of the analyte [52].

Dilution linearity is another tool of validation. Here, the diluted samples should be in the linear range of 100 +/-25%. The accuracy indicates how close the values determined by the method are to the actual concentration [52]. For this purpose, the WHO standard immunoglobulin with a known concentration can be used as a comparison. At the time of development, the WHO standard was not available yet.

Krähling et. al, in addition to precision testing, sensitivity and specificity, (which we also performed) also tested cross-reactivity to other coronaviruses and compared the ELISA to a SARS-CoV-2 neutralization assay [49]. This could complete the evaluation of the in-house ELISAs. Cross-reactivity of the in-house ELISAs is discussed later in this thesis.

With regard to the samples, one could test the thaw and freezing stability of the samples and check whether there is a difference in using plasma or sera as samples. Furthermore, one could examine, at which lipemic or hemolytic strength of the samples the signal is influenced, because one sample of the CoVNeg collection appeared with high OD values in the in-house IgA ELISA and a check of the

original sample tubes showed that the sample was hemolytic. This might be an explanation of the high background signal that was observed and could be examined in further experiments.

4.2.2 Evaluation of the choice of methods

We chose indirect ELISA as method, as mentioned in the introduction. At the beginning of our work, in early March 2020, there were no comparative studies to rely on. Only a pre-print of a protocol for the preparation of an ELISA by Stadlbauer et. al. [53]. Thus, we had decided to use ELISA. Also because this method is common in the institute and is used a lot.

In the meantime, the methods with regard to COVID-19 have been evaluated more. Gong et. al. compared ELISA, CLIA, LFIA and IFA, (which I already described in the introduction) in terms of feasibility, duration, cost, and the most important marker for evaluating diagnostic tests: sensitivity and specificity [35]. With a mean detection time of 2-8 h, ELISA is the longest lasting diagnostic tool. The CLIA, on the other hand, takes only 0.5-2 h. However, due to their complexity, both methods can only be used in laboratories or clinics [35]. The LFIA is the fastest at 3-30 min and the easiest to use. In addition, it is also very inexpensive. However, as with the IFA, the specific antibodies are not quantifiable, but this was a requirement for us. In addition, LFIA has low sensitivity and specificity compared to the other methods. With IFA, there is also a risk of infection, as infected cells are used. There is also some subjectivity in the evaluation of IFA due to the assessment of fluorescence [35]. Therefore, the test is less suitable for our purpose and has little application in COVID-19 diagnostics [35]. CLIA and ELISA both have relatively high accuracy. ELISA was slightly less sensitive and specific than CLIA but more accurate than the other two assays. Accordingly, CLIA performed best in this study [35].

Machado et. al. found a sensitivity of 82.5% with respect to IgG and 44.4% with respect to IgM and a specificity of 100% for the ELISAs in their review of methods for COVID-19 diagnosis. For CLIAs, on the other hand, a sensitivity of 71.4% for IgG and 57.2% for IgM was described, also with 100% specificity [54].

Accordingly, the data vary. Our in-house IgG ELISA with a sensitivity of 84.3%

and a specificity of 100% fits well into the picture and has a good performance. What both studies show is that the combination of IgG and IgM detection achieves the best result in sensitivity [35,54]. Therefore, it should be considered to combine the results of IgG and IgM ELISAs to also detect early immune responses and to achieve a higher sensitivity.

4.3 Measurement of the specimens with the in-house ELISAs

The screening of the study samples showed that COV HCQ is a study with generally high antibody levels, although it is noticeable that some samples gave negative results. The strong positivity of the samples could be attributed to the severity of symptoms in this cohort, as all of whom were hospitalized. It has been reported repeatedly that symptom severity correlates positively with the antibody level [27,28]. In the study by Rijkers et. al. hospitalized subjects had 100% detectable total antibodies and subjects with mild clinical symptoms only 87% with significantly lower titers [28].This observation is supported by our measurements. In comparison, the samples of the COMIHY study with mild symptoms and no hospitalized individuals had lower antibody levels. Part of the negative samples in the COMIHY and COV HCQ study could be explained by the fact that blood was drawn at different time points, including early timepoints of infection (day 1 and day 7 of symptom onset). It has been reported that especially IgG antibody formation is delayed after the onset of symptoms. In the case of COVID-19, a seropositive rate of approximately 50% in the first week was reported, compared to 100% in the third week after symptom onse t[30]. In the COMIHY cohort four participants out of 19 showed a seroconversion between day 01 and day 14. Interestingly, only two participants out of 18 patients from the COV HCQ cohort showed a seroconversion from day 01 to day 07. In both studies, inclusion did not occur exactly at symptom onset, especially in the COV HCQ cohort, since symptoms usually begin a while before hospital admission [55]. To make sure that there was enough time for the formation of the antibodies, we used only samples from day 14 of inclusion on for determining the sensitivity of the ELISAs. The COMIHY and CoV HCQ studies were chosen for antibody detection because in March 2020 there were not many other samples from COVID-19 recovered

individuals. In hindsight, it is questionable whether the subjects really all had COVID-19 or whether there were errors due to the urgency of recruitment and a low prevalence of COVID-19 in March 2020 (further discussion in 4.4.3). The TüCoV samples formed a cluster and is more representative than the COMIHY and CoV HCQ studies, which included only certain individuals. For this reason, this cohort was used to determine a threshold in further analysis.

4.4 Statistical analysis of data

4.4.1 Evaluation of the screening

The AUC ROC showed that the developed tests could reliably distinguish between positive and negative samples. When measuring all cohorts, the IgG in-house ELISA achieved a sensitivity of 84.3% (with a 95% CI of 75.0 – 90.6%) based on 83 PCR-positive subjects tested in a clinical laboratory, which initially did not seem optimal for screening. The IgA in-house ELISA also detected only 47.6% (with a 95% CI of 37.3 – 58.2%) of positive samples. The question is whether the test was not able to detect SARS-CoV-2 specific antibodies or whether some infected individuals did not develop antibodies. What impact did the timing of sample collection have had, considering that blood was also drawn at early time points of infection in the COMIHY and COV HCQ studies? Lei et al. observed that IgG levels in patients with mild symptoms were significantly higher than in asymptomatic individuals [56]. Furthermore, it was reported by Rijkers et.al., who measured total antibody levels with an ELISA, that about one quarter of the infected individuals with mild symptoms did not produce any antibodies against SARS-CoV-2 at all [28]. This was supported by our results, where 24.6% of the subjects showed no seroconversion and none of the participants of the TüCoV cohort indicating no symptoms at all (4%) had specific detectable antibodies. These findings had a negative impact on the sensitivity of the ELISAs when a positive RT-PCR test was taken as reference. The possibility that it could also be due to false positive PCR results will be discussed later.

The ELISAs presented a specificity of 98.5% for the IgG ELISA and 97.0% for the IgA ELISA based on the pre-pandemic and CoVNeg samples. None of the pre-pandemic samples were measured positive by the IgG in-house ELISA. The

few positive samples in the in-house ELISAs referred to the CoVNeg cohort. It cannot be excluded that the CoVNeg subjects were not infected, because recruitment already took place during the pandemic. Therefore, it was difficult to estimate the true specificity of the tests. More pre-pandemic negative controls would be necessary as well as more measurements in total, like testing the cross-reactivity to other coronaviruses. Cross-reactivity will be discussed later.
The in-house ELISAs were compared to commercial ELISAs to better assess its functionality.

4.4.2 Comparison with commercial tests

4.4.2.1 Comparison of separability, sensitivity and specificity

All ELISAs, except the Mediagnost IgA ELISA, had very similar AUC in the ROC curves and good diagnostic ability. This showed that although some PCR positive samples were measured negative it was not caused by the quality of the serological tests, but probably caused by the absence of antibodies. The IgA ELISA from Mediagnost had a low AUC and therefore a low degree of separability between positive and negative samples. This may be due to a poorer performance. Another reason for a smaller AUC could be that only 33 instead of 66 negative samples were measured, because only a limited amount of plates of Mediagnost were available. This was contradicted by the fact that the IgG ELISA of Mediagnost showed a high AUC even with less negative samples.

It is also to be noted that Wantai had the largest AUC of the IgA ELISAs but showed a lower sensitivity. The differences could be attributable to the fact that distinct reference groups were used. The PCR-positive TüCoV samples were included for the AUC measurements and to detect a cut-off value for the tests as mentioned before. In contrast to this, samples from all cohorts were used to measure the sensitivity and specificity of all ELISAs conducted.

Concerning the sensitivity and specificity, the in-house ELISAs could compete with the commercial assays very well. Moreover, the IgG in-house ELISA outperformed industrial ELISAs in sensitivity, although the true positive rate was not

very high (in-house: 73.94%; EUROIMMUN 69.01%; Mediagnost 47.89% based on PCR confirmed positive samples from all cohorts).

It is striking that Mediagnost's tests, although using the same antigen as our in-house ELISA, had a lower sensitivity. Hence, the low sensitivity could be due to the protocol, to the buffers used within the ELISA or to the definition of the threshold of the Mediagnost ELISAs. Another possibility is that they expressed the RBD protein differently or the structure has slight differences so that it loses sensitivity. The fact that the NCP ELISA from EUROIMMUN did not recognize many PCR-confirmed samples, may be caused by missing antibody production against the nucleocapsid antigen or caused by the protocol of the ELISA, as it was reported that the nucleocapsid antigen was as sensitive as the RBD antigen [24]. The SARS-CoV-2 ELISA from EUROIMMUN used the S1 domain as antigen and had a similar performance to the in-house ELISA. A concern regarding the use of RBD instead of the spike protein in an antibody assay, was a loss of sensitivity in the diagnostics. However, Brochot et al. observed that the detection of RBD was more sensitive than the detection of S1 protein in the use of their assays [24]. This was supported by our findings, as our results showed that the RBD antigen could compete in sensitivity with the S1 domain as antigen. Moreover, the IgG in-house ELISA outperformed the EUROIMMUN test in sensitivity with 74% compared to 69% respectively (based on PCR confirmed positive subjects from all cohorts) and the in-house IgA ELISA missed just two positive samples compared to the EUROIMMUN IgA ELISA. Also, the specificity of the RBD antigen appeared quite similar to the specificity of the S1 antigen and reached 100% for pre-pandemic samples in the IgG in-house ELISA. McAndrews et al. also observed that the specificity of the RBD antigen in pre-pandemic samples was 100% (0 positives out of 104 pre-pandemic samples) in their study using IgG SARS-CoV-2 RDB ELISA [25]. Another study measured 99% specificity in using RBD antigen [32].

It would also be interesting to investigate our in-house ELISA in terms of cross-reactivity to other coronaviruses, as these are widely distributed in the population [57]. Krähling et. al. tested their aforementioned IgG SARS-CoV-2 S1 ELISA

for cross-reactivity with antibody-positive samples of human coronavirus HKU1 (n = 27) and on samples from subjects vaccinated against Middle east respiratory syndrome-related coronavirus (n = 20). No cross-reactivity was detected in either [49].

Cross-reactivity of the developed ELISAs to SARS-CoV cannot be excluded. Lv et. al. observed that cross-reactivity of SARS-CoV and SARS-CoV-2 in binding S protein is common [58]. But the low seroprevalence of SARS-CoV antibodies in humans reduces the possible impact of this cross-reactivity on our in-house ELISA.

Additionally, Piccoli et al. observed that SARS-CoV-2 RBD-specific IgG antibodies dominated the IgG response [59]. Prior studies have noted that the main part of the neutralizing humoral immune activity is caused by antibodies targeting the RBD protein [33,59]. Accordingly, RBD was a good choice as an antigen for our ELISA, since thus detection of RBD specific antibody is indicative of protection against infection. Another factor that supports the choice of RBD as an antigen is that the S protein and thereby RBD epitopes are widely used in vaccine trials, because it is suggested that the RBD region is immunogenic [29]. Therefore, it is possible to use this assay to assess immune responses to vaccines. This assumption is supported by the work of Beck et. al. In their cohort, all subjects vaccinated against SARS-CoV-2 formed IgG or IgM antibodies against RBD [60].

The drawback is that only the determination of RBD specific antibodies cannot distinguish whether the immune response relates to vaccination, to a passed through infection, or whether both occurred. Brochot et. al. observed that infection often results in antibody formation against multiple viral epitopes (N, S1, S2, RBD, N-terminal domain) [61]. Vaccine antibodies, on the other hand, are directed only against the vaccinated protein, usually parts of S, and are therefore only detectable with serological tests that use parts of S as antigen [60]. According to the algorithm of Beck et. al. subjects with IgG antibodies against S1 but no total antibodies against the N protein are most likely vaccinated [60]. In their cohort of 428 vaccinated but not infected subjects, all were IgG S1 positive and IgG/IgM RBD positive, but no antibodies against N could be detected. In contrast, in the infected

subjects, IgG antibodies to S1 could be detected in 89%, IgM/IgG antibodies to RBD in 91%, and antibodies to N in 91% [60]. Accordingly, it would be useful to test samples not only for multiple antibody classes but also for multiple antigens to obtain a complete picture of the subject's serology. Brochot et. al. recommend a combination of anti N and anti S for discrimination [61].

4.4.3 RT-PCR as gold standard

Is a RT-PCR positive test, currently the gold standard for the diagnosis of COVID-19 [62], a good reference for antibody positivity? The analytical specificity of RT-PCR was usually rated at 100% with no false positive results [63]. However, this calculation did not take user errors and contaminations into account. A rate of false positives about 0.3 to 6.3% for SARS-CoV-2 RT-PCR testing was assumed [64,65]. The wide range shows that the number of false positives seems to vary strongly, depending on the laboratory and the region. The rate of false positives has a great impact for the tested individuals. Among other things, they are wrongly subjected to quarantine and cannot perform their work, what might also cause economic damage [65]. In addition, there is a risk that those affected may feel a false sense of security, fail to get vaccinated, and run the risk of infection for themselves and those around them. Also, the assessment of ELISAs was affected negatively, when compared to the gold standard RT-PCR. Our results indicated a rate of 24.6% of PCR-confirmed positive samples showing no antibodies. Certainly, not all of these antibody-negative cases were false positive PCR results. However, false positive PCR results should be considered as a factor, along with factors such as the length of time and cases with few symptoms that developed lower antibody levels that faded over time or no specific antibodies at all.

Especially in the samples of the COV HCQ study, which included patients with severe symptoms, we would expect antibody formation. However, even in this cohort there were subjects who remained negative across all time points and in all eight ELISA tests as well (33.33%, n = 6). Healy et al. assessed RT-PCR results with positivity in only one gene and a cycle threshold (Ct) value higher than 35 as falsely positive considered results [66]. Therefore, it would be interesting to

inspect the RT-PCR results closer. Unfortunately, we did not have the exact RT-PCR results with Ct values for the individual genes used for the RT-PCR. This shows the limitations of my work, as I cannot verify the quality of recruitment for COMIHY and CoV HCQ. Therefore, we could not draw any conclusions from the RT-PCR. However, it is possible that the subjects who did not develop antibodies had a low viral load with very high Ct values and would be more likely to be SARS-CoV-2 negative samples according to the study of Healy et al [66]. Moreover, the CoV HCQ study recruited at the very beginning of the pandemic. At that time, the rate of false positive RT-PCRs may have been higher because there was less experience in technique and interpretation of results. Moreover, at the time of recruitment, the prevalence of COVID-19 was very low, which may also have had an impact on the level of false-positive PCR results [66].

Thus, voices were rising to argue that a RT-PCR result alone should not establish a diagnosis of COVID-19. Rather, the whole picture should be considered. Do the persons have symptoms? Has there been contact with infected individuals? In summary, how great is the pre-test probability of infection? If in doubt, further testing should be done [64-66].

The RT-PCR result also plays a major role in vaccination recommendation. Accordingly, people who can prove a RT-PCR positive test will not be offered vaccination until six months after infection, according to the current status[67] (22/10/2021). After these six months, they will receive one dose of vaccination. This decision is also based solely on the RT-PCR result. However, as we have seen, a RT-PCR positive result is not immediately followed by a humoral immune response. Thus, people who have not developed antibodies may be at risk of infection. This study suggests that seroconversion could be a criterion for a vaccination recommendation to protect RT-PCR positive individuals without antibodies. Another consideration is whether it would not make more sense to have antibody titers determined before the third vaccination - especially at times when many countries of the Global South still do not have enough doses available to vaccinate their populations.

Further studies are needed to assess the occurrence of false positive RT-PCR

results and to evaluate, whether a RT-PCR result with high Ct values should be assessed as positive or negative result and thus to gain knowledge of the context of low virus load and sero-negativity.
For further evaluation of our ELISA, we could only compare with other ELISA tests to get as close as possible to the truth, whether a sample contained SARS-CoV-2 specific antibodies and how high the sensitivity of the in-house ELISA was.

4.4.3.1 Comparison of individual samples

To ascertain whether a sample had specific antibodies against SARS-CoV-2, we looked at individual samples. What stands out was that EUROIMMUN IgG and the in-house IgG test agreed in many RT-PCR confirmed samples. Interestingly, these tests predominantly assessed the same RT-PCR confirmed samples as negative. Therefore, the ELISAs achieved only moderate sensitivity, as RT-PCR was taken as a reference. However, it is questionable whether antibodies could be detected at all in these samples. Therefore, the sensitivity of the in-house ELISA was probably distinctly higher as the calculations showed. In the IgA tests, it is also noticeable that many positively confirmed samples were measured negative, even more than in the IgG ELISAs. The absence of detectable IgA antibodies could be caused by the partly long time period between symptom onset and blood collection in the TüCoV study, as IgA is an antibody, which appears in the early stage of immune reaction and has a short half-life of six days compared to the IgG antibody class [68]. Since the IgA ELISA is behind the IgG test in sensitivity and specificity, no additional value has been shown for this test. Tré-Hardy et. al. also found lower sensitivity in the IgA ELISAs compared with the IgG ELISA (94.9% compared to 89.7%) [69].

Regarding the negative samples, it is noticeable that a negative sample was considered positive in the IgG in-house test. This was a CoVNeg sample belonging to a health care worker who had reported symptoms such as fever in April 2020. Therefore, it may be that this participant had COVID-19 and thus, the IgG in-house ELISA may have detected the infection. This conclusion is somewhat hypothetical as the in-house IgG ELISA was the only one to detect the sample as

positive. EUROIMMUN IgG had classified the same sample as an intermediate positive sample and all other IgG ELISAs performed evaluated the sample as negative.

For IgA testing, the same samples were not considered false positives by the different ELISAs. The in-house IgA ELISA evaluated a sample as false positive, which was previously noticed by hemolytic discoloration. Hence, hemolysis might have had an impact on the in-house IgA ELISA. For more accurate evaluation of the tests, further examinations of the samples would be necessary to get closer to the truth of whether a sample is antibody positive or negative. Thus, it would be interesting to determine the neutralization titers of the samples.

It was also presented that industrial tests provide only semi-quantitative results, as they reached saturation, whereas the in-house ELISAs could be evaluated as quantitative assays. Therefore, it was difficult to examine a correlation between industrial and in-house ELISAs.

4.4.4 Influences on level of IgG antibodies

Fever and gustatory disorders had a statistically significant positive impact on the IgG antibody level (measured with the in-house ELISA) in the TÜCoV cohort. Hence, these symptoms served as predictors for high antibody levels. These findings were supported by Taziki B. et al. who observed a higher IgG antibody level in individuals with olfactory disorders [70]. Indeed, they did study olfactory disorders, whereas we related taste disorders to IgG antibody level. However, these symptoms are strongly overlapping because olfactory and taste disorders almost always occur simultaneously. Taste has only five qualities, namely sweet, sour, salty, bitter and umami. The sensations beyond that are created by our sense of smell. According to this, our ability to taste in a differentiated way is also affected when our sense of smell is disturbed [71]. The high level of antibodies in these patients may lead to a longer lasting immunity against SARS-CoV-2, as RBD-targeting IgG antibodies correlate with neutralizing antibody titers [33]. Therefore, our results indicate that fever and gustatory disorders may be predictors for a good immunity. However, so far no published work can be found that supports this hypothesis.

The t-test showed that participants without symptoms developed significantly fewer antibodies. This result is supported by the report of Rijkers et al., who found fewer antibodies in subjects with mild symptoms [28]. However, the group of recovered subjects who reported absolutely no symptoms was very small (n = 5). More cases would need to be tested to better estimate the effect of asymptomatic cases on the antibody development.

We expected a decreasing trend in antibody level with time, because the smallest time interval between symptom onset and blood draw was 23 days and ranged up to 173 days. Previous literature described a peak of IgG antibodies at day 27 [29]. Our data did not reflect a decrease of antibody levels over time. No downward trend was evident ($p>0.05$). Antibody levels appeared to be stable. This could be caused by the fact that we did not have extreme peaks of antibody levels in our cohort, as these were non-hospitalized subjects who tended to have a mild course. However, we cannot trace an exact course, as we had only one timepoint of blood collection. Nevertheless, current research findings support our analyses. These show stability of antibody levels for at least 6 six months [72,73].

Finally, we were able to complete the picture of the influence of taste disorders. It has been described that taste and smell disorders are associated with a higher viral load [45]. We showed evidence that taste disorders lead to higher antibody titers and may result in longer lasting immunity. Because the number of study participants was limited and a possible bias of the cohort may exist, further research on these associations is needed to support these findings.

4.4.5 Prediction of positive or negative ELISA results

RT-PCR remains the gold standard for diagnosis of COVID-19 [62]. German guidelines (January, 2021) consider a RT-PCR positive tested person as immune for the next six month and do not require further quarantines, even if the person became a first degree contact [74]. Since RT-PCR alone, as our study showed, was not a reliable indicator of SARS-CoV-2 antibodies (and thus immunity)

in our cohort the following question arised: Is this procedure based on the RT-PCR test result useful or should other parameters besides the test be used? Gustatory disorder has been shown to be an additional predictor of antibody positivity with a 4.3-fold higher probability of seroconversion in addition to a positive RT-PCR test. Unfortunately, a large 95% CI was shown, which is due to a low number of participants without taste disturbance (n = 26). Nevertheless, the result was significant and we can assume that RT-PCR positive convalescents who had taste disorders were more likely to appear positive in the RBD-seeking IgG antibody test than those who did not have taste disorders. The low number of RT-PCR positives without loss of taste indicated that this is a common symptom of COVID-19 in the first and second infection wave in Germany. The association of gustatory and olfactory disturbances and a positive RT-PCR had been extensively studied. These symptoms had been described as strong predictors of PCR positivity [42,43,75-77]. However, it was not related to antibody production up to now. In this work, we have obtained the additional information that RT-PCR positivity does not automatically lead to a seroconversion, but that positive RT-PCR and taste disorders together carry a higher probability of the availability of detectable and specific IgG antibodies against SARS-CoV-2.

Surprisingly, fever in addition to a positive RT-PCR result was not a statistically significant predictor, although it is a systemic response that would be expected to result in high antibody production. However, other factors seem to have more influence, which then diminish the effect of fever. In addition, the variable fever could also be biased because, especially during the beginning of the pandemic, in the first and the beginning of the second infection wave in Germany, when there was less testing capacity, fever was evaluated as a criterion for a RT-PCR test.

What then is the effect of taste disorders? What triggers high antibody production? Makaronidis et al. evaluated a CRF from which it became clear that, in the case of COVID-19, it was not a matter of ordinary taste disturbances that occur in a cold with a congested nose but infected individuals reported that they could not taste anything, not even very spicy or hot food [40]. This was quite interesting, because the spiciness of food is not determined by taste receptors, but by

nociceptors [78]. Xu et al. observed that there were many ACE2-expressing cells in the oral cavity, which were considered entry cells of the virus. Interestingly, they found higher expressions in tongue than in buccal and gingival tissues [79]. Accordingly, it can be assumed that infected persons with loss of taste have a high viral load in the oral cavity and that because of this high viral load the antibody titer is high, too.

4.5 Benefits of the in-house ELISA

At the end, as a summary, I would like to pursue the following questions. What are the benefits of the developed IgG in-house ELISA, what are its disadvantages and where can it be used?

As an advantage especially compared to RT-PCR I see that the ELISA has a high throughput rate. This means that in times of limited capacities it is possible to measure several samples at the same time. In addition, a serological test has the advantage over PCR that it allows the diagnosis of a passed through infection in a time frame where virus detection is no longer possible. Thus, in-house ELISA can be used to retrospectively investigate and assess a local outbreak of COVID-19.

By choosing the RBD antigen we have the possibility to measure with our test, by comparing antibodies before and after immunization, a reaction of the immune system to the vaccination. The quantitative determination of antibodies allows to study the course of antibody levels after infection or vaccination over time. In addition, the severity of the disease can be reflected by the level of the antibodies.

As a disadvantage I see, as already mentioned, that the test cannot differentiate between vaccine antibodies and antibodies after infection. An alternative would be a test with combinations of antibody classes and antigens to detect vaccine antibodies and achieve even better sensitivity [54,61].

I see different scenarios for the use of in-house ELISA, which have also changed over time. At the beginning of the pandemic, it was also used for diagnostics to retrospectively determine if infection occurred when RT-PCR was not available at the time of acute illness. Later, it became more about whether protective antibodies were present. And after vaccines came on the market, the question was

whether the vaccine produced specific antibodies.

Today, I see the application mainly in epidemiologic and serologic studies, as well as for when there is a clinical suspicion of COVID-19, but RT-PCR gives a negative result. In this case, the in-house ELISA could be used to exclude or confirm false negative RT-PCR results.

4.6 Conclusion

In conclusion, a quantitative IgG and IgA antibody screening test with high diagnostic quality has been developed. These ELISAs can compete very well with commercial tests in terms of sensitivity and specificity. In fact, the IgG ELISA outperformed all commercial tests in sensitivity without sacrificing specificity. Thus, RBD has been shown to be an antigen with high separability.

COVID-19 patients with fever and taste disorders had higher antibody levels than patients without these symptoms. Therefore, these symptoms may be an indicator for longer lasting immunity. RT-PRC positivity alone was found to not be a good predictor of seroconversions. But RT-PCR positive confirmed individuals with taste disorders had a 4.3-fold higher probability of seroconversion.

One quarter of all measured samples had no detectable antibodies. 6 out of 18 participants of the COV HCQ study (33.3%) did not produce any specific antibodies over time and partly may be false positive RT-PCR results.

5 Zusammenfassung

Die durch das 2019 neu aufgetretene Coronavirus, schweres-akutes-Atemwegssyndrom-Coronavirus Typ 2 (SARS-CoV-2), verursachte Pandemie beeinflusst unser aller Leben in den verschiedensten Bereichen. Der Wissensstand um das Virus und die Erkrankung wächst seit dem Beginn der Pandemie enorm. Zu Beginn unserer Arbeit im März 2020 war noch kein Antikörper-Suchtest kommerziell verfügbar und wenig über den Erkrankungsverlauf und die humorale Immunantwort bekannt. Inzwischen wurde die Kinetik der Antikörper gut untersucht. Wenig ist bisher darüber bekannt wie Symptome oder andere Faktoren mit der Höhe des Antikörperlevels assoziiert sind. Es fehlt auch die Information, welche Faktoren zusätzlich zur Reverse-Transkriptase-Polymerase-Kettenreaktion (RT-PCR) - Positivität eine höhere Wahrscheinlichkeit der Serokonversion und damit potentiell der Immunität vorhersagen können.

Um diesen Fragen nachzugehen und zur Etablierung eines eigenen Enzyme-linked Immunosorbent Assay (ELISA) im Institut, wurde ein quantitativer Immunglobulin G (IgG) und Immunglobulin A (IgA) rezeptorbindende Domäne (RBD)-SARS-CoV-2 ELISA entwickelt und mit mittlerweile verfügbaren kommerziellen ELISAs verglichen. Des Weiteren wurden 131 Studienteilnehmer:innen im Rahmen der TüCoV Studie rekrutiert, die eine Coronavirus-Krankheit-19 (COVID-19) durchgemacht haben. Ihnen wurde Blut abgenommen und sie füllten einen Fragebogen aus, der unter anderem Symptome abfragte.

Als Ergebnis entstand ein in-house IgG ELISA, welcher die Kommerziellen bezüglich der Sensitivität und Spezifität mit 84,3% und 100% übertrifft. Der IgA ELISA erreicht eine Sensitivität von 47,6% und eine Spezifität von 96,8%, jeweils bezogen auf 83 RT-PCR-positive Proben der TüCoV Studie und 66 negative Proben. In der statistischen Analyse konnte in der Kohorte ein positiver Zusammenhang von Fieber und Geschmacksstörungen mit der Höhe der IgG Antikörperlevel festgestellt werden, wobei das Symptom Geschmacksstörungen den stärksten Einfluss zeigte. Geschmacksstörungen erwiesen sich außerdem in Kombination mit der RT-PCR-Positivität, als guter Prädiktor für eine Serokonversion mit

einer 4,3 mal höheren Wahrscheinlichkeit für eine IgG Antikörper-Positivität.

Schwierigkeiten bei der Interpretation der ELISA-Resultate entstanden, da ungefähr ein Viertel der RT-PCR-positiven Proben von verschiedenen Studien beim Antikörper-Screening negativ blieben. Dies führte zum kritischen Hinterfragen von RT-PCR-positiven Ergebnissen, vor allem in Fällen, bei denen alle acht durchgeführten Antikörpersuchtests negativ blieben. Die in anderen Studien ermittelte Rate der falsch positiven RT-PCR Ergebnisse liegt deutlich unter einem Viertel. Demnach nehme ich an, dass noch andere Ursachen der Seronegativität dieser Beobachtung zugrunde liegen, wie beispielsweise der Zusammenhang von milden Verläufen und niedrigen Antikörpertitern. Insgesamt zeigen die Ergebnisse deutlich, dass ein positiver RT-PCR Test allein, zumindest für die untersuchte Kohorte, kein guter Indikator für eine Antikörperbildung ist.

Es wäre interessant in weiterführenden Studien zu überprüfen, ob sich die Ergebnisse bezüglich der Kombination von RT-PCR-Positivität und Geschmacksstörungen als Prädiktor für Seropositivität auch in anderen Kohorten mit mehreren Proband:innen reproduzieren lassen. Bezüglich der entwickelten Tests wären weitere Prüfungen, wie die Messung von Proben mit bekannten Konzentrationen spezifischer Antikörper sinnvoll, um die Genauigkeit der gemessenen Konzentrationen zu überprüfen.

6 Abstract

The Coronavirus disease 19 (COVID-19) pandemic has kept the world on tenterhooks for over a year. At the beginning of our work (by March 2020), very little was known about the new virus. No commercial antibody screening test was available yet. The aim of this doctoral thesis was to establish a Severe acute respiratory syndrome coronavirus type 2 (SARS-CoV-2) antibody test at the Institute for Tropical Medicine in Tübingen, which was then used to explore, whether there is a correlation of symptoms and antibody levels and which factors additional to a RT-PCR positive test predict antibody positivity.

For this purpose, an immunoglobulin G (IgG) and an immunoglobulin A (IgA) SARS-CoV2-RBD ELISA were developed and evaluated by comparing it to commercial tests. For the statistical analysis of IgG antibody levels, blood was drawn from 131 subjects with COVID-19 disease and a Case Report Form was administered.

The IgG ELISA outperformed commercial tests in comparison with a sensitivity of 84.3% and a specificity of 100% related to 83 RT-PCR-positive samples of the TüCoV study and 66 negative samples. The IgA ELISA reached 47.6% and 96.8% in sensitivity and specificity respectively. We have found that the symptoms of fever and loss of taste correlated positively with the level of antibody titers. Moreover, we found taste loss to be a factor additionally to RT-PCR positivity that increased the probability of seroconversion 4.3-fold, as about one quarter of the RT-PCR-confirmed infected test persons did not develop detectable antibodies at all. Thus, fever and especially loss of taste may be predictors for a stable immunity.

It would be interesting to verify in further studies whether the results regarding the combination of RT-PCR positivity and taste disturbance as a predictor for seropositivity can be reproduced in other cohorts with more subjects. Regarding the developed assays, further testing, such as measuring samples with known concentrations of specific antibodies, would be useful to verify the accuracy of the measured concentrations.

7 References

1. Wu D, Wu T, Liu Q, Yang Z. The SARS-CoV-2 outbreak: What we know. *Int J Infect Dis.* 2020;94:44-48. doi:10.1016/j.ijid.2020.03.004.
2. World Health Organization WHO Director-General's opening remarks at the media briefing on COVID-19 - 11 March 2020. https://www.who.int/director-general/speeches/detail/who-director-general-s-opening-remarks-at-the-media-briefing-on-covid-19---11-march-2020. Published 2020. Accessed 04th October, 2022.
3. World Health Organization Coronavirus Disease (COVID-19) Dashboard. Web site. https://covid19.who.int. Published 2021. Accessed January 03, 2021.
4. Dbouk T, Drikakis D. On coughing and airborne droplet transmission to humans. *Phys Fluids (1994).* 2020;32(5):053310. doi:10.1063/5.0011960.
5. Adams-Prassl A, Cloyne J, Costa Dias M, Parey M, Ziliak JP. The COVID-19 Economic Crisis. *Fisc Stud.* 2020;41(3):489-492. doi:10.1111/1475-5890.12248.
6. Jin Y, Sun T, Zheng P, An J. Mass quarantine and mental health during COVID-19: A meta-analysis. *J Affect Disord.* 2021;295:1335-1346. doi:10.1016/j.jad.2021.08.067.
7. De Kock JH, Ann Latham H, Cowden RG, et al. The mental health of NHS staff during the COVID-19 pandemic: two-wave Scottish cohort study. *BJPsych Open.* 2022;8(1):e23. doi:10.1192/bjo.2021.1079.
8. Leshem E, Lopman BA. Population immunity and vaccine protection against infection. *The Lancet.* 2021;397(10286):1685-1687. doi:10.1016/S0140-6736(21)00870-9.
9. Robert-Koch-Institut. Hinweise zur Testung von Patienten auf Infektion mit dem neuartigen Coronavirus SARS-CoV-2. Robert Koch Institute. COVID-19 (Coronavirus SARS-CoV-2) Web site. https://www.rki.de/DE/Content/InfAZ/N/Neuartiges_Coronavirus/Vorl_Testung_nCoV.html;jsessionid=A5764AF9F0F7BB99663B2D0F4C64DDB8.internet061?nn=2386228#doc13490982bodyText4. Published 2020. Updated December 23. Accessed December 23, 2020.
10. Grasselli G, Zangrillo A, Zanella A, et al. Baseline Characteristics and Outcomes of 1591 Patients Infected With SARS-CoV-2 Admitted to ICUs of the Lombardy Region, Italy. *Jama.* 2020;323(16):1574-1581. doi:10.1001/jama.2020.5394.
11. Weng LM, Su X, Wang XQ. Pain Symptoms in Patients with Coronavirus Disease (COVID-19): A Literature Review. *J Pain Res.* 2021;14:147-159. doi:10.2147/jpr.S269206.
12. Santos REA, da Silva MG, do Monte Silva MCB, et al. Onset and duration of symptoms of loss of smell/taste in patients with COVID-19: A systematic review. *Am J Otolaryngol.* 2021;42(2):102889. doi:10.1016/j.amjoto.2020.102889.
13. Fehr AR, Perlman S. Coronaviruses: an overview of their replication and pathogenesis. *Methods Mol Biol.* 2015;1282:1-23. doi:10.1007/978-1-4939-2438-7_1.

14. Nagesha S. N. , Ramesh B.N. , Pradeep C. , et al. SARS-CoV 2 spike protein S1 subunit as an ideal target for stable vaccines: A bioinformatic study. *Mater Today Proc.* 2022;49:904-912. doi:10.1016/j.matpr.2021.07.163.
15. Jackson CB, Farzan M, Chen B, Choe H. Mechanisms of SARS-CoV-2 entry into cells. *Nature Reviews Molecular Cell Biology.* 2022;23(1):3-20. doi:10.1038/s41580-021-00418-x.
16. Li F. Structure, Function, and Evolution of Coronavirus Spike Proteins. *Annu Rev Virol.* 2016;3(1):237-261. doi:10.1146/annurev-virology-110615-042301.
17. Hamming I, Timens W, Bulthuis ML, Lely AT, Navis G, van Goor H. Tissue distribution of ACE2 protein, the functional receptor for SARS coronavirus. A first step in understanding SARS pathogenesis. *J Pathol.* 2004;203(2):631-637. doi:10.1002/path.1570.
18. Dai L, Gao GF. Viral targets for vaccines against COVID-19. *Nature Reviews Immunology.* 2021;21(2):73-82. doi:10.1038/s41577-020-00480-0.
19. Scheiblauer H, Nübling CM, Wolf T, et al. Antibody response to SARS-CoV-2 for more than one year − kinetics and persistence of detection are predominantly determined by avidity progression and test design. *Journal of Clinical Virology.* 2022;146:105052. doi:10.1016/j.jcv.2021.105052.
20. Vollmar A, Dingermann T. I.3. Die erworbene Immunantwort. In: *Immunologie - Grundlagen und Wirkstoffe.* 1st ed.: Wissenschaftliche Verlagsgesellschaft mbH Stuttgart; 2005:33-84.
21. Murphy K, Weaver C. Verteilung und Funktionen der Immunglobulinisotypen. In. *Janeway's immunobiology*. 9th ed. Berlin: Springer Spektrum; 2018:549-557.
22. Vollmar A, Dingermann T. II.5. Seren und Immunglobuline. In: *Immunologie - Grundlagen und Wirkstoffe.* 1st ed.: Wissenschaftliche Verlagsgesellschaft mbH Stuttgart; 2005:301-303.
23. Lalkhen AG, McCluskey A. Clinical tests: sensitivity and specificity. *Continuing Education in Anaesthesia Critical Care & Pain.* 2008;8(6):221-223. doi:10.1093/bjaceaccp/mkn041.
24. Brochot E, Demey B, Touzé A, et al. Anti-spike, Anti-nucleocapsid and Neutralizing Antibodies in SARS-CoV-2 Inpatients and Asymptomatic Individuals. *Front Microbiol.* 2020;11. doi:10.3389/fmicb.2020.584251.
25. McAndrews KM, Dowlatshahi DP, Dai J, et al. Heterogeneous antibodies against SARS-CoV-2 spike receptor binding domain and nucleocapsid with implications for COVID-19 immunity. *JCI Insight.* 2020;5(18). doi:10.1172/jci.insight.142386.
26. Post N, Eddy D, Huntley C, et al. Antibody response to SARS-CoV-2 infection in humans: A systematic review. *PLoS One.* 2020;15(12):e0244126. doi:10.1371/journal.pone.0244126.
27. Wang Y, Zhang L, Sang L, et al. Kinetics of viral load and antibody response in relation to COVID-19 severity. *J Clin Invest.* 2020;130(10):5235-5244. doi:10.1172/jci138759.
28. Rijkers G, Murk JL, Wintermans B, et al. Differences in Antibody Kinetics and Functionality Between Severe and Mild Severe Acute Respiratory Syndrome Coronavirus 2 Infections. *J Infect Dis.* 2020;222(8):1265-1269. doi:10.1093/infdis/jiaa463.

29. Yin S, Tong X, Huang A, et al. Longitudinal anti-SARS-CoV-2 antibody profile and neutralization activity of a COVID-19 patient. *J Infect.* 2020;81(3):e31-e32. doi:10.1016/j.jinf.2020.06.076.
30. Sun B, Feng Y, Mo X, et al. Kinetics of SARS-CoV-2 specific IgM and IgG responses in COVID-19 patients. *Emerg Microbes Infect.* 2020;9(1):940-948. doi:10.1080/22221751.2020.1762515.
31. Yao X-Y, Liu W, Li Z-Y, et al. Neutralizing and binding antibody kinetics of COVID-19 patients during hospital and convalescent phases. *medRxiv.* 2020. doi:10.1101/2020.07.18.20156810.
32. Premkumar L, Segovia-Chumbez B, Jadi R, et al. The RBD Of The Spike Protein Of SARS-Group Coronaviruses Is A Highly Specific Target Of SARS-CoV-2 Antibodies But Not Other Pathogenic Human and Animal Coronavirus Antibodies. *medRxiv : the preprint server for health sciences.* 2020. doi:10.1101/2020.05.06.20093377.
33. To KK-W, Tsang OT-Y, Leung W-S, et al. Temporal profiles of viral load in posterior oropharyngeal saliva samples and serum antibody responses during infection by SARS-CoV-2: an observational cohort study. *The Lancet Infectious Diseases.* 2020;20(5):565-574. doi:10.1016/S1473-3099(20)30196-1.
34. Sidiq Z, Hanif M, Dwivedi KK, Chopra KK. Benefits and limitations of serological assays in COVID-19 infection. *Indian J Tuberc.* 2020;67(4s):163-166. doi:10.1016/j.ijtb.2020.07.034.
35. Gong F, Wei H-x, Li Q, Liu L, Li B. Evaluation and Comparison of Serological Methods for COVID-19 Diagnosis. *Frontiers in Molecular Biosciences.* 2021;8. doi:10.3389/fmolb.2021.682405.
36. Lequin RM. Enzyme immunoassay (EIA)/enzyme-linked immunosorbent assay (ELISA). *Clin Chem.* 2005;51(12):2415-2418. doi:10.1373/clinchem.2005.051532.
37. Butler JE. Enzyme-linked immunosorbent assay. *J Immunoassay.* 2000;21(2-3):165-209. doi:10.1080/01971520009349533.
38. Raem A, Rauch P. *Immunoassays; Kapitel 8. Auswertung und Validierung* 1st ed. München: ELSEVIER Spektrum Akademischer Verlag; 2006: 275-291.
39. Lee Y, Min P, Lee S, Kim SW. Prevalence and Duration of Acute Loss of Smell or Taste in COVID-19 Patients. *J Korean Med Sci.* 2020;35(18):e174. doi:10.3346/jkms.2020.35.e174.
40. Makaronidis J, Mok J, Balogun N, et al. Seroprevalence of SARS-CoV-2 antibodies in people with an acute loss in their sense of smell and/or taste in a community-based population in London, UK: An observational cohort study. *PLoS Med.* 2020;17(10):e1003358. doi:10.1371/journal.pmed.1003358.
41. Hannum ME, Koch RJ, Ramirez VA, et al. Taste loss as a distinct symptom of COVID-19: A systematic review and meta-analysis. *medRxiv.* 2021. doi:10.1101/2021.10.09.21264771.
42. Roland LT, Gurrola JG, 2nd, Loftus PA, Cheung SW, Chang JL. Smell and taste symptom-based predictive model for COVID-19 diagnosis. *Int Forum Allergy Rhinol.* 2020;10(7):832-838. doi:10.1002/alr.22602.
43. Clemency BM, Varughese R, Scheafer DK, et al. Symptom Criteria for COVID-19 Testing of Heath Care Workers. *Acad Emerg Med.* 2020;27(6):469-474. doi:10.1111/acem.14009.

44. Callejon-Leblic MA, Moreno-Luna R, Del Cuvillo A, et al. Loss of Smell and Taste Can Accurately Predict COVID-19 Infection: A Machine-Learning Approach. *Journal of Clinical Medicine.* 2021;10(4):570. doi:10.3390/jcm10040570.
45. Nakagawara K, Masaki K, Uwamino Y, et al. Acute onset olfactory/taste disorders are associated with a high viral burden in mild or asymptomatic SARS-CoV-2 infections. *Int J Infect Dis.* 2020;99:19-22. doi:10.1016/j.ijid.2020.07.034.
46. Thomsson O, Ström-Holst B, Sjunnesson Y, Bergqvist A-S. Validation of an enzyme-linked immunosorbent assay developed for measuring cortisol concentration in human saliva and serum for its applicability to analyze cortisol in pig saliva. *Acta Vet Scand.* 2014;56(1):55-55. doi:10.1186/s13028-014-0055-1.
47. Amanat F, Stadlbauer D, Strohmeier S, et al. A serological assay to detect SARS-CoV-2 seroconversion in humans. *Nature Medicine.* 2020;26(7):1033-1036. doi:10.1038/s41591-020-0913-5.
48. Pruslin FH, To SE, Winston R, Rodman TC. Caveats and suggestions for the ELISA. *J Immunol Methods.* 1991;137(1):27-35. doi:10.1016/0022-1759(91)90390-2.
49. Krähling V, Halwe S, Rohde C, et al. Development and characterization of an indirect ELISA to detect SARS-CoV-2 spike protein-specific antibodies. *Journal of Immunological Methods.* 2021;490:112958. doi:10.1016/j.jim.2021.112958.
50. INTERNATIONAL CONFERENCE ON HARMONISATION OF TECHNICAL REQUIREMENTS VALIDATION OF ANALYTICAL PROCEDURES: TEXT AND METHODOLOGY. https://database.ich.org/sites/default/files/Q2%28R1%29%20Guideline.pdf. Published 2005. Accessed October 12th, 2022.
51. Armbruster DA, Pry T. Limit of blank, limit of detection and limit of quantitation. *Clin Biochem Rev.* 2008;29 Suppl 1(Suppl 1):S49-52. Published 2008/10/15.
52. Wallwitz J, Aigner P, Gadermaier E, et al. Validation of an enzyme-linked immunosorbent assay (ELISA) for quantification of endostatin levels in mice as a biomarker of developing glomerulonephritis. *PLoS ONE.* 2019;14(8): e0220935. doi:10.1371/journal.pone.0220935.
53. Stadlbauer D, Amanat F, Chromikova V, et al. SARS-CoV-2 Seroconversion in Humans: A Detailed Protocol for a Serological Assay, Antigen Production, and Test Setup. *Curr Protoc Microbiol.* 2020;57(1):e100. doi:10.1002/cpmc.100.
54. Machado BAS, Hodel KVS, Barbosa-Júnior VG, Soares MBP, Badaró R. The Main Molecular and Serological Methods for Diagnosing COVID-19: An Overview Based on the Literature. *Viruses.* 2021;13. doi:10.3390/v13010040.
55. Faes C, Abrams S, Van Beckhoven D, et al. Time between Symptom Onset, Hospitalisation and Recovery or Death: Statistical Analysis of Belgian COVID-19 Patients. *Int J Environ Res Public Health.* 2020;17(20):7560. doi:10.3390/ijerph17207560.
56. Lei Q, Li Y, Hou HY, et al. Antibody dynamics to SARS-CoV-2 in asymptomatic COVID-19 infections. *Allergy.* 2020. doi:10.1111/all.14622.

57. Dijkman R, Jebbink MF, El Idrissi NB, et al. Human coronavirus NL63 and 229E seroconversion in children. *J Clin Microbiol.* 2008;46(7):2368-2373. doi:10.1128/jcm.00533-08.
58. Lv H, Wu NC, Tsang OT, et al. Cross-reactive Antibody Response between SARS-CoV-2 and SARS-CoV Infections. *Cell Rep.* 2020;31(9):107725. doi:10.1016/j.celrep.2020.107725.
59. Piccoli L, Park Y-J, Tortorici MA, et al. Mapping Neutralizing and Immunodominant Sites on the SARS-CoV-2 Spike Receptor-Binding Domain by Structure-Guided High-Resolution Serology. *Cell.* 2020. doi:10.1016/j.cell.2020.09.037.
60. Beck EJ, Hsieh YH, Fernandez RE, et al. Differentiation of Individuals Previously Infected with and Vaccinated for SARS-CoV-2 in an Inner-City Emergency Department. *J Clin Microbiol.* 2022;60(3):e0239021. doi:10.1128/jcm.02390-21.
61. Brochot E, Souplet V, Follet P, et al. A multiplex serological assay for the characterization of IgG immune response to SARS-CoV-2. *PLoS ONE.* 2022;17(1): e0262311. doi:10.1371/journal.pone.0262311.
62. Robert-Koch Institut DIrekter Erregernachweis durch RT-PCR. https://www.rki.de/DE/Content/InfAZ/N/Neuartiges_Coronavirus/Vorl_Testung_nCoV.html;jsessionid=68A18555E672754F8FB30948B7869922.internet062?nn=13490888#doc13490982bodyText11. Published 2022. Updated 07.03.2022. Accessed 14.03.2022, 2022.
63. Sethuraman N, Jeremiah SS, Ryo A. Interpreting Diagnostic Tests for SARS-CoV-2. *JAMA.* 2020;323(22):2249-2251. doi:10.1001/jama.2020.8259.
64. Cohen AN, Kessel B, Milgroom MG. Diagnosing COVID-19 infection: the danger of over-reliance on positive test results. *medRxiv.* 2020. doi:10.1101/2020.04.26.20080911.
65. Surkova E, Nikolayevskyy V, Drobniewski F. False-positive COVID-19 results: hidden problems and costs. *The Lancet Respiratory Medicine.* 2020;8(12):1167-1168. doi:10.1016/S2213-2600(20)30453-7.
66. Healy B, Khan A, Metezai H, Blyth I, Asad H. The impact of false positive COVID-19 results in an area of low prevalence. *Clinical Medicine.* 2020:0839. doi:10.7861/clinmed.2020-0839.
67. Robert-Koch Institut Durchführung der COVID-19-Impfung. https://www.rki.de/SharedDocs/FAQ/COVID-Impfen/FAQ_Liste_Durchfuehrung_Impfung.html#FAQId16072404. Published 2021. Updated 18.10.2021. Accessed 22.10.2021, 2021.
68. Dietzen DJ. 13 - Amino Acids, Peptides, and Proteins. In: Rifai N, Horvath AR, Wittwer CT, eds. *Principles and Applications of Molecular Diagnostics.* Elsevier; 2018:345-380.
69. Tré-Hardy M, Wilmet A, Beukinga I, et al. Analytical and clinical validation of an ELISA for specific SARS-CoV-2 IgG, IgA, and IgM antibodies. *J Med Virol.* 2021;93(2):803-811. doi:10.1002/jmv.26303.
70. Taziki Balajelini MH, Vakili MA, Saeidi M, Tabarraei A, Hosseini SM. Using Anti-SARS-CoV-2 IgG and IgM Antibodies to Detect Outpatient Cases with Olfactory and Taste Disorders Suspected as Mild Form of COVID-19: a Retrospective Survey. *SN Compr Clin Med.* 2020:1-7. doi:10.1007/s42399-020-00623-3.

71. Neto FXP, Targino MN. Sensorial abnormalities: Smell and taste. *Thieme.* 2011:3. doi:10.1590/S1809-48722011000300014.
72. Pradenas E, Trinité B, Urrea V, et al. Stable neutralizing antibody levels 6 months after mild and severe COVID-19 episodes. *Med (N Y).* 2021;2(3):313-320.e314. doi:10.1016/j.medj.2021.01.005.
73. Ortega N, Ribes M, Vidal M, et al. Seven-month kinetics of SARS-CoV-2 antibodies and role of pre-existing antibodies to human coronaviruses. *Nature Communications.* 2021;12(1):4740. doi:10.1038/s41467-021-24979-9.
74. Robert-Koch-Institut. 3.1.2. Empfohlenes Management von Kontaktpersonen der Kategorie 1. Robert Koch-Institute. https://www.rki.de/DE/Content/InfAZ/N/Neuartiges_Coronavirus/Kontaktperson/Management.html;jsessionid=11FDF25C897680C3DE00FF45873A4327.internet062?nn=13490888#doc13516162bodyText10. Published 2020. Updated 21.12.2020. Accessed January 06, 2021.
75. Beltrán-Corbellini Á, Chico-García JL, Martínez-Poles J, et al. Acute-onset smell and taste disorders in the context of COVID-19: a pilot multicentre polymerase chain reaction based case-control study. *Eur J Neurol.* 2020;27(9):1738-1741. doi:10.1111/ene.14273.
76. Dawson P, Rabold EM, Laws RL, et al. Loss of Taste and Smell as Distinguishing Symptoms of COVID-19. *Clin Infect Dis.* 2020. doi:10.1093/cid/ciaa799.
77. Benazzo M, Cassaniti I, Maiorano E, et al. SARS-CoV-2 Virologic and Immunologic Correlates in Patients with Olfactory and Taste Disorders. *Microorganisms.* 2020;8(7). doi:10.3390/microorganisms8071052.
78. Simon SA, de Araujo IE. The salty and burning taste of capsaicin. *J Gen Physiol.* 2005;125(6):531-534. doi:10.1085/jgp.200509329.
79. Xu H, Zhong L, Deng J, et al. High expression of ACE2 receptor of 2019-nCoV on the epithelial cells of oral mucosa. *International Journal of Oral Science.* 2020;12(1):8. doi:10.1038/s41368-020-0074-x.

8 Erklärung zum Eigenanteil

Die Arbeit wurde in der Klinik / Institut für Tropenmedizin, Reisemedizin und Humanparasitologie unter Betreuung von Professor Dr. Benjamin Mordmüller durchgeführt.

Die Konzeption der Studie erfolgte in Zusammenarbeit mit Dr. rer. nat. Rolf Fendel, Gruppenleiter.

Die Versuche wurden, nach Einarbeitung durch die Labormitglieder Constanze Heinzel, Karoline Lenckner und Dr. Rolf Fendel von mir durchgeführt. Die Klonierung des RBDs in den CMV Vektor wurde von Andrea Weierich durchgeführt.

Die statistische Auswertung erfolgte nach Beratung durch das Institut für Biometrie durch mich.

Ich versichere, das Manuskript selbständig verfasst zu haben und keine weiteren als die von mir angegebenen Quellen verwendet zu haben.

Tübingen, den 08.12.2022

9 Appendix

Materials

Chemicals and reagents

All chemicals and reagents were purchased from Merck (Darmstadt), Sigma-Aldrich (Munich), Carl Roth (Karlsruhe), Honeywell (Morristown, US), Sarstedt (Nümbrecht), Serva (Heidelberg), GE healthcare (Munich), Gibco (Carlsbad, USA), Candor Bioscience GmbH (Wangen).

Biologicals, plasmids and antibodies used throughout this thesis, are listed below.

Table 8: Biologicals and Plasmids used throughout this thesis.

Biologicals/ Plasmids	Company	Cat.
Stellar competent cells, E. coli HST08 strain	Takara	#636766
Top 10 chemically competent cells, E. coli	Thermo Fischer	#C404010
Expi293F™ Cells, Human embryonal kidney cells, 1 ml aliquot at $1*10^7$ cells/ml, frozen by Freia-Raphaella Lorenz		
pCAGGs-CoV2-RBD	obtained through BEI Resources	#52309
CMV-CoV2-RBD cloned by Andrea Weierich		
GFP vector 1.87 µg/µl; Maxiprep on 15.02.2019 by Martina Rausch		

Sequences of the CMV-Sport-CoV-2-RBD Plasmid:

LOCUS pCMV_Sport_Albmod_RBD_Spike_TwinSH 5182 bp DNA circular UNA 15-Feb.-2019
DEFINITION
FEATURES Location/Qualifiers
Vector join(1..693,1558..5182)
/origin="pCMV_Sport_bGal (7.854bp linear)Target vector:
from start of vector to HindIII cut at 693^694 and from
EcoRI cut at 4229^4230 to end of vector,
4.318bpOrientation: originalPlus strand 5': no
changePlus strand 3': no changeMinus strand 5': no
changeMinus strand 3': no change"
Vector join(1558..5182,1..693)
/origin="pCMV_Sport_Alb_Pfs230_CO (4.882bp
circular)Target vector: from EcoRI cut at 1257^1258 to

HindIII cut at 693^694, 4.318bpOrientation: originalPlus
strand 5': no changePlus strand 3': no changeMinus
strand 5': no changeMinus strand 3': no change"
Vector join(1498..5182,1..818)
/origin="pCMV_Sport_Albmod_Pfs230_TwinSH (4.945bp
circular)Target vector: from XbaI cut at 1260^1261 to
NotI cut at 818^819, 4.503bpOrientation: originalPlus
strand 5': no changePlus strand 3': no changeMinus
strand 5': no changeMinus strand 3': no change"
CDS complement(699..1550)
/cds_type="ORF"
/note="Length: 852"
/note="Found at strand: negative"
/note="Start codon: ATG"
misc_feature complement(<823..>1501)
/note="Spike_protein_RBP_319-541"
source complement(<823..>1501)
/organism="synthetic DNA construct"
/mol_type="other DNA"
CDS complement(3578..4438)
/cds_type="ORF"
/note="Length: 861"
/note="Found at strand: negative"
/note="Start codon: ATG"
CDS complement(3578..4438)
/cds_type="ORF"
/note="Length: 861"
/note="Found at strand: negative"
/note="Start codon: ATG"
ORIGIN
1 CATTCGCCAT TCAGGCTGCG CAACTGTTGG GAAGGGCGAT CGGTGCGGGC CTCTTCGCTA
61 TTACGCCAGC CAATACGCAA ACCGCCTCTC CCCGCGCGTT GGCCGATTCA TTAATGCAGG
121 ATCGATCCAG ACATGATAAG ATACATTGAT GAGTTTGGAC AAACCACAAC TAGAATGCAG
181 TGAAAAAAAT GCTTTATTTG TGAAATTTGT GATGCTATTG CTTTATTTGT AACCATTATA
241 AGCTGCAATA AACAAGTTAA CAACAACAAT TGCATTCATT TTATGTTTCA GGTTCAGGGG
301 GAGGTGTGGG AGGTTTTTTA AAGCAAGTAA AACCTCTACA AATGTGGTAT GGCTGATTAT
361 GATCATGAAC AGACTGTGAG GACTGAGGGG CCTGAAATGA GCCTTGGGAC TGTGAATCTA
421 AAATACACAA ACAATTAGAA TCACTAGCTC CTGTGTATAA TATTTTCATA AATCATACTC
481 AGTAAGCAAA ACTCTCAAGC AGCAAGCATA TGCAGCTAGT TTAACACATT ATACACTTAA
541 AAATTTTATA TTTACCTTAG AGCTTTAAAT CTCTGTAGGT AGTTTGTCCA ATTATGTCAC
601 ACCACAGAAG TAAGGTTCCT TCACAAAGAT CCCAAGCTAG CTTATAATAC GACTCACTAT
661 AGGGAGAGAG CTATGACGTC GCATGCACGC GTAAGCTTTC AGTGATGATG GTGATGGTGG
721 TGGTGGTCGA CTTTTTCGAA CTGCGGGTGG CTCCACGCCG AACCTCCCGA TCCACCTCCG

781 GAACCTCCAC CTTTCTCGAA CTGCGGGTGG CTCCACGCGG CCGCAAAGTT CACACACTTG
841 TTCTTCACCA GGTTTGTGCT CTTCTTTGGT CCGCACACTG TGGCGGGGGC GTGCAGCAGC
901 TCAAAGCTCA GCACCACCAC CCTGTAGGGC TGGTAGCCCA CGCCGTTGGT AGGCTGGAAG
961 CCGTAGCTCT GCAGAGGGAA GTAACAGTTA AAGCCCTCCA CGCCATTACA GGGTGTGCTG
1021 CCGGCCTGGT AGATCTCTGT GGAGATGTCT CTCTCAAAAG GCTTCAGATT GCTCTTCCTG
1081 AACAGCCTGT ACAGGTAGTT GTAGTTGCCG CCCACCTTGC TGTCCAGGTT ATTGCTATTC
1141 CAGGCGATCA CACAGCCGGT GAAATCATCA GGCAGCTTGT AGTTGTAGTC GGCGATCTTG
1201 CCTGTCTGGC CAGGGGCGAT CTGCCTCACC TCGTCGCCTC TGATCACAAA GCTATCGGCG
1261 TACACGTTTG TGAAGCACAG ATCGTTCAGC TTGGTGGGGC TCACGCCGTA GCACTTGAAG
1321 GTGGAAAAGG AGGCGCTGTT GTACAGCACG CTGTAGTCGG CCACACAGTT GCTGATCCTC
1381 TTCCTGTTCC AGGCGTACAC GGAGGCGAAT CTGGTGGCGT TAAACACCTC GCCAAAGGGA
1441 CACAGATTGG TGATGTTAGG GAATCTCACG ATGGACTCTG TAGGCTGCAC CCTGGCTCTA
1501 GAGGAGCTGC TGAACAGGAA CAGCAGGCTG ATAAAGGTGA CCCATTTCAT GGTGGCGAAT
1561 TCCGGACCGG TACCTGCAGG CGTACCTTCT ATAGTGTCAC CTAAATAGCT TTTTGCAAAA
1621 GCCTAGGCTA GAGTCCGGAG GCTGGATCGG TCCCGGTGTC TTCTATGGAG GTCAAAACAG
1681 CGTGGATGGC GTCTCCAGGC GATCTGACGG TTCACTAAAC GAGCTCTGCT TATATAGACC
1741 TCCCACCGTA CACGCCTACC GCCCATTTGC GTCAATGGGG CGGAGTTGTT ACGACATTTT
1801 GGAAAGTCCC GTTGATTTTG GTGCCAAAAC AAACTCCCAT TGACGTCAAT GGGGTGGAGA
1861 CTTGGAAATC CCCGTGAGTC AAACCGCTAT CCACGCCCAT TGATGTACTG CCAAAACCGC
1921 ATCACCATGG TAATAGCGAT GACTAATACG TAGATGTACT GCCAAGTAGG AAAGTCCCAT
1981 AAGGTCATGT ACTGGGCATA ATGCCAGGCG GGCCATTTAC CGTCATTGAC GTCAATAGGG
2041 GGCGTACTTG GCATATGATA CACTTGATGT ACTGCCAAGT GGGCAGTTTA CCGTAAATAC
2101 TCCACCCATT GACGTCAATG GAAAGTCCCT ATTGGCGTTA CTATGGGAAC ATACGTCATT
2161 ATTGACGTCA ATGGGCGGGG GTCGTTGGGC GGTCAGCCAG GCGGGCCATT TACCG-TAAGT
2221 TATGTAACGA CCTGCACGAT GCTGTTTCCT GTGTGAAATT GTTATCCGCT CACAATTCCA
2281 CACATTATAC GAGCCGGAAG CTATAAAGTG TAAAGCCTGG GGTGCCTAAT GAGTGAAAGG
2341 GCCTCGTATC ACGCCTATTT TTATAGGTTA ATGTCATGAT AATAATGGTT TCTTAGACGT
2401 CAGGTGGCAC TTTTCGGGGA AATGTGCGCG GAACCCCTAT TTGTTTATTT TTCTAAATAC
2461 ATTCAAATAT GTATCCGCTC ATGAGACAAT AACCCTGATA AATGCTTCAA TAATATTGAA
2521 AAACGCGCGA ATTGCAAGCT CTGCATTAAT GAATCGGCCA ACGCGCGGGG AGAGGCGGTT
2581 TGCGTATTGG GCGCTCTTCC GCTTCCTCGC TCACTGACTC GCTGCGCTCG GTCGTTCGGC
2641 TGCGGCGAGC GGTATCAGCT CACTCAAAGG CGGTAATACG GTTATCCACA GAATCAGGGG
2701 ATAACGCAGG AAAGAACATG TGAGCAAAAG GCCAGCAAAA GGCCAGGAAC CGTAAAAAGG
2761 CCGCGTTGCT GGCGTTTTTC CATAGGCTCC GCCCCCCTGA CGAGCATCAC AAAAATCGAC
2821 GCTCAAGTCA GAGGTGGCGA AACCCGACAG GACTATAAAG ATACCAGGCG TTTCCCCCTG
2881 GAAGCTCCCT CGTGCGCTCT CCTGTTCCGA CCCTGCCGCT TACCGGATAC CTGTCCGCCT
2941 TTCTCCCTTC GGGAAGCGTG GCGCTTTCTC AATGCTCACG CTGTAGGTAT CTCAGTTCGG
3001 TGTAGGTCGT TCGCTCCAAG CTGGGCTGTG TGCACGAACC CCCCGTTCAG CCCGAC-CGCT
3061 GCGCCTTATC CGGTAACTAT CGTCTTGAGT CCAACCCGGT AAGACACGAC TTATCGCCAC

3121 TGGCAGCAGC CACTGGTAAC AGGATTAGCA GAGCGAGGTA TGTAGGCGGT GCTACAGAGT

3181 TCTTGAAGTG GTGGCCTAAC TACGGCTACA CTAGAAGGAC AGTATTTGGT ATCTGCGCTC

3241 TGCTGAAGCC AGTTACCTTC GGAAAAAGAG TTGGTAGCTC TTGATCCGGC AAACAAACCA

3301 CCGCTGGTAG CGGTGGTTTT TTTGTTTGCA AGCAGCAGAT TACGCGCAGA AAAAAAGGAT

3361 CTCAAGAAGA TCCTTTGATC TTTTCTACGG GGTCTGACGC TCAGTGGAAC GAAAACTCAC

3421 GTTAAGGGAT TTTGGTCATG CCATAACTTC GTATAGCATA CATTATACGA AGTTATGGCA

3481 TGAGATTATC AAAAAGGATC TTCACCTAGA TCCTTTTAAA TTAAAAATGA AGTTTTAAAT

3541 CAATCTAAAG TATATATGAG TAAACTTGGT CTGACAGTTA CCAATGCTTA ATCAGTGAGG

3601 CACCTATCTC AGCGATCTGT CTATTTCGTT CATCCATAGT TGCCTGACTC CCCGTCGTGT

3661 AGATAACTAC GATACGGGAG GGCTTACCAT CTGGCCCCAG TGCTGCAATG ATACCGCGAG

3721 ACCCACGCTC ACCGGCTCCA GATTTATCAG CAATAAACCA GCCAGCCGGA AG-GGCCGAGC

3781 GCAGAAGTGG TCCTGCAACT TTATCCGCCT CCATCCAGTC TATTAATTGT TGCCGGGAAG

3841 CTAGAGTAAG TAGTTCGCCA GTTAATAGTT TGCGCAACGT TGTTGCCATT GCTACAGGCA

3901 TCGTGGTGTC ACGCTCGTCG TTTGGTATGG CTTCATTCAG CTCCGGTTCC CAACGATCAA

3961 GGCGAGTTAC ATGATCCCCC ATGTTGTGCA AAAAAGCGGT TAGCTCCTTC GGTCCTCCGA

4021 TCGTTGTCAG AAGTAAGTTG GCCGCAGTGT TATCACTCAT GGTTATGGCA GCACTGCATA

4081 ATTCTCTTAC TGTCATGCCA TCCGTAAGAT GCTTTTCTGT GACTGGTGAG TACTCAACCA

4141 AGTCATTCTG AGAATAGTGT ATGCGGCGAC CGAGTTGCTC TTGCCCGGCG TCAATACGGG

4201 ATAATACCGC GCCACATAGC AGAACTTTAA AAGTGCTCAT CATTGGAAAA CGTTCTTCGG

4261 GGCGAAAACT CTCAAGGATC TTACCGCTGT TGAGATCCAG TTCGATGTAA CCCACTCGTG

4321 CACCCAACTG ATCTTCAGCA TCTTTTACTT TCACCAGCGT TTCTGGGTGA GCAAAAACAG

4381 GAAGGCAAAA TGCCGCAAAA AAGGGAATAA GGGCGACACG GAAATGTTGA ATACTCATAC

4441 TCTTCCTTTT TCAATATTAT TGAAGCATTT ATCAGGGTTA TTGTCTCATG CCAGGGGTGG

4501 GCACACATAT TTGATACCAG CGATCCCTAC ACAGCACATA ATTCAATGCG ACTTCCCTCT

4561 ATCGCACATC TTAGACCTTT ATTCTCCCTC CAGCACACAT CGAAGCTGCC GAGCAAGCCG

4621 TTCTCACCAG TCCAAGACCT GGCATGAGCG GATACATATT TGAATGTATT TAGAAAAATA

4681 AACAAATAGG GGTTCCGCGC ACATTTCCCC GAAAAGTGCC ACCTGAAATT GTAAACGTTA

4741 ATATTTTGTT AAAATTCGCG TTAAATTTTT GTTAAATCAG CTCATTTTTT AACCAATAGG

4801 CCGAAATCGG CAAAATCCCT TATAAATCAA AAGAATAGAC CGAGATAGGG TTGAGTGTTG

4861 TTCCAGTTTG GAACAAGAGT CCACTATTAA AGAACGTGGA CTCCAACGTC AAAGGGCGAA

4921 AAACCGTCTA TCAGGGCGAT GGCCCACTAC GTGAACCATC ACCCTAATCA AGTTTTTTGG

4981 GGTCGAGGTG CCGTAAAGCA CTAAATCGGA ACCCTAAAGG GAGCCCCCGA TTTAGAGCTT

5041 GACGGGGAAA GCCGGCGAAC GTGGCGAGAA AGGAAGGGAA GAAAGCGAAA GGAGCGGGCG

5101 CTAGGGCGCT GGCAAGTGTA GCGGTCACGC TGCGCGTAAC CACCACACCC GCCGCGCTTA

5161 ATGCGCCGCT ACAGGGCGCG TC

Sequences of the pCAGGS-SARS-CoV-2-RBD plasmid

>pCAGGs_Spike_RBD .

GTCGACATTGATTATTGACTAGTTATTAATAGTAATCAATTACGGGGTCATTAGTTCATA
GCCCATATATGGAGTTCCGCGTTACATAACTTACGGTAAATGGCCCGCCTGGCTGACCGC
CCAACGACCCCCGCCCATTGACGTCAATAATGACGTATGTTCCCATAGTAACGCCAATAG
GGACTTTCCATTGACGTCAATGGGTGGACTATTTACGGTAAACTGCCCACTTGGCAGTAC
ATCAAGTGTATCATATGCCAAGTACGCCCCCTATTGACGTCAATGACGGTAAATGGCCCG
CCTGGCATTATGCCCAGTACATGACCTTATGGGACTTTCCTACTTGGCAGTACATCTACG
TATTAGTCATCGCTATTACCATGGGTCGAGGTGAGCCCCACGTTCTGCTTCACTCTCCCC
ATCTCCCCCCCCTCCCCACCCCCAATTTTGTATTTATTTATTTTTTAATTATTTTGTGCA
GCGATGGGGGCGGGGGGGGGGGGGGCGCGCGCCAGGCGGGGCGGGGCGGGGCGAGGGGCG
GGGCGGGGCGAGGCGGAGAGGTGCGGCGGCAGCCAATCAGAGCGGCGCGCTCCGAAAGTT
TCCTTTTATGGCGAGGCGGCGGCGGCGGCGGCCCTATAAAAAGCGAAGCGCGCGGCGGGC
GGGAGTCGCTGCGTTGCCTTCGCCCCGTGCCCCGCTCCGCGCCGCCTCGCGCCGCCCGCC
CCGGCTCTGACTGACCGCGTTACTCCCACAGGTGAGCGGGCGGGACGGCCCTTCTCCTCC
GGGCTGTAATTAGCGCTTGGTTTAATGACGGCTCGTTTCTTTTCTGTGGCTGCGTGAAAG
CCTTAAAGGGCTCCGGGAGGGCCCTTTGTGCGGGGGGGAGCGGCTCGGGGGGTGCGTGCG
TGTGTGTGTGCGTGGGGAGCGCCGCGTGCGGCCCGCGCTGCCCGGCGGCTGTGAGCGCTG
CGGGCGCGGCGCGGGGCTTTGTGCGCTCCGCGTGTGCGCGAGGGGAGCGCGGCCGGGGGC
GGTGCCCCGCGGTGCGGGGGGGCTGCGAGGGGAACAAAGGCTGCGTGCGGGGTGTGTGCG
TGGGGGGGTGAGCAGGGGGTGTGGGCGCGGCGGTCGGGCTGTAACCCCCCCCTGCACCCC
CCTCCCCGAGTTGCTGAGCACGGCCCGGCTTCGGGTGCGGGGCTCCGTGCGGGGCGTGGC
GCGGGGCTCGCCGTGCCGGGCGGGGGGTGGCGGCAGGTGGGGGTGCCGGGCGGGGCGGGG
CCGCCTCGGGCCGGGGAGGGCTCGGGGGAGGGGCGCGGCGGCCCCGGAGCGCCGGCGGCT
GTCGAGGCGCGGCGAGCCGCAGCCATTGCCTTTTATGGTAATCGTGCGAGAGGGCGCAGG
GACTTCCTTTGTCCCAAATCTGGCGGAGCCGAAATCTGGGAGGCGCCGCCGCACCCCCTC
TAGCGGGCGCGGGCGAAGCGGTGCGGCGCCGGCAGGAAGGAAATGGGCGGGGAGGGCCTT
CGTGCGTCGCCGCGCCGCCGTCCCCTTCTCCATCTCCAGCCTCGGGGCTGCCGCAGGGGG
ACGGCTGCCTTCGGGGGGGACGGGGCAGGGCGGGGTTCGGCTTCTGGCGTGTGACCGGCG
GCTCTAGAGCCTCTGCTAACCATGTTCATGCCTTCTTCTTTTTCCTACAGCTCCTGGGCA
ACGTGCTGGTTGTTGTGCTGTCTCATCATTTTGGCAAAGGCCACCATGTTCGTGTTTCTG
GTGCTGCTGCCTCTGGTGTCCAGCCAGCGGGTGCAGCCCACCGAATCCATCGTGCGGTTC
CCCAATATCACCAATCTGTGCCCCTTCGGCGAGGTGTTCAATGCCACCAGATTCGCCTCT
GTGTACGCCTGGAACCGGAAGCGGATCAGCAATTGCGTGGCCGACTACTCCGTGCTGTAC
AACTCCGCCAGCTTCAGCACCTTCAAGTGCTACGGCGTGTCCCCTACCAAGCTGAACGAC
CTGTGCTTCACAAACGTGTACGCCGACAGCTTCGTGATCCGGGGAGATGAAGTGCGGCAG
ATTGCCCCTGGACAGACAGGCAAGATCGCCGACTACAACTACAAGCTGCCCGACGACTTC
ACCGGCTGTGTGATTGCCTGGAACAGCAACAACCTGGACTCCAAAGTCGGCGGCAACTAC
AATTACCTGTACCGGCTGTTCCGGAAGTCCAATCTGAAGCCCTTCGAGCGGGACATCTCC
ACCGAGATCTATCAGGCCGGCAGCACCCCTTGTAACGGCGTGGAAGGCTTCAACTGCTAC
TTCCCACTGCAGTCCTACGGCTTTCAGCCCACAAATGGCGTGGGCTATCAGCCCTACAGA
GTGGTGGTGCTGAGCTTCGAACTGCTGCATGCCCCTGCCACAGTGTGCGGCCCTAAGAAA
AGCACCAATCTCGTGAAGAACAAATGCGTGAACTTCCACCATCACCATCACCATTGATAA
AATTCGAGCTCGCGGCCGCATCGATCTTAAGTCGCGACTCGAGCTAGCAGATCTTTTTCC
CTCTGCCAAAAATTATGGGGACATCATGAAGCCCCTTGAGCATCTGACTTCTGGCTAATA

AAGGAAATTTATTTTCATTGCAATAGTGTGTTGGAATTTTTTGTGTCTCTCACTCGGAAG
GACATATGGGAGGGCAAATCATTTAAAACATCAGAATGAGTATTTGGTTTAGAGTTTGGC
AACATATGCCCATATGCTGGCTGCCATGAACAAAGGTTGGCTATAAAGAGGTCATCAGTA
TATGAAACAGCCCCCTGCTGTCCATTCCTTATTCCATAGAAAAGCCTTGACTTGAGGTTA
GATTTTTTTTATATTTTGTTTTGTGTTATTTTTTTCTTTAACATCCCTAAAATTTTCCTT
ACATGTTTTACTAGCCAGATTTTTCCTCCTCTCCTGACTACTCCCAGTCATAGCTGTCCC
TCTTCTCTTATGAAGATCCCTCGACCTGCAGCCCAAGCTTGGCGTAATCATGGTCATAGC
TGTTTCCTGTGTGAAATTGTTATCCGCTCACAATTCCACACAACATACGAGCCGGAAGCA
TAAAGTGTAAAGCCTGGGGTGCCTAATGAGTGAGCTAACTCACATTAATTGCGTTGCGCT
CACTGCCCGCTTTCCAGTCGGGAAACCTGTCGTGCCAGCGGATCCGCATCTCAATTAGTC
AGCAACCATAGTCCCGCCCCTAACTCCGCCCATCCCGCCCCTAACTCCGCCCAGTTCCGC
CCATTCTCCGCCCCATGGCTGACTAATTTTTTTTATTTATGCAGAGGCCGAGGCCGCCTC
GGCCTCTGAGCTATTCCAGAAGTAGTGAGGAGGCTTTTTTGGAGGCCTAGGCTTTTGCAA
AAAGCTAACTTGTTTATTGCAGCTTATAATGGTTACAAATAAAGCAATAGCATCACAAAT
TTCACAAATAAAGCATTTTTTTCACTGCATTCTAGTTGTGGTTTGTCCAAACTCATCAAT
GTATCTTATCATGTCTGGATCCGCTGCATTAATGAATCGGCCAACGCGCGGGGAGAGGCG
GTTTGCGTATTGGGCGCTCTTCCGCTTCCTCGCTCACTGACTCGCTGCGCTCGGTCGTTC
GGCTGCGGCGAGCGGTATCAGCTCACTCAAAGGCGGTAATACGGTTATCCACAGAATCAG
GGGATAACGCAGGAAAGAACATGTGAGCAAAAGGCCAGCAAAAGGCCAGGAACCGTAAAA
AGGCCGCGTTGCTGGCGTTTTTCCATAGGCTCCGCCCCCCTGACGAGCATCACAAAAATC
GACGCTCAAGTCAGAGGTGGCGAAACCCGACAGGACTATAAAGATACCAGGCGTTTCCCC
CTGGAAGCTCCCTCGTGCGCTCTCCTGTTCCGACCCTGCCGCTTACCGGATACCTGTCCG
CCTTTCTCCCTTCGGGAAGCGTGGCGCTTTCTCAATGCTCACGCTGTAGGTATCTCAGTT
CGGTGTAGGTCGTTCGCTCCAAGCTGGGCTGTGTGCACGAACCCCCCGTTCAGCCCGACC
GCTGCGCCTTATCCGGTAACTATCGTCTTGAGTCCAACCCGGTAAGACACGACTTATCGC
CACTGGCAGCAGCCACTGGTAACAGGATTAGCAGAGCGAGGTATGTAGGCGGTGCTACAG
AGTTCTTGAAGTGGTGGCCTAACTACGGCTACACTAGAAGGACAGTATTTGGTATCTGCG
CTCTGCTGAAGCCAGTTACCTTCGGAAAAAGAGTTGGTAGCTCTTGATCCGGCAAACAAA
CCACCGCTGGTAGCGGTGGTTTTTTTGTTTGCAAGCAGCAGATTACGCGCAGAAAAAAAG
GATCTCAAGAAGATCCTTTGATCTTTTCTACGGGGTCTGACGCTCAGTGGAACGAAAACT
CACGTTAAGGGATTTTGGTCATGAGATTATCAAAAAGGATCTTCACCTAGATCCTTTTAA
ATTAAAAATGAAGTTTTAAATCAATCTAAAGTATATATGAGTAAACTTGGTCTGACAGTT
ACCAATGCTTAATCAGTGAGGCACCTATCTCAGCGATCTGTCTATTTCGTTCATCCATAG
TTGCCTGACTCCCCGTCGTGTAGATAACTACGATACGGGAGGGCTTACCATCTGGCCCCA
GTGCTGCAATGATACCGCGAGACCCACGCTCACCGGCTCCAGATTTATCAGCAATAAACC
AGCCAGCCGGAAGGGCCGAGCGCAGAAGTGGTCCTGCAACTTTATCCGCCTCCATCCAGT
CTATTAATTGTTGCCGGGAAGCTAGAGTAAGTAGTTCGCCAGTTAATAGTTTGCGCAACG
TTGTTGCCATTGCTACAGGCATCGTGGTGTCACGCTCGTCGTTTGGTATGGCTTCATTCA
GCTCCGGTTCCCAACGATCAAGGCGAGTTACATGATCCCCCATGTTGTGCAAAAAAGCGG
TTAGCTCCTTCGGTCCTCCGATCGTTGTCAGAAGTAAGTTGGCCGCAGTGTTATCACTCA
TGGTTATGGCAGCACTGCATAATTCTCTTACTGTCATGCCATCCGTAAGATGCTTTTCTG
TGACTGGTGAGTACTCAACCAAGTCATTCTGAGAATAGTGTATGCGGCGACCGAGTTGCT
CTTGCCCGGCGTCAATACGGGATAATACCGCGCCACATAGCAGAACTTTAAAAGTGCTCA

TCATTGGAAAACGTTCTTCGGGGCGAAAACTCTCAAGGATCTTACCGCTGTTGAGATCCA
GTTCGATGTAACCCACTCGTGCACCCAACTGATCTTCAGCATCTTTTACTTTCACCAGCG
TTTCTGGGTGAGCAAAAACAGGAAGGCAAAATGCCGCAAAAAAGGGAATAAGGGCGACAC
GGAAATGTTGAATACTCATACTCTTCCTTTTTCAATATTATTGAAGCATTTATCAGGGTT
ATTGTCTCATGAGCGGATACATATTTGAATGTATTTAGAAAAATAAACAAATAGGGGTTC
CGCGCACATTTCCCCGAAAAGTGCCACCTG

Table 9: Antibodies used throughout this doctoral thesis.

Antibody	Company	Cat.
Goat-anti-human IgG (Fc specific), HRP conjugated, Fc fragment specific	Jackson	# 109-035-098
Goat-anti-human Serum IgA (alpha-chain specific), HRP conjugated	Jackson	#109-035-011
Goat anti-human IgM (u chain) – Affinity Pure, HRP Conjugate	Immuno Reagents	# GtxHu-006-DHRPX
Goat-anti-human IgG (Fc specific), biotin-conjugated, Fc fragment specific	Jackson	#109-065-008
ChromePure Human IgG	Jackson	#009-000-003

Consumables and devices

All consumables used in this doctoral thesis were purchased from Sarstedt (Nümbrecht), Greiner bio-one (Frickenhausen), Corning (Corning, USA), Eppendorf (Hamburg), nerbe plus GmbH (Winsen/Luhe), TPP Techno Plastic Products (Trasadingen, Switzerland), Thermo Fisher Scientific (Waltham, USA), Miltenyi Biotec (Bergisch Gladbach), Bio-Rad (Feldkirchen), VWR (Darmstadt) and R. Langenbrinck GmbH (Emmendingen).

The kits and devices used in the doctoral research study are listed below.

Table 10: Kits used throughout this doctoral thesis.

Kit	Company	Cat.
Maxi Prep Kit	QIAGEN	#12163
Expi293^{TM} Expression System Kit	Thermo Fischer	#A14635
ELISA SARS-CoV-2 IgG	EUROIMMUN	#EI 2606-9601 G
ELISA SARS-CoV-2 IgA	EUROIMMUN	#EI 2606-9601 A
ELISA SARS-CoV-2 NCP	EUROIMMUN	#EI 2606-9601-2 G
Anti-SARS-CoV-2 Antikörper ELISA IgG	Mediagnost	#E111-IVD

Table 11: Devices used throughout this doctoral thesis.

Devices	Company
Accu-jet pro pipeting aid	Brand GmbH + Co KG, Wertheim
ÄKTAprime plus	GE Healthcare
Autoclave Systec VX 150	Systec GmbH, Linden
Bunsen Burner	

CLARIOstar *plus* microplate reader	BMG LABTECH GmbH
CO_2 Incubator HERAcell 150 i	Thermo scientific
Eclipse E200 microscope	Nikon, Japan
Hemocytometer (Neubauer-improved counting chamber)	Hecht Assistent, Sondheim von der Rhön
Heraeus Megafuge 1.0R	Heraeus Thermo scientific
Heraeus Pico 17 Centrifuge	Thermo scientific
HisTrap HP column	Sigma-Aldrich
Laboratory balance PM4000	Mettler Toledo, Columbus, Ohio
Microbiological safety cabinet	BDK Luft und Reinraumtechnik GmbH, Sonnenbühl-Genkingen
Microbiological safety cabinet Heraeus HERA safe	Thermo scientific
Millipore water system Astacus	membraPure GmbH, Henningsdorf/ Berlin
NanoDrop 2000/2000c	Thermo scientific
Pipettes Discovery Comfort (several volumes)	HTL lab solution, Poland
Pipettes Eppendorf Research plus (several volumes)	Eppendorf, Hamburg
Polycarbonate Erlenmeyer Flask with Vent Cap	Corning, USA
StrepTrap™ HP column	Sigma-Aldrich
ThermoMixer F1.5	Eppendorf, Hamburg
Vacuum-driven filtration system	

Media and buffers

Media for Transformation in competent cells

Terrific Broth Medium

Chemicals	End conc.
Bacto Tryptone	12 g/L
Bacto Yeast Extract	24 g/L
Glycerol	4 ml/L
KH_2PO_4	0.17 M
K_2HPO_4	0.72 M
MilliQ H_2O	

Solution of KH_2PO_4 and K_2HPO_4 sterilized by filtration, solution of other components sterilized by autoclaving

SOC Medium

Chemicals	End conc.
Tryptone	2% w/v
Yeast extract	0.5 % w/v
NaCl	10 mM
KCl	2.5 mM
MgCl2	10 mM
MgSO4	10 mM
Glucose	20 mM
MilliQ H_2O	
	pH 6.7-7.0

Agar plate with ampicillin

Chemicals	End conc.
Tryptone	10 g/L
Yeast extract	5 g/L
NaCl	10 g/L
Bacto agar	15 g/L
MilliQ H_2O	

Sterilized by autoclaving, cooled down to 50°C to add 100 mg/L carbenicillin.

Buffer for Agarose gel electrophoresis

TBE Buffer 10x

Chemicals	End conc.
TRIS	108 g/L
Boric acid	55.6 g/L
EDTA(Na2)	7.44 g/L
MilliQ H_2O	

Media for cell culture and transfection

The Gibco Expi293™ Expression medium by Thermo Fischer Scientific, cat. number A1435102 and the Expi293™ Expression System Kit by Thermo Fischer Scientific, cat. number A14635 were used throughout this thesis to maintain the cell cultures and to perform transfection.

Buffers for His-Tag purification with the Äkta system

Wash buffer 1x

Chemicals	End conc.
$NaH_2PO_4H_2O$	7.94 g/L
NaCl	17.54 g/L
MilliQ H_2O	

pH adjusted to 7.4 with HCl

Elution buffer

Chemicals	End conc.
$NaH_2PO_4H_2O$	7.94 g/L
NaCl	17.54 g/L
Imidazole	64.0 g/L
MilliQ H_2O	

pH adjusted to 7.4 with HCl

Buffer for Strep-Tag purification with the Äkta system

Wash buffer

Chemicals	End conc.
Tris-HCl	100 mM
NaCl	150 mM
EDTA	1 mM

pH adjusted to 8.0

Elution buffer:

2.5 mM Desthiobiotin in wash buffer.

Buffer for SDS Page

Runningbuffer 10 x TGS

Chemicals	End conc.
TRIZMA Base	250 mM
Glycin	192 mM
SDS	0.1% (w/v)
MilliQ H_2O	

10 M HCl for adjusting the pH to 8.3

SDS Loading-buffer 5x

Chemicals	End conc.
Dithiothreitol	0.5 M
Glycerol	50% (v/v)
10% SDS	10% (v/v)
Bromphenol blue	0.25% (w/v)
Tris-HCl, pH 6.8	0.25 M
MilliQ H_2O	

8 ml Stracking gel 6%

Chemicals	amount
MilliQ H2O	5.4 ml
Acrylamide (30%)	1.6 ml
1 M Tris pH 6.8	1 ml
SDS (10%)	80 µl
APS (10%)	80 µl
TEMED	8 µl

Separating gel 10%

Chemicals	amount
MilliQ H2O	4.1 ml
Acrylamide (30%)	3.3 ml
1 M Tris pH 8.8	2.5 ml
SDS (10%)	100 µl
APS (10%)	32 µl
TEMED	10 µl

Buffer and media for IgG and IgA inhouse ELISA

Coating buffer: Phosphate buffered saline (PBS 1x) pH 7,4

Coating antigen: CMV-RBD

Blocking buffer by Candor: The Blocking Solution

Wash buffer: PBS, PBS-T

Sample diluent: The Blocking Solution by Candor

Conjugate: Roti Block 1x by ROTH #A151.2

HRP substrate: Tetramethylbenzidine (TMB ONE™, ECO-TEK®)

Stopping solution: 1M Hydrochloric acid

Data

Intra-assay precision in-house SARS-CoV-2 IgG ELISA

Table 1: IgG in-house ELISA, intra-assay precision values of 12- fold determinations in dilution series.

dilution	*Average*	*Standard deviation* s	*Variation coefficient* v
1:50	3.314	0.052	1.622
1:150	2.790	0.029	1.031
1:450	1.356	0.053	3.939
1:1350	0.529	0.022	4.236
1:4050	0.184	0.010	5.174
1:12150	0.068	0.003	4.706
1:36450	0.028	0.002	7.326
blank	0.007	0.001	9.770

Inter-assay precision of the in-house SARS-CoV-2 IgG ELISA

Table 2: Average, standard deviation and variation coefficient of OD values of the inter-assay precision test of the in-house SARS-CoV-2 IgG ELISA.

A: Average			
Samle	1:100	1:500	1:2,500
TüCoV 003	2.833	0.943	0.212
	2.822	0.929	0.208
	2.773	0.872	0.195
TüCoV 004	3.398	2.564	0.756
	3.429	2.600	0.791
	3.357	2.593	0.761
TüCoV 005	1.505	0.371	0.085
	1.458	0.357	0.081
	1.270	0.329	0.071

B: Standard deviation *s*			
Samle	1:100	1:500	1:2,500
TüCoV 003	0.177	0.081	0.018
	0.045	0.041	0.008
	0.145	0.083	0.026
TüCoV 004	0.120	0.211	0.151
	0.065	0.091	0.044
	0.046	0.024	0.046
TüCoV 005	0.113	0.038	0.012
	0.091	0.024	0.007
	0.062	0.008	0.009

C: Variation coefficient [%]			
Samle	1:100	1:500	1:2,500
TüCoV 003	6.238	8.585	8.429
	1.589	4.361	3.997
	5.214	9.467	13.240
TüCoV 004	3.517	8.235	19.924
	1.895	3.486	5.595
	1.371	0.926	6.092
TüCoV 005	7.538	10.239	13.981
	6.239	6.840	8.723
	4.907	2.374	13.026
Average	4.279	6.057	10.334

D: Average of variation coefficients [%]			
Sample	1:100	1:500	1:2,500
TüCoV 003	2.261	4.216	10.537
TüCoV 004	4.347	7.471	8.555
TüCoV 005	6.228	6.484	11.910
Average	4.279	6.057	10.334

Intra-assay precision in-house SARS-COV-2 IgA ELISA

Table: IgA in-house ELISA, intra-assay precision values of 7 serial 12-fold dilutions.

dilution	***Average***	***Standard deviation* s**	***variation coefficient* v**
1:100	3.093	0.045	1.47
1:300	2.111	0.071	3.36
1:900	0.841	0.044	5.27
1:2700	0.281	0.018	6.53
1:8100	0.097	0.007	6.72
1:24300	0.035	0.004	11.66
1:72900	0.016	0.002	13.40

Inter-assay precision in-house SARS-COV-2 IgA ELISA

A: Average of the days

	1 to 100	1 to 500	1 to 2500
very strong positivity	1.314	0.312	0.072
strong positivity	1.113	0.284	0.066
intermediate positivity	0.582	0.161	0.039
low positivity	0.528	0.127	0.033

B: Standard deviation

	1 to 100	1 to 500	1 to 2500
very strong positivity	0.154	0.042	0.008
strong positivity	0.062	0.030	0.007
intermediate positivity	0.147	0.033	0.008
low positivity	0.064	0.018	0.003

C: Variation coefficient [%]

	1 to 100	1 to 500	1 to 2500
very strong positivity	11.710	13.518	11.615
strong positivity	5.593	10.569	10.585
intermediate positivity	25.226	20.724	21.571
low positivity	12.138	13.925	10.000
Average	13.667	14.684	13.443

CRF

ProbandenID:

Datenblatt COVID-19 Immunstudien

COVID-19 Antikörperstudie	Ja	Nein	ID
Covid -19 Zelluläre Immunstudie	Ja	Nein	ID

Name:

Alter:

Datum der Untersuchung (DDMMMYYYY): _____

Hatten Sie Symptome, die mit COVID-19 In Zusammenhang stehen könnten?	Ja	Nein
Wann traten die Symptome auf (DDMMMYYYY)?	_____	
Wie lange dauerten die Symptome?:	_____ Tage	
Mussten Sie im Krankenhaus behandelt werden?:	Ja	Nein

Welche Symptome traten auf?

Ermüdung	Ja	Nein
Erschöpfung	Ja	Nein
Halsschmerzen	Ja	Nein
Fieber	Ja	Nein
Wenn ja wie hoch?	_____ ^{0}C	
Wie viele Tage?	_____	
Kopfschmerzen	Ja	Nein
Gliederschmerzen	Ja	Nein
Schmerzen des Skeletts	Ja	Nein
Gelenkschmerzen	Ja	Nein
Andere Schmerzen	Ja	Nein
Wenn ja, welche?	_____	

CRF_V01_08APR2020